

# **Solvent Isotope Effect ( $D_2O$ ) in Photocatalytic Systems**

Von der Naturwissenschaftlichen Fakultät der  
Gottfried Wilhelm Leibniz Universität Hannover

Zur Erlangung des Grades

**Doktor der Naturwissenschaften**  
**(Dr. rer. nat.)**

genehmigte Dissertation

von

**Hamza Belhadj, Magistere (Algerien)**

2017

Referent: Prof. Dr. rer. nat. Detlef W. Bahnemann

Korreferent: Prof. Dr. rer. nat. Thomas Scheper

Korreferent: Prof. D.Phil. Peter K. J. Robertson

Tag der Promotion: 27.10.2017

## **Declaration**

The work described in the current thesis was carried out at the Institute of Technical Chemistry, Leibniz University of Hannover under the guidance of Prof. Dr. Detlef Bahnemann. I hereby declare that the present work is my own and to the best of my knowledge and belief, it contains no material previously either published or written by another person, or submitted by another person for the award of any other university degree, except where acknowledgement has been made in the text.

Hamza Belhadj

Hannover, 2017

## Preface

This cumulative dissertation is submitted for the degree of Dr.rer.nat. at the Gottfried Wilhelm Leibniz University of Hannover. The research described herein was conducted under the supervision of Prof. Dr. Detlef Bahnemann in the Institute of Technical Chemistry between October 2013 and October 2017.

This work is to the best of my knowledge original, except where acknowledgements and references are made to previous studies. The results of the work were published in peer-reviewed journals and presented in international congresses. The structure of the thesis is adapted in the form of “Cumulative dissertation” where experimental investigations, figure lists, as well as references were organized according to their appearance in the respective publications.

Hamza Belhadj

Hannover, 2017

## Acknowledgement

First and foremost, I would like to express my deepest gratitude to Prof. Dr. Detlef Bahnemann for giving me the chance to work under his supervision in such an interesting area, for his valuable guidance, inspiring reviews, and stimulating discussions.

I am appreciative to Prof. Dr. Thomas Scheper and Prof. Dr. Jürgen Caro for their kindness of being members of the examination committee.

I also would like to express my special appreciation to Prof. Peter K.J. Robertson for his willingness to be co-supervisor of this work, for many insightful discussions and ideas during my research, as well as for his co-authorship in my publications.

I owe special thanks to Dr. Ralf Dillert and Dr. Amer Hakki for numerous scientific discussions and their help in this research area.

I am also deeply thankful to my colleagues and office mates for their assistance in lab related issues and for the very good atmosphere of work.

I would like to express my deepest gratitude to my family especially to my parents. They are devoted to me and always do all they can to help me and encourage me to overcome the difficulties.

Every single day I thank my wonderful wife Kamilia Derradji for her love, support and her presence in my life.

My dear son Eyad I thank for his patience and love. You are the greatest discovery of my life.

Finally, I would like to gratefully acknowledge the Deutscher Akademischer Austauschdienst (DAAD) for the financial support to perform my PhD. studies in Germany.

## Abstract

There is increasing evidence that water adsorbed on the TiO<sub>2</sub> surface plays an important role in photocatalytic systems such as photoinduced hydrophilicity, photocatalytic degradation and hydrogen production. However, it is important to elucidate the role of water on the photocatalytic reaction mechanism of TiO<sub>2</sub>.

This thesis presents four original research articles focusing on the mechanistic studies of photocatalytic reactions at the TiO<sub>2</sub>/aqueous solution interface. The main objectives of this work are: (i) Investigating the behaviour of surface hydroxyl groups and of water adsorption on the TiO<sub>2</sub> surface under UV irradiation. (ii) Understanding the interaction between H<sub>2</sub>O/D<sub>2</sub>O and substrate adsorption, i.e., ethanol and acetate at the TiO<sub>2</sub> surface. (iii) Determining the role of H<sub>2</sub>O/D<sub>2</sub>O adsorption on the reaction mechanism for the simultaneous photocatalytic hydrogen production and formaldehyde oxidation over platinumized TiO<sub>2</sub>.

In Chapter 2, the effect of H<sub>2</sub>O and D<sub>2</sub>O adsorption on the surface hydroxyl group behaviour are investigated before and after UV irradiation using ATR-FTIR spectroscopy. Adsorption of H<sub>2</sub>O with different ratios of D<sub>2</sub>O on TiO<sub>2</sub> revealed that the deuteride ions exhibit stronger adsorption ability than hydroxyl ions resulting in an isotopic exchange reaction which takes place in the dark. Under UV irradiation, the oxygen molecule seems to play an important role for the adsorption of water molecules which in turn increases the hydrophilicity of the TiO<sub>2</sub> surface. The effect of the presence of hole scavengers (ethanol) on water and D<sub>2</sub>O adsorption behaviour was thoroughly investigated in Chapter 3. This *In situ* ATR-FTIR study showed that in the dark, ethanol can adsorb on the TiO<sub>2</sub> surface in both molecular and dissociative form. These adsorption forms of ethanol show a stronger adsorption capacity compared to water and D<sub>2</sub>O on the TiO<sub>2</sub> surface. Under UV irradiation, the typical ethanol bands decreased on the surface while the adsorption of water and D<sub>2</sub>O increased. Several mechanisms regarding the photoinduced charge transfer process (adsorption/desorption and photocatalytic reaction) and the thermal process (thermal desorption and de-aggregation of particle agglomerates) are discussed.

In Chapter 4, the interfacial acetate/TiO<sub>2</sub> interaction in H<sub>2</sub>O and D<sub>2</sub>O together with the influence of pH, as well as the formation of reactive species (ROS) on the TiO<sub>2</sub> surface were extensively studied during UV irradiation by ATR-FTIR and EPR spectroscopy,

respectively. Isotopic exchange during the adsorption of D<sub>2</sub>O on the TiO<sub>2</sub> surface led to different interactions between acetate and OD groups. The experimental results revealed that the interaction of acetate with the TiO<sub>2</sub> surface depends strongly on the pH of the suspension. EPR studies indicate that the degradation of acetate at higher pH mainly occurred by indirect oxidation via hydroxyl radical attack whereas at lower pH the degradation of acetate occurs via direct oxidation of surface-bound acetate by valence band holes.

In Chapter 5, the effect and the role of H<sub>2</sub>O/D<sub>2</sub>O adsorption on the photocatalytic hydrogen production from the oxidation of formaldehyde over platinized TiO<sub>2</sub> are addressed. The study of the solvent isotope effect on the degradation of formaldehyde indicates that the mineralization rate of formaldehyde decreases considerably when increasing the concentration of D<sub>2</sub>O. The solvent isotopic effect indicated that the photocatalytic oxidation of formaldehyde takes place at the valence band through <sup>•</sup>OH radicals while the photocatalytic hydrogen production mainly occurred at the conduction band by the reduction of two protons originating from water and formaldehyde. A detailed mechanism for the simultaneous hydrogen production with formaldehyde oxidation in D<sub>2</sub>O is presented.

**Keywords:** Titanium dioxide, Adsorption, D<sub>2</sub>O, Photocatalytic reaction, Isotopic-exchange, Acetate, Formaldehyde, Hydrogen production, Mechanistic study.

## Kurzzusammenfassung

Untersuchungen der photoinduzierten Hydrophilie, des photokatalytischen Abbaus und der Wasserstoffproduktion haben gezeigt, dass das an der TiO<sub>2</sub> Oberfläche adsorbierte Wasser eine wichtige Rolle in photokatalytischen Systemen spielt. Aus diesem Grund ist es wichtig, die Rolle von Wasser beim photokatalytischen Reaktionsmechanismus an der TiO<sub>2</sub> Oberfläche aufzuklären.

Diese Arbeit enthält vier originale Forschungsartikel, die sich auf die mechanistischen Studien der photokatalytischen Reaktion an der Titandioxid-Flüssigkeits-Grenzfläche fokussieren. Die Ziele dieser Arbeit sind (i) die Untersuchung des Verhaltens von Hydroxylgruppen und der Wasseradsorption an der TiO<sub>2</sub> Oberfläche unter UV-Bestrahlung. (ii) das Verständnis der Wechselwirkungen zwischen H<sub>2</sub>O/D<sub>2</sub>O- und der Substratadsorption, z.B. von Methanol und Acetat an der Wasser/TiO<sub>2</sub> Grenzfläche, (iii) die Ermittlung der Rolle von der H<sub>2</sub>O/D<sub>2</sub>O-Adsorption auf den Reaktionsmechanismus für die gleichzeitige Wasserstoffproduktion und Formaldehyd-Oxidation an platinisiertem Titandioxid.

In Kapitel 2 wird der Effekt der H<sub>2</sub>O- und D<sub>2</sub>O-Adsorption auf Oberflächen-Hydroxylgruppen vor und nach einer UV-Bestrahlung mittels ATR-FTIR Spektroskopie untersucht. Die Adsorption von H<sub>2</sub>O in verschiedenen Verhältnissen zu D<sub>2</sub>O an TiO<sub>2</sub> zeigte, dass deuterierte Ionen eine stärkere Adsorption eingehen als Hydroxylionen. Dies führt zu einer Isotopen-Austauschreaktion, die im Dunkeln stattfindet. Unter UV-Bestrahlung scheint das Sauerstoffmolekül eine wichtige Rolle in der Adsorption von Wassermolekülen zu spielen, was im Gegenzug die Hydrophilie der TiO<sub>2</sub> Oberfläche erhöht. Der Effekt der Anwesenheit von Lochfängern wie Ethanol auf das H<sub>2</sub>O- und D<sub>2</sub>O-Adsorptionsverhalten wurden in Kapitel 3 eingehend untersucht. *In-situ* ATR-FTIR Adsorptionsmessungen zeigten, dass Ethanol im Dunkeln sowohl in seiner molekularen, als auch in seiner dissoziierten Form an der TiO<sub>2</sub> Oberfläche adsorbiert. Die Adsorption von Ethanol zeigt eine höhere Adsorptionskapazität im Vergleich zu H<sub>2</sub>O und D<sub>2</sub>O auf der Titandioxidoberfläche. Unter UV-Bestrahlung verringern sich die typischen Ethanolbänder im IR, während die Adsorption von Wasser und D<sub>2</sub>O steigt. Verschiedene Mechanismen bezüglich des photoinduzierten Ladungstransfers (Adsorption/Desorption und photokatalytische Reaktion) und der thermischen Prozesse (thermische Desorption und Deaggregation von Partikeln) werden diskutiert.



Kapitel 4 beschäftigt sich mit der Grenzflächenwechselwirkung von Acetat und  $\text{TiO}_2$  in Wasser und  $\text{D}_2\text{O}$ . Außerdem wird der Einfluss des pH-Wertes, sowie die Bildung von reaktiven Sauerstoff Spezies (engl.: Reactive Oxygen Species, ROS) an der  $\text{TiO}_2$ -Oberfläche unter UV-Bestrahlung mittels ATR-FTIR und EPR Spektroskopie untersucht. Isotopen-Austauschreaktionen während der Adsorption von  $\text{D}_2\text{O}$  an der  $\text{TiO}_2$  Oberfläche führen zu verschiedenen Wechselwirkungen zwischen Acetat- und OD-Gruppen. Die experimentellen Ergebnisse zeigen, dass die Wechselwirkung von Acetat mit der  $\text{TiO}_2$  Oberfläche sehr stark vom pH-Wert der Suspension abhängig ist. EPR Untersuchungen zeigen außerdem, dass der Acetatabbau bei höheren pH-Werten hauptsächlich durch die indirekte Oxidation mittels Hydroxylradikalen abläuft, während bei niedrigen pH-Werten der Abbau von Acetat über die direkte Oxidation von oberflächengebundenem Acetat durch Löcher aus dem Valenzband erfolgt.

In Kapitel 5 werden der Effekt und die Rolle der  $\text{H}_2\text{O}/\text{D}_2\text{O}$ -Adsorption auf die photokatalytische Wasserstoffproduktion und die Oxidation von Formaldehyd an platinisiertem  $\text{TiO}_2$  betrachtet. Die Studie des Lösungs-Isotopen-Effekts auf den Abbau von Formaldehyd deutet an, dass die Mineralisierung von Formaldehyd zu  $\text{CO}_2$  sich signifikant verringert, wenn die Konzentration von  $\text{D}_2\text{O}$  erhöht wird. Der Lösungs-Isotopen-Effekt erklärt, dass die photokatalytische Oxidation von Formaldehyd aus dem Valenzband durch OH-Radikale abläuft, während die photokatalytische Wasserstoffentwicklung hauptsächlich am Leitungsband durch die Reduktion von zwei Protonen aus Wasser und Formaldehyd erfolgt. Des Weiteren wird der detaillierte Mechanismus für die gleichzeitige Oxidation von Formaldehyd und die Wasserstoffproduktion in  $\text{D}_2\text{O}$  gezeigt.

**Stichwörter:** Titandioxid, Adsorption,  $\text{D}_2\text{O}$ , Photokatalytische Reaktion, Isotopen-Austauschreaktion, Formaldehyd, Wasserstoffproduktion, Mechanistische Studien.



---

# Table of Contents

<b>Introduction and Objectives</b>	1
<b>Chapter 1</b>	5
<b>1. Theoretical Background</b>	5
1.1. Photocatalysis Mechanism of TiO <sub>2</sub>	5
1.1.1. Photoinduced Hydrophilicity of TiO <sub>2</sub>	6
1.1.2. Photocatalytic Degradation of Organic Pollutants in Water	9
1.1.3. Photocatalytic Hydrogen Production	10
1.1.4. Novel Mechanistic Concepts of TiO <sub>2</sub> Photocatalysis	12
1.2. Impact of H <sub>2</sub> O/D <sub>2</sub> O Adsorption on Photocatalytic Reaction Mechanism	14
1.3. References	16
<b>Chapter 2</b>	21
<b>2. <i>In Situ</i> ATR-FTIR Study of H<sub>2</sub>O and D<sub>2</sub>O Adsorption on TiO<sub>2</sub> Under UV Irradiation</b>	22
2.1. Abstract	22
2.2. Introduction	23
2.3. Experimental	24
2.4. Results	26
2.5. Discussion	32
2.6. Conclusions	35
2.7. Acknowledgments	36
2.8. References	36
2.9. Supplementary information	39
<b>Chapter 3</b>	42

---

<b>3. <i>In Situ</i> ATR-FTIR Investigation of the Effects of H<sub>2</sub>O and D<sub>2</sub>O Adsorption on the TiO<sub>2</sub> Surface</b>	42
3.1. Abstract	42
3.2. Introduction	42
3.3. Experimental	43
3.4. Results and discussion	45
3.5. Conclusions	55
3.6. Acknowledgments	55
3.7. References	55
<b>Chapter 4</b>	57
<b>4. Pathways of the Photocatalytic Reaction of Acetate in H<sub>2</sub>O and D<sub>2</sub>O: A Combined EPR and ATR-FTIR Study</b>	58
4.1. Abstract	58
4.2. Introduction	59
4.3. Experimental section	60
4.4. Results	62
4.5. Discussion	72
4.6. Conclusions	76
4.7. Acknowledgments	77
4.8. References	77
4.9. Supplementary information	80
<b>Chapter 5</b>	85
<b>5. Mechanisms of Simultaneous Hydrogen Production and Formaldehyde Oxidation in H<sub>2</sub>O and D<sub>2</sub>O over Platinized TiO<sub>2</sub></b>	86
5.1. Abstract	86
5.2. Introduction	87

5.3. Experimental Section	88
5.4. Results	90
5.5. Discussion	96
5.6. Conclusions	99
5.7. Acknowledgments	99
5.8. References	102
5.9. Supplementary information	102
<b>Chapter 6</b>	105
<b>6. Summary and Outlook</b>	105
6.1. Summary and Conclusion	105
6.1.1. Photoinduced Hydrophilicity of TiO <sub>2</sub>	105
6.1.2. Photocatalytic Degradation of Organic Compounds	108
6.1.3. Photocatalytic Hydrogen Production	110
6.2. Outlook	114
<b>List of Publications</b>	115
<b>Curriculum Vitae</b>	117



## Introduction and Objectives

Photocatalysts have been widely applied for environmental cleaning (i.e., self-cleaning, wastewater purification and antifogging) and solar fuel production (i.e., Hydrogen production and CO<sub>2</sub> reduction). Among many kinds of photocatalysts, titanium dioxide (TiO<sub>2</sub>) is the most promising material because it is inexpensive, chemically stable and nontoxic. As most photocatalysis applications of TiO<sub>2</sub> involve an aqueous environment, the investigation of photocatalytic reactions at the TiO<sub>2</sub>/water interface has attracted strong interest in recent years.

The photocatalytic process is initiated by the formation of valence band holes ( $h^+_{vb}$ ) and conduction band electrons ( $e^-_{cb}$ ) in a TiO<sub>2</sub> particle upon band gap illumination. Consequently, the TiO<sub>2</sub> particles act as electron donors and electron acceptors for molecules in the surrounding medium. Elucidation of the photocatalytic reaction mechanism is vital to gain insight into the current limitations of titanium dioxide and also to improve the efficiency and stability of the photocatalysts by rational design. However, more in situ studies at the TiO<sub>2</sub> surface under working conditions are needed to reveal all mechanistic details.

It has been well reported that UV(A) irradiation of the TiO<sub>2</sub> surface induces photocatalytic reactions and photoinduced hydrophilicity which can take place simultaneously on the same photocatalyst surface even though the mechanisms are completely different. The photoinduced hydrophilicity of TiO<sub>2</sub> surfaces is initially explained by an increase in the amount of hydroxyl groups on this surface, while the photocatalytic reaction is based on redox reactions with molecules adsorbed on the photocatalyst surface to yield the final products.

Under aerated conditions, photocatalytic degradation of organic pollutants takes place at the photocatalyst surface, with the participation of photogenerated holes, which act either directly or indirectly via the generation of reactive oxygen species such as hydroxyl radicals ( $\bullet\text{OH}$ ), superoxide radical anions ( $\text{O}_2^{\bullet-}$ ) and hydrogen peroxide ( $\text{H}_2\text{O}_2$ ). Since the reaction ability of the hydroxyl radical ( $\bullet\text{OH}$ ) is high enough to attack any organic molecules, it has been assigned as a key species in the mineralization mechanism of organic compounds yielding CO<sub>2</sub> and H<sub>2</sub>O. Although the mechanism of hydroxyl

radical formation has been suggested via the photocatalytic oxidation of water or OH groups adsorbed on the catalyst surface, the detailed mechanism at the TiO<sub>2</sub>/water interface is so far still unclear.

Under oxygen free conditions, adsorption of electron donors such as water and organic compounds has been found to yield key species for the initiation of the photocatalytic hydrogen production. The rate of hydrogen production depends strongly on a range of experimental parameters including the nature of metal deposition, the catalyst concentration, the pH and the concentration of electron donors. The metal deposits act as an active site for H<sub>2</sub> production, in which the trapped photogenerated electrons are transferred to protons to produce hydrogen molecules. Since competitive reactions may take place between the adsorption of water and organic compounds at the TiO<sub>2</sub> surface, the primary events and the source of molecular hydrogen formed during the oxidation of organic molecules have not been clarified in a unified mechanism yet. An elucidation of this mechanism requires direct experimental investigations of the effect of water adsorption on the catalyst surface and on the photocatalytic reaction mechanism of hydrogen production.

Moreover, the effect of light on the particle network of TiO<sub>2</sub> has recently received special attention in view of mechanistic studies of the photocatalytic reaction behaviour introducing the additional effect of UV light on the chemical reaction at the interface TiO<sub>2</sub>/aqueous solution. Novel mechanistic concepts of TiO<sub>2</sub> photocatalysis have been proposed such such as the antenna mechanism and the deaggregation concept which may give an alternative or additional explanation for open questions concerning the photocatalytic reaction mechanism at the TiO<sub>2</sub> surface.

In order to understand the photocatalytic reaction mechanism at the TiO<sub>2</sub>/aqueous solution interface, it is necessary to determine the role of water adsorption for photoinduced hydrophilicity, photocatalytic degradation and hydrogen production. Therefore, a study of the solvent isotope effect appears to be a rational strategy to elucidate the mechanistic details of the photocatalytic process by looking closely at the surface phenomena using *in situ* ATR-FTIR, QMS, and EPR spectroscopy.



This thesis presents a chronological sequence of the research performed on interfacial photocatalytic processes at the liquid/solid interface, with the objective to resolve the following three issues:

- i. Understand the fundamental process of photoinduced hydrophilicity and determine the source of hydroxyl groups formed on the TiO<sub>2</sub> surface under UV irradiation.
- ii. Investigate the interaction between water and substrate at the TiO<sub>2</sub>/aqueous solution interface with photocatalytic reaction pathways.
- iii. Determine the primary events and the source of molecular hydrogen formed during the oxidation of organic molecules.

The first issue is reported in Chapters 2 and 3, where the adsorption behaviour of H<sub>2</sub>O and D<sub>2</sub>O on the TiO<sub>2</sub> surface was investigated in the absence and presence of both electron scavengers (molecular oxygen) and hole scavengers (ethanol) using *in situ* ATR-FTIR spectroscopy. This work focuses on the analysis of the behaviour of water adsorption before and after UV irradiation considering the effect of UV irradiation on the TiO<sub>2</sub> particle network to provide new insight into the mechanism of photoinduced hydrophilicity during UV illumination.

The second issue is reported in Chapter 4, where the photocatalytic reaction pathways of acetate was determined in terms of the adsorption behaviour of acetate on TiO<sub>2</sub> surfaces as well as the formation of primary intermediate radicals by ATR-FTIR and EPR spectroscopy.

The third issue is discussed in Chapter 5, where a detailed mechanism of photocatalytic hydrogen evolution on platinumized TiO<sub>2</sub> from aqueous formaldehyde solution was investigated in different concentrations of D<sub>2</sub>O. This work considers the solvent isotope effect to determine whether the origin of the evolved molecular hydrogen is from water or formaldehyde.



# Chapter 1

## 1. Theoretical background

### 1.1 Photocatalysis Mechanism of TiO<sub>2</sub>

Titanium dioxide (TiO<sub>2</sub>) is an interesting material for photocatalytic reactions due to its high stability, low cost, nontoxicity and excellent photoactivity [1],[2]. When TiO<sub>2</sub> absorbs a photon of energy equal to or greater than its band gap width (3.2 eV), electrons are promoted from the valance band (VB) to the conduction band (CB) to generate electron-hole pairs. The photogenerated electron and holes can either recombine, releasing energy in the form of heat, or can separate and migrate to the surface of the photocatalyst where they are ultimately trapped by adsorbed electron donors (D) and acceptors (A) (Figure 1.1).

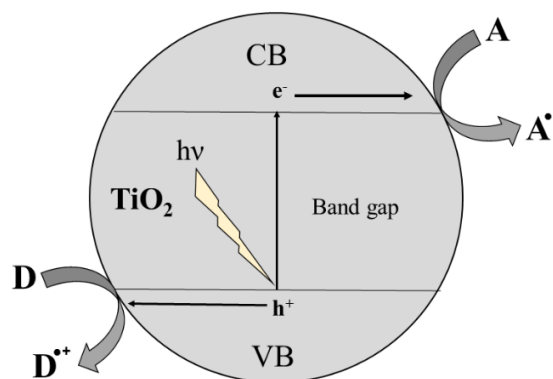


**Figure 1.1:** Mechanism of photocatalysis.

The photocatalytic reactions of TiO<sub>2</sub> have been extensively studied because of its promising applications for environmental problems (self-cleaning, water and air purification and antifogging) and for solar energy conversion (Hydrogen production and CO<sub>2</sub> reduction) [3],[4].

### 1.1.1 Photoinduced Hydrophilicity of TiO<sub>2</sub>

Self-cleaning TiO<sub>2</sub> films have gained considerable attention for their unique properties and practical application such as window glasses and anti-fogging mirrors [5]. The surface wettability of TiO<sub>2</sub> is generally evaluated by water contact angle measurements. Upon irradiation by UV light, the surface gradually converts to a hydrophilic state with the contact angle finally reaching 0° after water spreads over the entire surface (Figure 1.2).

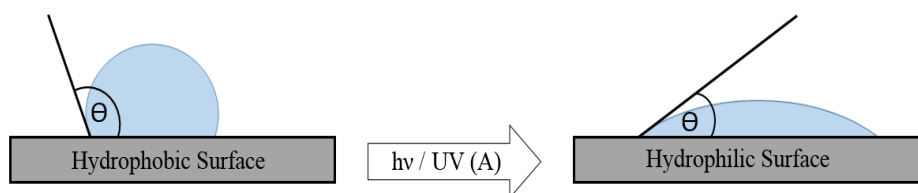


**Figure 1.2:** Effect of UV irradiation on the wettability conversion of titanium dioxide.

The mechanism for photoinduced hydrophilicity of titanium dioxide is still not well understood, however, different models have been proposed for the hydrophilicity phenomenon on TiO<sub>2</sub> surfaces such as (i) the formation of oxygen vacancies [6], (ii) the photo-induced reconstruction of Ti–OH [7] and (iii) the photocatalytic decomposition of organic adsorbents [8].

### 1.1.1.1 Mechanisms

- **Generation of oxygen vacancies**

When  $\text{TiO}_2$  is irradiated by UV light, electron and hole pairs are generated. The conduction band electrons are trapped at titanium sites to reduce titanium (IV) to titanium (III), while the photogenerated holes produced in the bulk of  $\text{TiO}_2$  diffuse to the surface and oxidize lattice oxygen anions causing oxygen atoms to be liberated leaving oxygen vacancies behind [9],[10]. Adsorbed water molecules can then dissociate in these oxygen vacancies resulting in the formation of adsorbed OH groups thereby increasing the surface hydrophilicity (Figure 1.3) [11].

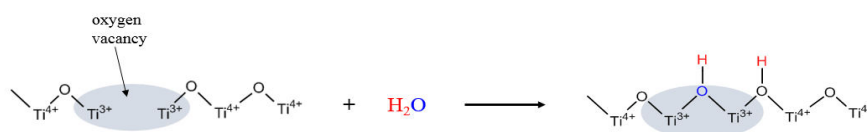


**Figure 1.3:** Scheme for water dissociation on oxygen vacancies.

- **Photo-induced reconstruction of Ti–OH**

Upon excitation of  $\text{TiO}_2$  by UV(A) light, the photogenerated holes produced in the bulk of  $\text{TiO}_2$  diffuse to the surface where they are trapped at lattice oxygen sites [12]. The trapped holes are consumed by breaking the bond between the lattice titanium and oxygen upon the coordination of water molecules at the titanium site. Subsequently, the water molecule releases a proton for charge compensation to produce new OH groups [13],[14]. When the  $\text{TiO}_2$  surface is stored in the dark, the surface is converted to a less hydrophilic state, due to the desorption of surface hydroxyl groups (Figure 1.4) [15].

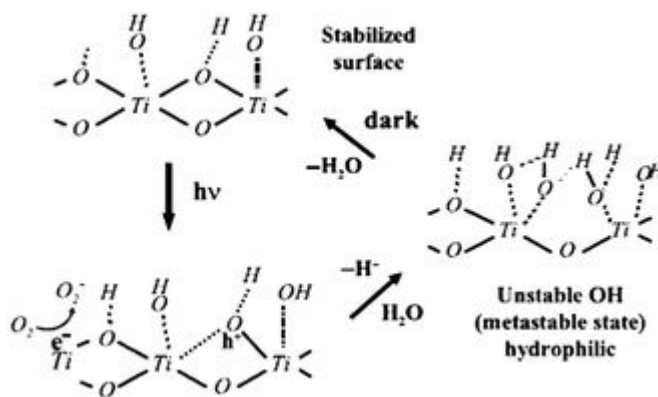


**Figure 1.4:** Schematic illustration of the reconstruction of Ti–OH in the dark and under UV irradiation [15]. (Copyright 2005 Springer.)

- **Photocatalytic decomposition of organic adsorbents**

This mechanism occurs on the surface of  $\text{TiO}_2$  when UV light induces the photocatalytic decomposition of organic compounds. The contamination then decreases continuously which is followed by a decrease of the contact angle (Figure 1.5). It has been suggested that in addition to the photocatalytic decomposition, UV light can also induce the desorption of water from the surface by the heating effect from a light source. As soon as the organic pollutants are removed from the  $\text{TiO}_2$  surface and the amount of water molecules is decreased, the surface exhibits high wettability towards water [16],[17].

As discussed above, different possible mechanisms have been suggested to explain the photoinduced hydrophilicity, however, no common mechanism has been proposed so far.

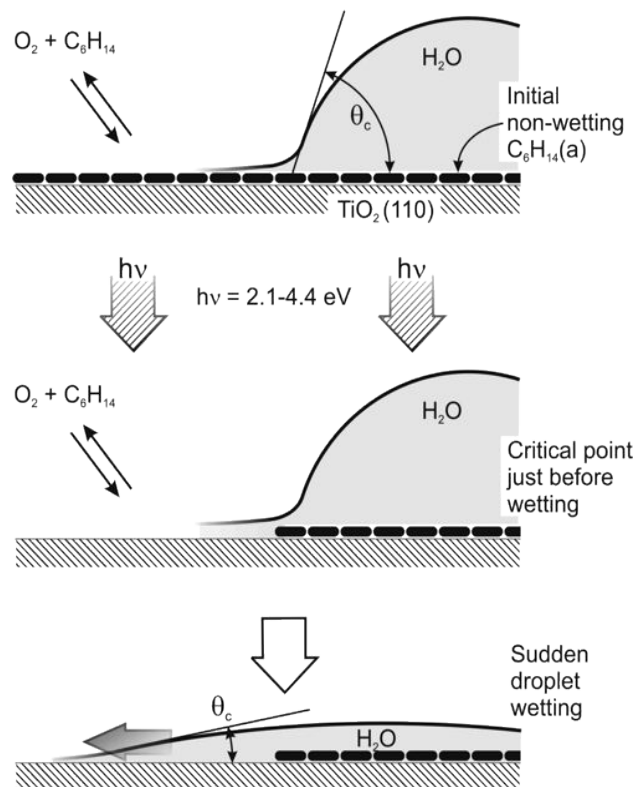
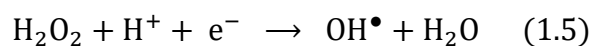
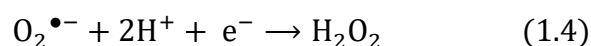
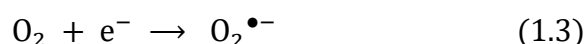
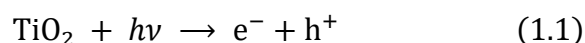


**Figure 1.5:** Mechanism of the UV induced photocatalytic process for hydrophilicity proposed by Yates et al. [16]. (Copyright 2005 American Chemical Society.)

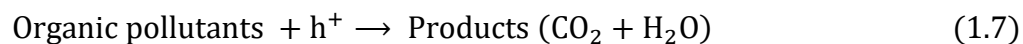
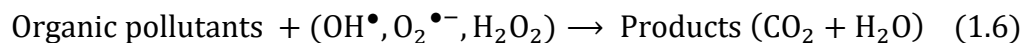
## 1.1.2 Photocatalytic Degradation of Organic Pollutants in Water

### 1.1.2.1 Mechanism and Reaction Pathways

Photocatalysis is one of the most effective approaches to degrade organic and inorganic pollutants in water or air. According to the mechanism illustrated in Figure 1, excitation of TiO<sub>2</sub> by UV light irradiation results in the promotion of an electron from the valence band to the conduction band leaving behind a hole in the valence band. The hole in the valence band may react with surface bound Ti–OH and/or adsorbed water to produce the hydroxyl radicals (•OH) [18], while molecular oxygen adsorbed at the TiO<sub>2</sub> surface is reduced by conduction band electrons to yield reactive oxygen species (ROS) such as the superoxide radical anion (O<sub>2</sub><sup>•-</sup>) and hydrogen peroxide (H<sub>2</sub>O<sub>2</sub>), as indicated in the following Eqs. (1.1)-(1.5) [19],[20]:



The hydroxyl radical (•OH) is a powerful oxidizing species which aggressively attacks a wide range of organic compounds [21]. However, it has been reported that the valence band hole potential is positive enough to oxidize not only the adsorbed water but also adsorbed organic pollutants via direct oxidation. Thus, it was suggested that two types of reaction pathways may be responsible for the oxidation of organic pollutants on the surface of TiO<sub>2</sub>. Eqs. (1.6)-(1.7) [22],[23]:

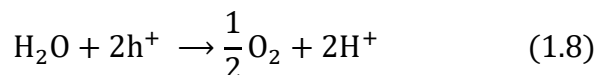
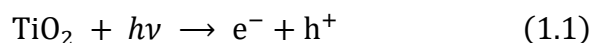


Although the photocatalytic degradation of organic pollutants proceeds to mineralized product, the photocatalytic processes, the surface species and the reaction intermediates are quite complicated and the degradation pathways are still not well understood.

### 1.1.3 Photocatalytic Hydrogen Production

#### 1.1.3.1 Photocatalytic Hydrogen Production from Water Splitting

The interest in photocatalytic hydrogen production has significantly increased in recent years in prospect to its environmental and economic potential [3],[24]. Fujishima and Honda discovered the photoinduced splitting of water into molecular hydrogen and molecular oxygen on a TiO<sub>2</sub> electrode under UV irradiation [25]. The overall photocatalytic water splitting reaction over a semiconductor photocatalyst (TiO<sub>2</sub>) is composed of two half-reactions, that is the hydrogen evolution reaction and the oxygen evolution reaction Eqs. (1.8)-(1.9). From the viewpoint of thermodynamics, the bottom of the conduction band must be located at a more negative potential than the reduction potential of H<sup>+</sup> to H<sub>2</sub> (0 V vs. NHE at pH 0), while the top of valence band must be positioned more positive than the oxidation potential of H<sub>2</sub>O to O<sub>2</sub> (1.23 V vs. NHE) [26].



The disadvantage of this system is that the recombination electrons and holes is very fast resulting in the reduction of the photocatalytic efficiency and also the backward reaction of H<sub>2</sub> and O<sub>2</sub> to form H<sub>2</sub>O is thermodynamically favorable.

#### 1.1.3.2 Photocatalytic Hydrogen Production from Oxidation of Organic Compounds

Hydrogen production from organic compound is one of the most effective ways to overcome the disadvantages mentioned above and to improve the efficiency of the photocatalytic reaction [27].

The principle of hydrogen production from the oxidation of organic compounds is based on the photo-induced charge transfer of valence band (VB) holes and conduction band (CB) electrons under oxygen free conditions. The photogenerated holes can either react with surface-bound H<sub>2</sub>O and/or hydroxyl ions producing •OH radicals or they might be transferred directly to adsorbed organic molecules. Simultaneously, the conduction band



electrons could provide a sufficient reduction ability to reduce protons towards molecular hydrogen [28],[29].

Loading of noble metal islands on the  $\text{TiO}_2$  surface is known to enhance the efficiency of the photocatalytic process thus serving as active sites for the hydrogen production, in which the trapped photogenerated electrons reduce protons ( $\text{H}^+$ ) to produce molecular  $\text{H}_2$  (Figure 1.6) [30],[31].

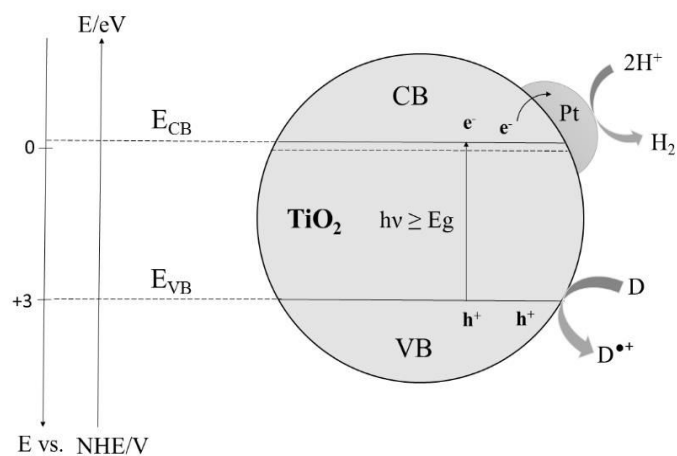


**Figure 1.6:** Mechanism of simultaneous hydrogen production with oxidation of organic compounds over platinized titanium dioxide.

Several molecules such as alcohols and carboxylic acids used as electron donors called “sacrificial systems” are usually required to increase the hole consumption and thereby reduce the electron/hole pair recombination resulting in a significantly enhanced photocatalytic hydrogen production [31],[32]. Although simultaneous hydrogen production with oxidation of organic pollutants has been extensively studied, however, only a few mechanistic investigation of this system have been addressed in the literature. It is generally acknowledged that the photocatalytic hydrogen formation can occur either directly by water splitting or initiated by photoreforming of organic compounds [33]. However, the primary events and the source of molecular hydrogen formed during the oxidation of organic molecules have not yet been clearly determined.

### 1.1.4 Novel Mechanistic Concepts of TiO<sub>2</sub> Photocatalysis

Based upon the respective mechanistic investigations, additional mechanistic concept in photocatalysis have been proposed recently to provide new insights into the mechanism of TiO<sub>2</sub> photocatalysis during UV irradiation.

#### 1.1.4.1 The Antenna Mechanism

It was reported that metal oxide nanoparticles tend to form 3D networks via a self-aggregation mechanism when suspended in aqueous solution [34]. The aggregation behaviour of the photocatalysts particles allows the transfer of charge carriers without much interference of interfacial trapping processes. The antenna mechanism is initiated once the light has reached one of the nanoparticles within the particle network [35]. The photogenerated electron hole pairs are likely to be transported throughout until arriving at a suitable trap site thus acting as an antenna system transferring the photon energy from the location of light absorption to the location of reaction [34]. Hence, the network will subsequently be available to promote redox processes anywhere within the structure thereby leading to an improved photocatalytic performance of the overall system (Figure 1.7).

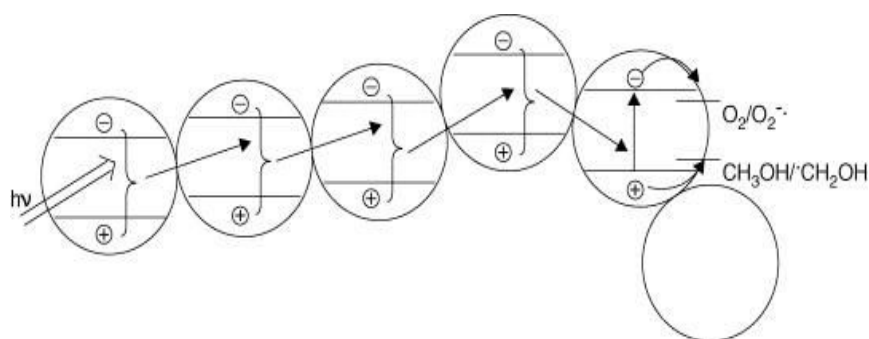


**Figure 1.7:** Scheme representing the Antenna Mechanism [35]. (Copyright 2003 The Royal Society of Chemistry.)

### 1.1.4.2 The Deaggregation Concept

Until recently, there was no clear concept concerning the interaction of UV light with such a particle network. Pagel et al. and Mendive et al. have observed another interesting aspect of these self-assembled network of nanoparticles during UV irradiation leading to increasing photonic efficiencies [36],[37].

To explain these observation as well as the effect of UV irradiation on the nanoparticle behavior, a new mechanistic concept called “deaggregation effect” has been proposed. The deaggregation model assumes that part of the absorbed light energy is used to break the bonds between the particles (most likely hydrogen bonds), thus producing additional surface area for the photocatalytic process resulting in an increased photonic efficiency (Figure 1.8). It has been earlier reported that the energetic requirements for deaggregation are met under laser-pulsed conditions [36]. The average photon energy deposited in the particle is around  $341 \text{ kJ mol}^{-1}$  per laser pulse at 351 nm. The inter-particle bond energy is only ca.  $30 \text{ kJ mol}^{-1}$ . The energy supplied for photolysis would therefore be sufficient for the supposed stepwise deaggregation of even larger agglomerates [35],[4].

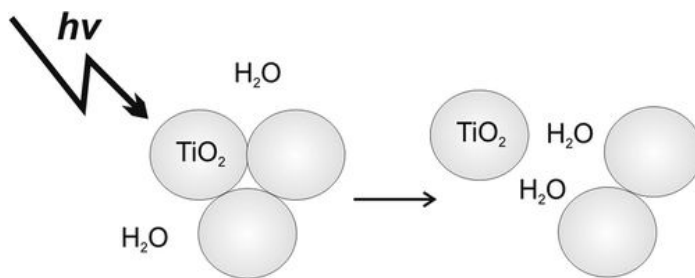


**Figure 1.8:** Scheme representing the Deaggregation Concept. [37] (Copyright 2011 American Chemical Society.)

## 1.2 Impact of H<sub>2</sub>O/D<sub>2</sub>O Adsorption on the Photocatalytic Mechanism

### 1.2.1 Effect of Water

Studies concerning the substrate adsorption/desorption on TiO<sub>2</sub> surfaces and the formation of reactive oxygen species (ROS) during photocatalytic processes are of substantial importance for the understanding of the mechanism of the underlying reaction pathways. In aerated aqueous solution, adsorbed species such as water, organic molecules and molecular oxygen together with the influence of pH are expected to affect the degradation pathway on TiO<sub>2</sub> surfaces [38],[39]. However, their overall influence has not yet been clearly determined. Several experimental and theoretical work has been carried out concerning the interaction of water adsorption at the TiO<sub>2</sub>/aqueous solution interface. Guan and coworkers reported a competitive reaction between the adsorption of water and organic compounds, which was dominated by the water adsorption because of the surface acidity [40]. In an another study, Medlin et al., revealed that the adsorption of water on the TiO<sub>2</sub> surface causes a change in the adsorbed structure of the substrate (formate) and that these transformations can have an important influence on elementary steps in the photocatalytic decomposition on TiO<sub>2</sub> [41].

Additionally, it has been pointed out previously that the adsorption of water on the TiO<sub>2</sub> surface plays a vital role in the formation of hydroxyl radicals. Cunningham et al. [42] and Robertson et al., [43] observed a primary kinetic solvent isotope effect of 3.3 for the destruction of organic compounds when the photocatalytic reactions were performed in pure D<sub>2</sub>O. They suggested that the reduced rate of photocatalytic decomposition in D<sub>2</sub>O was due to a lower oxidation potential compared to that of the hydroxyl radical.

Because of the complexity of the behaviour of adsorbed H<sub>2</sub>O and D<sub>2</sub>O and the interaction of water/D<sub>2</sub>O adsorption with different adsorbates at the TiO<sub>2</sub>/solution interface, detail of the underlying processes are still not well understood.

### 1.2.2 Physical and Chemical Properties of Water and Deuterium Oxide

According to the literature data [44],[45],[46],[47], the physicochemical properties of D<sub>2</sub>O are quite distinct compared to those of water as shown in Table 1.1.

**Table 1.1:** Physical and chemical properties of water and deuterium oxide

Color	H <sub>2</sub> O: Slight blue color D <sub>2</sub> O: Colorless
Molar mass	H <sub>2</sub> O: 18.015268 g mol <sup>-1</sup> D <sub>2</sub> O: 20.027508 g mol <sup>-1</sup>
Molar concentration (25 °C)	H <sub>2</sub> O: 55.345 mol L <sup>-1</sup> D <sub>2</sub> O: 55.142 mol L <sup>-1</sup>
Dissociation in liquid phase, ΔG (25 °C)	2H <sub>2</sub> O → H <sub>3</sub> O <sup>+</sup> + OH <sup>-</sup> 79.90 kJ mol <sup>-1</sup> 2D <sub>2</sub> O → D <sub>3</sub> O <sup>+</sup> + OD <sup>-</sup> 84.88 kJ mol <sup>-1</sup>
Dissociation constant (25 °C), K = [H <sub>3</sub> O <sup>+</sup> ][OH <sup>-</sup> ]/[H <sub>2</sub> O]	H <sub>2</sub> O: 1.82 × 10 <sup>-16</sup> mol <sup>-1</sup> D <sub>2</sub> O: 3.54 × 10 <sup>-17</sup> mol <sup>-1</sup>
Self-ionization of water (pK <sub>w</sub> )	H <sub>2</sub> O: 13.995 (25 °C) D <sub>2</sub> O: 14.87 (25 °C)
Dissociation constant (pK <sub>a</sub> and pK <sub>b</sub> ) pK <sub>a</sub> (D <sub>2</sub> O)=1.076 pK <sub>a</sub> (H <sub>2</sub> O)-0.41	pK <sub>a</sub> H <sub>2</sub> O = pK <sub>b</sub> H <sub>2</sub> O = 15.738 (25 °C) pK <sub>a</sub> D <sub>2</sub> O = pK <sub>b</sub> D <sub>2</sub> O = 16.610
Potential of hydrogen (pH) pD = pH+ 0.41	H <sub>2</sub> O: 6.9976 (pH) D <sub>2</sub> O: 7.43 (pD) HDO: 7.266 (pHD)
Enthalpy of formation, ΔH <sub>f</sub> (liquid)	H <sub>2</sub> O: -286.629 kJ mol <sup>-1</sup> (0 °C) D <sub>2</sub> O: -294.6 kJ mol <sup>-1</sup> (25 °C)
Bond dissociation energy (O-H), average at 0 K	H <sub>2</sub> O, (H-O-H), 458.9 kJ mol bond <sup>-1</sup> D <sub>2</sub> O, (D-O-D), 466.4 kJ mol bond <sup>-1</sup>

### 1.3 References

- [1] M.R. Hoffmann, S.T. Martin, W. Choi, D.W. Bahnemann, Environmental Applications of Semiconductor Photocatalysis, *Chem. Rev.* 95 (1995) 69–96. doi:10.1021/cr00033a004.
- [2] A.L. Linsebigler, G. Lu, J.T. Yates, Photocatalysis on TiO<sub>2</sub> Surfaces: Principles, Mechanisms, and Selected Results, (1995) 735–758.
- [3] Y. Ma, X. Wang, Y. Jia, X. Chen, H. Han, C. Li, Titanium Dioxide-Based Nanomaterials for Photocatalytic Fuel Generations, *Chem. Rev.* 114 (2014) 9987–10043. doi:10.1021/cr500008u.
- [4] J. Schneider, M. Matsuoka, M. Takeuchi, J. Zhang, Y. Horiuchi, M. Anpo, D.W. Bahnemann, Understanding TiO<sub>2</sub> Photocatalysis: Mechanisms and Materials, *Chem. Rev.* 114 (2014) 9919–9986. doi:10.1021/cr5001892.
- [5] L. Zhang, R. Dillert, D. Bahnemann, M. Vormoor, Photo-induced hydrophilicity and self-cleaning: models and reality, *Energy Environ. Sci.* 5 (2012) 7491. doi:10.1039/c2ee03390a.
- [6] S. Banerjee, D.D. Dionysiou, S.C. Pillai, Self-cleaning applications of TiO<sub>2</sub> by photo-induced hydrophilicity and photocatalysis, *Appl. Catal. B Environ.* 176–177 (2015) 396–428. doi:10.1016/j.apcatb.2015.03.058.
- [7] M. Takeuchi, K. Sakamoto, G. Martra, S. Coluccia, M. Anpo, Mechanism of photoinduced superhydrophilicity on the TiO<sub>2</sub> photocatalyst surface, *J. Phys. Chem. B.* 109 (2005) 15422–15428. doi:10.1021/jp058075i.
- [8] A. Eshaghi, A. Eshaghi, Investigation of superhydrophilic mechanism of titania nano layer thin film—Silica and indium oxide dopant effect, *Bull. Mater. Sci.* 35 (2012) 137–142. doi:10.1007/s12034-012-0277-7.
- [9] R. Wang, K. Hashimoto, A. Fujishima, M. Chikuni, E. Kojima, A. Kitamura, M. Shimohigoshi, T. Watanabe, Photogeneration of Highly Amphiphilic TiO<sub>2</sub> Surfaces, *Adv. Mater.* 10 (1998) 135–138. doi:10.1002/(SICI)1521-4095(199801)10:2<135::AID-ADMA135>3.3.CO;2-D.
- [10] R. Wang, K. Hashimoto, A. Fujishima, M. Chikuni, E. Kojima, A. Kitamura, M. Shimohigoshi, T. Watanabe, Light-induced amphiphilic surfaces, *Nature.* 388 (1997) 431–432. doi:10.1038/41233.
- [11] Z. Zhang, O. Bondarchuk, B.D. Kay, J.M. White, Z. Dohnálek, Imaging water dissociation on TiO<sub>2</sub> (110): Evidence for inequivalent geminate OH groups, *J. Phys. Chem. B.* 110 (2006) 21840–21845. doi:10.1021/jp063619h.
- [12] R. Fateh, R. Dillert, D. Bahnemann, Preparation and characterization of transparent hydrophilic photocatalytic TiO<sub>2</sub>/SiO<sub>2</sub> thin films on polycarbonate, *Langmuir.* 29 (2013) 3730–3739. doi:10.1021/la400191x.
- [13] N. Sakai, A. Fujishima, T. Watanabe, K. Hashimoto, Enhancement of the

- Photoinduced Hydrophilic Conversion Rate of TiO<sub>2</sub> Film Electrode Surfaces by Anodic Polarization, *J. Phys. Chem. B.* 105 (2001) 3023–3026. doi:10.1021/jp003212r.
- [14] N. Sakai, A. Fujishima, T. Watanabe, K. Hashimoto, Quantitative Evaluation of the Photoinduced Hydrophilic Conversion Properties of TiO<sub>2</sub> Thin Film Surfaces by the Reciprocal of Contact Angle, *J. Phys. Chem. B.* 107 (2003) 1028–1035. doi:10.1021/jp022105p.
- [15] H. Irie, K. Hashimoto, Photocatalytic Active Surfaces and Photo-Induced High Hydrophilicity/High Hydrophobicity, in: P. Boule, D.W. Bahnemann, P.K.J. Robertson (Eds.), *Environ. Photochem. Part II*, Springer-Verlag, Berlin/Heidelberg, 2005: pp. 425–450. doi:10.1007/b138190.
- [16] T. Zubkov, D. Stahl, T.L. Thompson, D. Panayotov, O. Diwald, J.T. Yates, Ultraviolet Light-Induced Hydrophilicity Effect on TiO<sub>2</sub>(110)(1×1). Dominant Role of the Photooxidation of Adsorbed Hydrocarbons Causing Wetting by Water Droplets, *J. Phys. Chem. B.* 109 (2005) 15454–15462. doi:10.1021/jp058101c.
- [17] M. Miyauchi, A. Nakajima, T. Watanabe, K. Hashimoto, Photocatalysis and photoinduced hydrophilicity of various metal oxide thin films, *Chem. Mater.* 14 (2002) 2812–2816. doi:10.1021/cm020076p.
- [18] J. Zhang, Y. Nosaka, Mechanism of the OH Radical Generation in Photocatalysis with TiO<sub>2</sub> of Different Crystalline Types, *J. Phys. Chem. C.* 118 (2014) 10824–10832. doi:10.1021/jp501214m.
- [19] T. Hirakawa, Y. Nosaka, Properties of O<sub>2</sub><sup>•-</sup> and OH<sup>•</sup> Formed in TiO<sub>2</sub> aqueous suspensions by photocatalytic reaction and the influence of H<sub>2</sub>O<sub>2</sub> and some ions, *Langmuir.* 18 (2002) 3247–3254. doi:10.1021/la015685a.
- [20] M.D. Hernández-Alonso, A.R. Almeida, J. a. Moulijn, G. Mul, Identification of the role of surface acidity in the deactivation of TiO<sub>2</sub> in the selective photo-oxidation of cyclohexane, *Catal. Today.* 143 (2009) 326–333. doi:10.1016/j.cattod.2008.09.025.
- [21] C. Minero, G. Mariella, V. Maurino, E. Pelizzetti, Photocatalytic Transformation of Organic Compounds in the Presence of Inorganic Anions. 1. Hydroxyl-Mediated and Direct Electron-Transfer Reactions of Phenol on a Titanium Dioxide–Fluoride System, *Langmuir.* 16 (2000) 2632–2641. doi:10.1021/la9903301.
- [22] M. Mohibbul, D. Bahnemann, M. Muneer, Photocatalytic Degradation of Organic Pollutants: Mechanisms and Kinetics, in: *Org. Pollut. Ten Years After Stock. Conv. - Environ. Anal. Updat.*, InTech, 2012. doi:10.5772/34522.
- [23] P.K.J. Robertson, D.W. Bahnemann, J.M.C. Robertson, F. Wood, Photocatalytic Detoxification of Water and Air, in: *Environ. Photochem. Part II*, Springer-Verlag, Berlin/Heidelberg, 2005: pp. 367–423. doi:10.1007/b138189.
- [24] A. a. Ismail, D.W. Bahnemann, Photochemical splitting of water for hydrogen production by photocatalysis: A review, *Sol. Energy Mater. Sol. Cells.* 128 (2014)

- 85–101. doi:10.1016/j.solmat.2014.04.037.
- [25] A. Fujishima, K. Honda, Electrochemical Photolysis of Water at a Semiconductor Electrode, *Nature*. 238 (1972) 37–38. doi:10.1038/238037a0.
- [26] M.J. Katz, S.C. Riha, N.C. Jeong, A.B.F. Martinson, O.K. Farha, J.T. Hupp, Toward solar fuels: Water splitting with sunlight and “rust”?, *Coord. Chem. Rev.* 256 (2012) 2521–2529. doi:10.1016/j.ccr.2012.06.017.
- [27] I. Rossetti, Hydrogen Production by Photoreforming of Renewable Substrates, *ISRN Chem. Eng.* 2012 (2012) 1–21. doi:10.5402/2012/964936.
- [28] S. Pasternak, Y. Paz, On the similarity and dissimilarity between photocatalytic water splitting and photocatalytic degradation of pollutants., *Chemphyschem.* 14 (2013) 2059–70. doi:10.1002/cphc.201300247.
- [29] J. Kim, D. Monllor-Satoca, W. Choi, Simultaneous production of hydrogen with the degradation of organic pollutants using TiO<sub>2</sub> photocatalyst modified with dual surface components, *Energy Environ. Sci.* 5 (2012) 7647. doi:10.1039/c2ee21310a.
- [30] T. a. Kandiel, R. Dillert, L. Robben, D.W. Bahnemann, Photonic efficiency and mechanism of photocatalytic molecular hydrogen production over platinumized titanium dioxide from aqueous methanol solutions, *Catal. Today.* 161 (2011) 196–201. doi:10.1016/j.cattod.2010.08.012.
- [31] X. Chen, S. Shen, L. Guo, S.S. Mao, Semiconductor-based Photocatalytic Hydrogen Generation, *Chem. Rev.* 110 (2010) 6503–6570. doi:10.1021/cr1001645.
- [32] N. Strataki, V. Bekiari, D.I. Kondarides, P. Lianos, Hydrogen production by photocatalytic alcohol reforming employing highly efficient nanocrystalline titania films, *Appl. Catal. B Environ.* 77 (2007) 184–189. doi:10.1016/j.apcatb.2007.07.015.
- [33] H. Lu, J. Zhao, L. Li, L. Gong, J. Zheng, L. Zhang, Z. Wang, J. Zhang, Z. Zhu, Selective oxidation of sacrificial ethanol over TiO<sub>2</sub>-based photocatalysts during water splitting, *Energy Environ. Sci.* 4 (2011) 3384–3388. doi:10.1039/c1ee01476e.
- [34] C. Wang, C. Böttcher, D.W. Bahnemann, J.K. Dohrmann, A comparative study of nanometer sized Fe(III)-doped TiO<sub>2</sub> photocatalysts: synthesis, characterization and activity, *J. Mater. Chem.* 13 (2003) 2322–2329. doi:10.1039/B303716A.
- [35] C. Wang, R. Pagel, J.K. Dohrmann, D.W. Bahnemann, Antenna mechanism and deaggregation concept: novel mechanistic principles for photocatalysis, *Comptes Rendus Chim.* 9 (2006) 761–773. doi:10.1016/j.crci.2005.02.053.
- [36] C.Y. Wang, R. Pagel, D.W. Bahnemann, J.K. Dohrmann, Quantum yield of formaldehyde formation in the presence of colloidal TiO<sub>2</sub>-based photocatalysts: Effect of intermittent illumination, platinization, and deoxygenation, *J. Phys. Chem. B.* 108 (2004) 14082–14092. doi:10.1021/jp048046s.



- [37] C.B. Mendive, D. Hansmann, T. Bredow, D. Bahnemann, New insights into the mechanism of TiO<sub>2</sub> photocatalysis: Thermal processes beyond the electron-hole creation, *J. Phys. Chem. C*. 115 (2011) 19676–19685. doi:10.1021/jp112243q.
- [38] A.Y. Nosaka, T. Fujiwara, H. Yagi, H. Akutsu, Y. Nosaka, Characteristics of water adsorbed on TiO<sub>2</sub> photocatalytic systems with increasing temperature as studied by solid-state <sup>1</sup>H NMR Spectroscopy, *J. Phys. Chem. B*. 108 (2004) 9121–9125. doi:10.1021/jp037297i.
- [39] D. Friedmann, C. Mendive, D. Bahnemann, TiO<sub>2</sub> for water treatment: Parameters affecting the kinetics and mechanisms of photocatalysis, *Appl. Catal. B Environ.* 99 (2010) 398–406. doi:10.1016/j.apcatb.2010.05.014.
- [40] K. Guan, Relationship between photocatalytic activity, hydrophilicity and self-cleaning effect of TiO<sub>2</sub>/SiO<sub>2</sub> films, *Surf. Coatings Technol.* 191 (2005) 155–160. doi:10.1016/j.surfcoat.2004.02.022.
- [41] K.L. Miller, C.W. Lee, J.L. Falconer, J.W. Medlin, Effect of water on formic acid photocatalytic decomposition on TiO<sub>2</sub> and Pt/TiO<sub>2</sub>, *J. Catal.* 275 (2010) 294–299. doi:10.1016/j.jcat.2010.08.011.
- [42] J. Cunningham, S. Srijaranai, Isotope-effect evidence for hydroxyl radical involvement in alcohol photo-oxidation sensitized by TiO<sub>2</sub> in aqueous suspension, *J. Photochem. Photobiol. A Chem.* 43 (1988) 329–335. doi:10.1016/1010-6030(88)80029-7.
- [43] P.K.J. Robertson, D.W. Bahnemann, L. a. Lawton, E. Bellu, A study of the kinetic solvent isotope effect on the destruction of microcystin-LR and geosmin using TiO<sub>2</sub> photocatalysis, *Appl. Catal. B Environ.* 108–109 (2011) 1–5. doi:10.1016/j.apcatb.2011.07.019.
- [44] N. N. Greenwood, A. Earnshaw, *Chemistry of the Elements*, Second Edi, 11<sup>th</sup> November 1997, Butterworth Heinemann, Oxford, 1997.
- [45] A. Krężel, W. Bal, A formula for correlating p*K*<sub>a</sub> values determined in D<sub>2</sub>O and H<sub>2</sub>O, *J. Inorg. Biochem.* 98 (2004) 161–166. doi:10.1016/j.jinorgbio.2003.10.001.
- [46] P.K. Glasoe, F.A. Long, Use of glass electrodes to measure acidities in deuterium oxide, *J. Phys. Chem.* 64 (1960) 188–190. doi:10.1017/CBO9781107415324.004.
- [47] O. V. Boyarkin, M.A. Koshelev, O. Aseev, P. Maksyutenko, T.R. Rizzo, N.F. Zobov, L. Lodi, J. Tennyson, O.L. Polyansky, Accurate bond dissociation energy of water determined by triple-resonance vibrational spectroscopy and ab initio calculations, *Chem. Phys. Lett.* 568–569 (2013) 14–20. doi:10.1016/j.cplett.2013.03.007.



## Chapter 2

### ***In situ* ATR-FTIR study of H<sub>2</sub>O and D<sub>2</sub>O adsorption on TiO<sub>2</sub> under UV irradiation**

Hamza Belhadj,<sup>a</sup> Amer Hakki,<sup>a</sup> Peter K. J. Robertson<sup>\*b</sup> and Detlef W. Bahnemann<sup>\*ac</sup>

<sup>a</sup>Institut für Technische Chemie, Leibniz Universität Hannover, Callinstraße 3, D-30167 Hannover, Germany

<sup>b</sup>Centre for the Theory and Application of Catalysis (CenTACat), School of Chemistry and Chemical Engineering, Queen's University Belfast, Stranmillis Road, Belfast, BT9 5AG, UK.

E-mail: p.robertson@qub.ac.uk

<sup>c</sup>Laboratory "Photoactive Nanocomposite Materials", Saint-Petersburg State University, Ulyanovskaya str. 1, Peterhof, Saint-Petersburg, 198504 Russia.

E-mail: bahnemann@iftc.uni-hannover.de

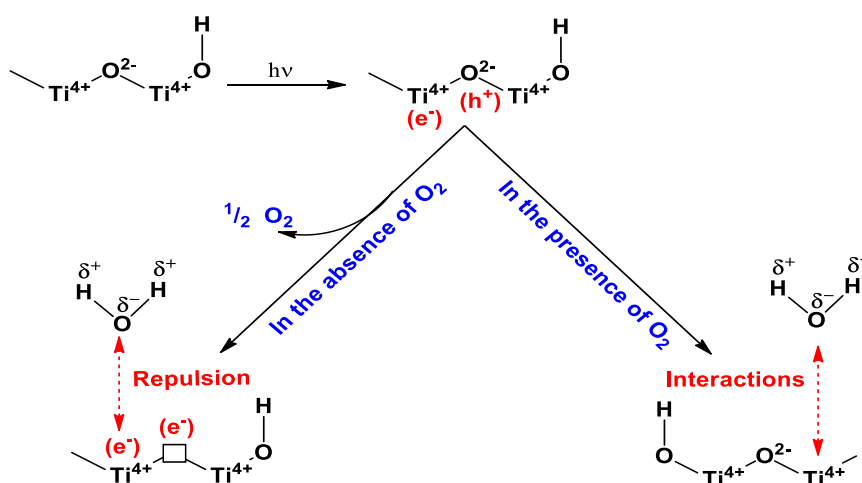
Published in Physical Chemistry Chemical Physics, 2015, 17, 22940-22946.

DOI: 10.1039/c5cp03947a

## 2. *In situ* ATR-FTIR study of H<sub>2</sub>O and D<sub>2</sub>O adsorption on TiO<sub>2</sub> under UV irradiation

### 2.1 Abstract

The adsorption of water and deuterium oxide on TiO<sub>2</sub> surfaces was investigated in the dark as well as under UV(A) irradiation using *in situ* ATR-FTIR spectroscopy under oxygen and oxygen free conditions. Adsorption of H<sub>2</sub>O-D<sub>2</sub>O mixtures revealed an isotopic exchange reaction occurring onto the surface of TiO<sub>2</sub> in the dark. Under UV(A) irradiation, the amount of both OH and OD groups was found to be increased by the presence of molecular oxygen. Furthermore, the photocatalytic formation of hydroperoxide under oxygenated condition has been recorded utilizing Attenuated Total Reflection Fourier Transformed Infrared (ATR-FTIR) spectroscopy which appeared as new band at 3483 cm<sup>-1</sup>. Different possible mechanisms are discussed in terms of the source of hydroxyl groups formed and/or hydration water on the TiO<sub>2</sub> surface for the photocatalytic reaction and photoinduced hydrophilicity.



## 2.2 Introduction

Photocatalytic reactions at the surface of titanium dioxide ( $\text{TiO}_2$ ) have been attracting much attention, in view of their practical applications including environmental aspects such as water purification, self-cleaning and antifogging.<sup>1,2</sup> UV(A) irradiation of the  $\text{TiO}_2$  surface induces photocatalytic reactions and photoinduced hydrophilicity.<sup>3</sup> In general, electrons and holes generated after the band gap excitation can respectively, reduce and oxidize electron acceptor and electron donor species which are already adsorbed on the  $\text{TiO}_2$  surface. The importance of the photogenerated active oxygen species, such as hydroxyl radicals ( $\bullet\text{OH}$ ), superoxide radicals ( $\text{O}_2^{\bullet-}$ ) and hydrogen peroxide ( $\text{H}_2\text{O}_2$ ) in photocatalytic applications has been extensively studied.<sup>4,5</sup> The mechanism of hydroxyl radical formation has been suggested as a result of the oxidation of water,<sup>6</sup> while hydrogen peroxide can be formed by both reduction and oxidation processes, such as dimerization of hydroxyl radicals, as well as disproportionation and reduction of superoxide radical anions.<sup>5</sup> On the other hand, the photoinduced hydrophilicity is reported as a result of increasing the number of hydroxyl groups on the  $\text{TiO}_2$  surface upon irradiation.<sup>7</sup> During these processes, the surface OH groups on the  $\text{TiO}_2$  surface have been assumed to play important roles in both photocatalytic reactions and photoinduced hydrophilicity.<sup>8</sup> Adsorbed species such as water and molecular oxygen, however are expected to affect the hydroxyl group behaviour on the  $\text{TiO}_2$  surface,<sup>9</sup> but their influences have to date not yet been clearly determined.

Several mechanisms regarding the interaction of UV(A) light and hydroxyl group formation on  $\text{TiO}_2$  have been proposed by different research groups.<sup>8</sup> One of the proposed mechanisms for the photoinduced hydrophilicity is based on the formation of oxygen vacancies and the reconstruction of Ti-OH bonds caused by the photogenerated electron-hole pairs.<sup>7,10</sup> Another mechanism has been suggested to involve the photocatalytic removal of organic contaminants from the surface.<sup>11</sup> Hashimoto and co-workers have followed the idea of photogenerated surface OH groups to introduce their surface reconstruction model of hydroxyl groups as the mechanism for the hydrophilic conversion.<sup>12,13</sup> Another mechanism was proposed by Yates *et al.*, who demonstrated that only under UV light illumination the decomposition of organic contaminants can take place leading to the creation of superhydrophilic surfaces.<sup>11</sup> In another studies, Munuera

*et al.* and Anpo *et al.* have reported that H<sub>2</sub>O desorbs from the TiO<sub>2</sub> surface during UV light irradiation, i.e., photodesorption of H<sub>2</sub>O, due to the heating effect of the light source.<sup>14,15</sup> Recently, special attention has been focused on the particle network before and after irradiation and how it changes during illumination.<sup>16,17</sup> Wang *et al.* reported that the metal oxide nanoparticles tend to form 3D networks via a self-aggregation mechanism when suspended in aqueous solution.<sup>16</sup> Some investigations indicated that UV light activation of TiO<sub>2</sub> leads to an increase in the surface area due to de-aggregation of particles agglomerates which in turn enhances the photonic efficiency.<sup>17,18</sup> The behaviours of the water adsorption and the associated hydroxyl groups during irradiation are, however, still not well understood. The relative roles of the active oxygen and the hydroxyl groups for the photocatalytic process and for the photoinduced hydrophilicity, which have been under debate for a long time, still need to be investigated in detail. From this point of view, one of the most important issues of the current investigations concerning photocatalytic reactions and photoinduced hydrophilicity is to understand the fundamental process of water adsorption and the source of hydroxyl groups formed on TiO<sub>2</sub> surface under UV irradiation.

Herein, a detailed investigation of the H<sub>2</sub>O and/or D<sub>2</sub>O adsorption on the TiO<sub>2</sub> surface is reported using Attenuated Total Reflection Fourier Transformed Infrared spectroscopy (ATR-FTIR). Qualitative and quantitative evaluations of the D<sub>2</sub>O effect and the isotopic exchange on the TiO<sub>2</sub> surface are presented. This work focuses on the analysis of the behaviours of OH and OD stretching groups before and after UV irradiation considering the role of molecular oxygen to provide new insights into the mechanism of photoinduced hydrophilicity during UV illumination.

## 2.3 Experimental

### 2.3.1 Materials

The photocatalyst, titanium dioxide PC-500 (Cristal Global) consisted of 100% pure anatase with a specific BET-surface area of 340 m<sup>2</sup> g<sup>-1</sup> and a primary particle size of 5-10 nm. Deuterium oxide (D<sub>2</sub>O) (99.9 atom % D) was purchased from Sigma Aldrich. Deionized water (H<sub>2</sub>O) was supplied from a Millipore Mill-Q system with a resistivity equal to 18.2 Ω cm at 25 °C.

## 2.3.2 ATR-FTIR Spectroscopic Measurements

### 2.3.2.1 Preparation of TiO<sub>2</sub> Films on the ATR-FTIR Crystal

An aqueous suspension of TiO<sub>2</sub> at a concentration of 5.75 g l<sup>-1</sup> was initially prepared and sonicated for 15 min in an ultrasonic cleaning bath. An aliquot of 400 μL of the TiO<sub>2</sub> suspension was placed on the surface of the ZnSe ATR crystal. This small volume was simply spread by balancing the unit manually. The suspension was then directly allowed to evaporate to dryness by storing the crystal in a semi-opened desiccator at room temperature. Prior to deposition of the TiO<sub>2</sub> films, the ZnSe surface (area = 6.8 mm×72 mm) was cleaned by polishing with 1 mm diamond paste (Metadi II, polishing grade) and rinsed with methanol and deionised water. The coverage of the final dry layer of particles obtained was 2.3 g m<sup>-2</sup> and the layer appeared homogeneous under visual inspection. In the original preparation by Hug *et al.*, AFM measurements of layers with coverage of 2.3 g m<sup>-2</sup> yielded a thickness of 1-3 μm.<sup>19,20</sup> The final resulting layers of particles remained stable over the entire course of the experiment. Thus, it can be assumed that the effective path lengths at all wavelengths remained unchanged.

### 2.3.2.2 ATR-FTIR Measurement

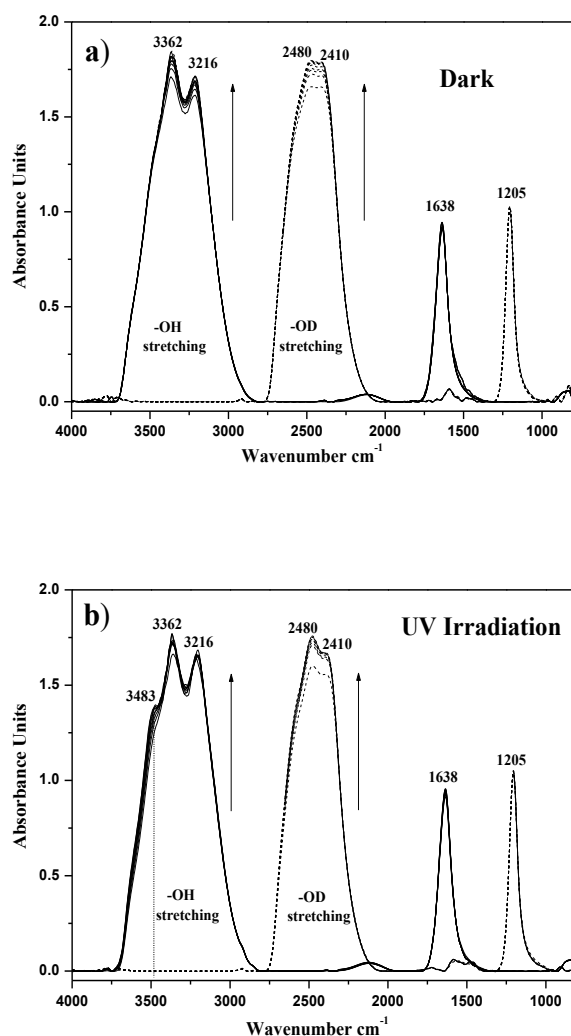
The ATR-FTIR spectra of the TiO<sub>2</sub> samples were monitored by a FTIR spectrometer (IFS 66 BRUKER) equipped with an internal reflection element 45° ZnSe crystal and a deuterated triglycine sulfate (DTGS) detector. The interferometer and the infrared light path in the spectrometer were constantly purged with Argon to avoid H<sub>2</sub>O and CO<sub>2</sub> contamination. The spectra were recorded with 350 scans at 4 cm<sup>-1</sup> resolution and analysed using OPUS version 6.5 software. The background was subtracted and baseline correction was made in order to eliminate minor fluctuations due to instrumental instability. Irradiation of samples with UV(A) light was carried out using an LED lamp (Model LED-Driver, THORLABS) emitting UV light (365 nm). The distance from the UV lamp to the surface of the test solution was kept at 30 cm on which the intensity of UV(A) light was of 1.0 mWcm<sup>-2</sup> as measured by an UV radiometer (Dr. Höhle GmbH, Martinsried, Germany). Prior to starting the irradiation experiments, spectra of adsorption of H<sub>2</sub>O and D<sub>2</sub>O on the TiO<sub>2</sub> were monitored in the dark. When the last spectrum of each experiment had been recorded, the UV(A) lamp was turned on and another sequence of spectra was

recorded. These two groups of spectra were considered as the blank reference spectra in the dark and under UV(A) illumination, respectively.

## 2.4 Results

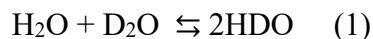
Fig. 1a shows the time evolution of the spectra of adsorbed H<sub>2</sub>O and D<sub>2</sub>O on TiO<sub>2</sub> in the dark. The signal of the adsorbed water on TiO<sub>2</sub> with maxima at 3362, 3216, and 1638 cm<sup>-1</sup> can be clearly seen. As is well known, the adsorption of H<sub>2</sub>O is represented by strong IR absorbances of O-H stretching in the region between 3200 and 3550 cm<sup>-1</sup> and  $\delta$  (H-O-H) bending at 1638 cm<sup>-1</sup> which is assigned to undissociated water molecules. When D<sub>2</sub>O was used instead of H<sub>2</sub>O, the results showed that all bands of adsorbed water on TiO<sub>2</sub> surface were shifted to lower frequency with exchanging H for D. Additionally, an increase in the intensities of OH and OD stretching has been observed by increasing the adsorption time in the dark, which can be explained by increased adsorption of water molecules as well as of deuterium oxide on the TiO<sub>2</sub> surface until attaining an equilibrium. It can be clearly seen from Fig. 1b that subsequent illumination with UV(A) light in the presence of O<sub>2</sub>, results in the formation of a shoulder in the FTIR spectrum of the adsorbed H<sub>2</sub>O at 3483 cm<sup>-1</sup> as well as an increase in the bands at 2480 cm<sup>-1</sup> in the case of D<sub>2</sub>O (Fig. 1b). The shoulder formed around 3483 cm<sup>-1</sup> can be attributed to the photocatalytically generated hydroperoxide. This was confirmed by recording the spectrum of H<sub>2</sub>O<sub>2</sub> added to the water-TiO<sub>2</sub> system in the dark in which a similar band (at 3483 cm<sup>-1</sup>) has been detected (Fig. S1, in ESI). Furthermore, no formation of such band around 3483 cm<sup>-1</sup> was observed in the absence of O<sub>2</sub> (Fig. S2, in ESI).





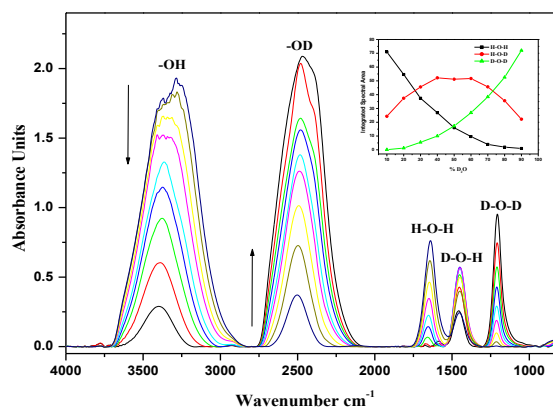
**Fig. 1** Time evolution of the ATR-FTIR spectra of adsorbed pure H<sub>2</sub>O (solid lines) and D<sub>2</sub>O (dashed lines) in the presence of O<sub>2</sub> on TiO<sub>2</sub> (a) in the dark for 4 h, (b) under 8 h of UV(A) illumination.

Fig. 2 shows the spectra of D<sub>2</sub>O-H<sub>2</sub>O mixtures adsorbed on TiO<sub>2</sub> in the dark. It is obvious from these spectra that the intensity of the band in the OH-stretching region decreased gradually with increasing dosage of D<sub>2</sub>O. Interestingly, the peak of the isotopologue HDO bending band centred at 1450  $\text{cm}^{-1}$  was formed and increased by increasing the concentration of H<sub>2</sub>O in D<sub>2</sub>O until it approached equimolar proportions (Fig.2 insert). This peak then decreased again with further increases in the amounts of H<sub>2</sub>O in D<sub>2</sub>O. The mixture of H<sub>2</sub>O and D<sub>2</sub>O reacted and equilibrated *via* transfer by self-dissociation and recombination to form HDO.<sup>21</sup>



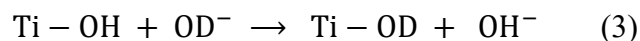
The equilibrium constant  $K$  of this reaction is given by

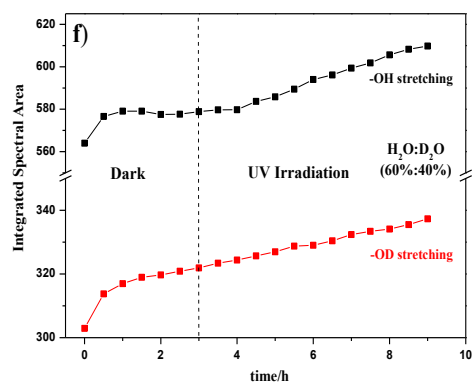
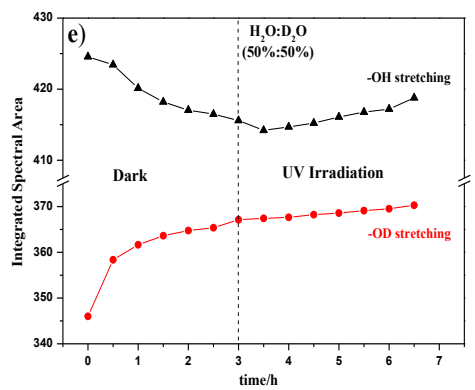
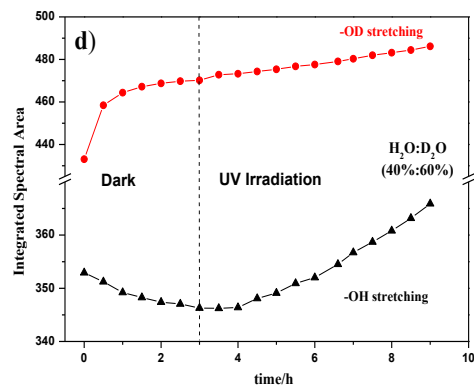
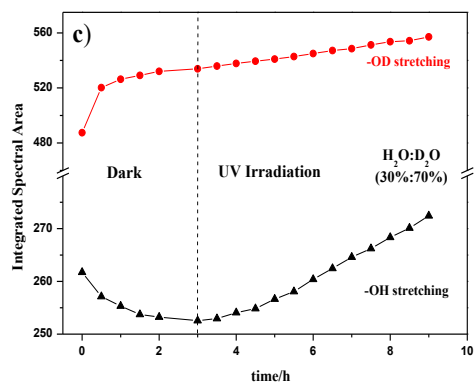
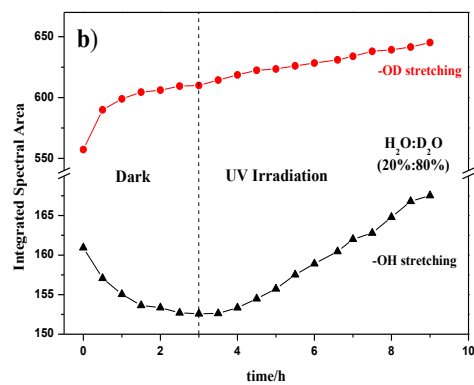
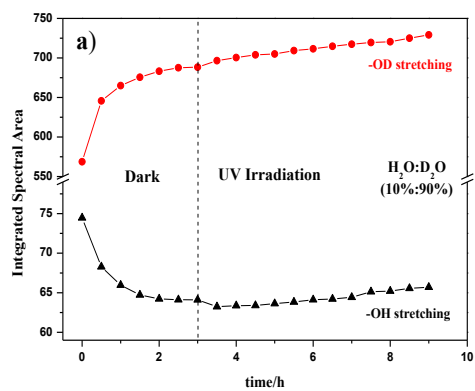
$$K = [\text{HOD}]^2/[\text{H}_2\text{O}][\text{D}_2\text{O}] \quad K_{eq} = 3.86 \text{ at } 25^\circ\text{C} \quad (2)$$



**Fig. 2** ATR-FTIR spectra of  $\text{D}_2\text{O}$ - $\text{H}_2\text{O}$  mixtures with different concentrations adsorbed on  $\text{TiO}_2$  in the dark. Inset: evolution of the intensity of the integrated spectral areas of  $\text{H}_2\text{O}$ ,  $\text{HOD}$  and  $\text{D}_2\text{O}$  bending modes.

To investigate the effect of  $\text{D}_2\text{O}$  on the hydroxyl group behaviour during UV irradiation, a series of experiments for water adsorption with different ratios of  $\text{D}_2\text{O}$  were performed under irradiation in the presence of oxygen. Fig. 3 shows the time evolution of the intensities of the integrated spectral areas of OH and OD stretching groups that are formed on the surface of  $\text{TiO}_2$  before and after UV irradiation. As can be clearly seen, in the dark, at low concentrations of  $\text{H}_2\text{O}$  ( $\text{H}_2\text{O}\% < \text{D}_2\text{O}\%$ ), a strong decrease in the amount of OH stretching was observed especially in the first hour. Simultaneously, the amount of OD stretching groups adsorbed on  $\text{TiO}_2$  increased during this period until the system reached equilibrium. In contrast, at higher concentrations of  $\text{H}_2\text{O}$  ( $\text{H}_2\text{O}\% > \text{D}_2\text{O}\%$ ), both OH and OD stretching bands increased. Interestingly, at an equimolar mixture of 50%  $\text{H}_2\text{O}$  and  $\text{D}_2\text{O}$ , a decrease in intensity of OH stretching with a simultaneous increase in the OD stretching could be observed in the dark. From these results we suggest that the deuteride ion in the dark shows a stronger adsorption ability than hydroxyl ions at the surface of  $\text{TiO}_2$ . Thus, the deuteride ions could lead to isotopic exchange by replacing hydroxyl groups adsorbed on the  $\text{TiO}_2$  surface (reaction 3):





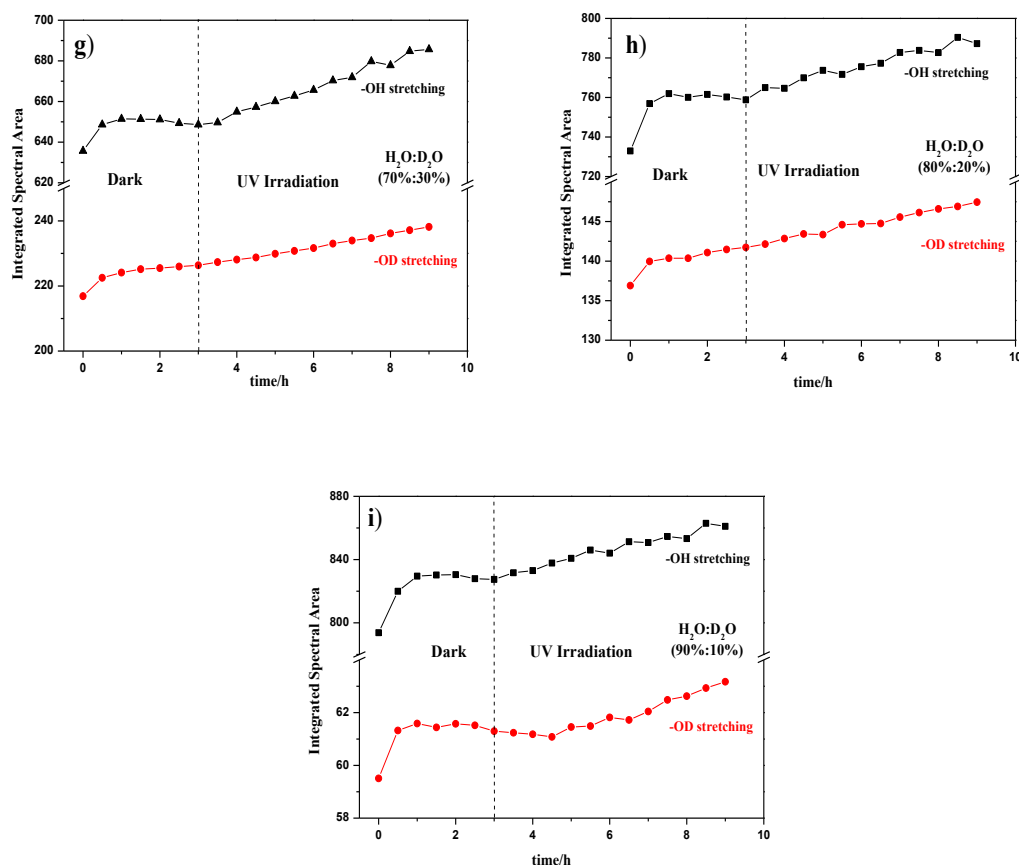


**Fig. 3** Time evolution of the intensity of the integrated spectral areas of the OH and OD stretching groups before and after UV(A) irradiation with different ratios (H<sub>2</sub>O:D<sub>2</sub>O).

It is worth noting that the time required to reach equilibrium for all experiments was nearly constant, i.e., it took almost 3 hours to approach isotopic exchange equilibrium. Furthermore, this evaluation of OD groups could be associated with the better exchange of the isolated Ti-OH species on TiO<sub>2</sub> at higher concentrations than at lower concentrations of D<sub>2</sub>O. Interestingly, upon UV(A) irradiation, an increase in the intensity of the OH stretching could be observed almost immediately as well as an increasing intensity of the OD stretching band, *i.e.*, Fig. S3 (see ESI). These results, however can be largely attributed to either an increase of the amount of OH and OD groups by the formation of new OH and OD groups on the surface or by increasing the amount of H<sub>2</sub>O and D<sub>2</sub>O molecules chemisorbed on the TiO<sub>2</sub> surface.

To determine the effect of molecular oxygen on the behaviour of the H<sub>2</sub>O and D<sub>2</sub>O adsorption on the TiO<sub>2</sub> surface, the solution was saturated and constantly purged with different types of gases, *i.e.*, oxygen, nitrogen, and argon during the ATR-FTIR measurements. As shown in Fig. 4, the integrated intensity of the OH and OD stretching group increased significantly upon illumination in the presence of molecular O<sub>2</sub>. By contrast, when the sample was purged with nitrogen or argon, no increase in the OH and/or OD stretching group was observed. A similar isotopic exchange behaviour, however, was observed during the dark period.

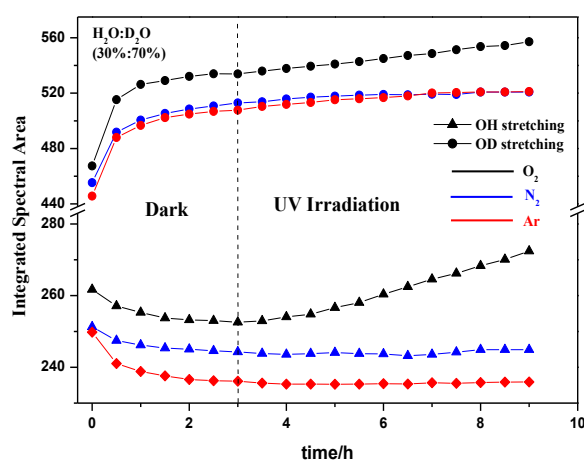


**Fig. 4** Evolution of the intensity of the integrated spectral areas of OH and OD stretching groups before and after UV irradiation: Effect of dissolved O<sub>2</sub>, N<sub>2</sub> and Ar on the adsorption of H<sub>2</sub>O-D<sub>2</sub>O on the TiO<sub>2</sub> surface.

The time evolution of the intensity of the integrated spectral areas of the OH and OD stretching groups before and after UV irradiation at prolonged time periods are shown in Fig. 5. Again as described above under dark conditions, the isotopic exchanges inevitably took place on the TiO<sub>2</sub> surface. When the system was subsequently stored again in the dark (after the UV illumination was turned off), however, no more isotopic exchange behaviour was detected and the amount of OH and OD groups remained steady during this period. Additionally, when the system was illuminated again, the amount of OH and OD groups immediately increased.

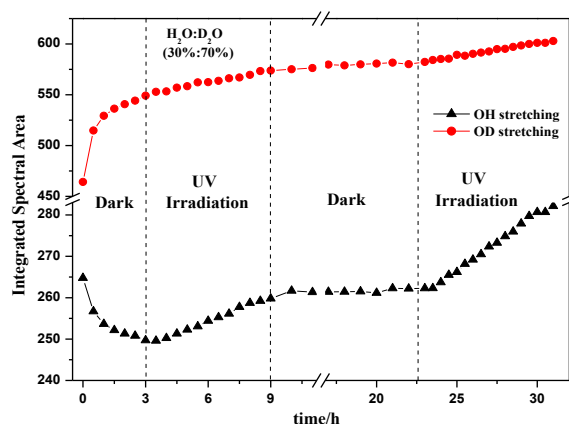


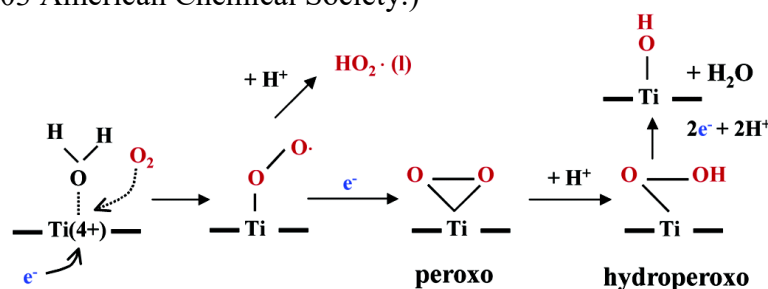
**Fig. 5** Time evolution of the intensity of the integrated spectral areas of OH and OD stretching groups before and after UV(A) irradiation with prolonged time (Alternately).

## 2.5 Discussion

When the  $\text{TiO}_2$  surface was illuminated with UV light, electron and hole pairs were generated, and they, respectively, reduced and oxidized adsorbates on the surface. As can be seen from the ATR-FTIR spectra (Fig. 1b), a clear shoulder appears at  $3483\text{ cm}^{-1}$  upon irradiation of the system by UV(A) in the presence of molecular oxygen ( $\text{O}_2$ ). This peak can most likely be assigned to a Ti-OOH vibration as has been confirmed from the spectrum of  $\text{H}_2\text{O}_2$  added to the water- $\text{TiO}_2$  system in the dark in which a similar band (at  $3483\text{ cm}^{-1}$ ) has been detected as shown in Fig. S1 (see ESI). The formation of this adsorbed hydroperoxy species only in the presence of ( $\text{O}_2$ ) can be considered as evidence that it is resulting from the reduction of molecular oxygen adsorbed at the  $\text{TiO}_2$  surface by the photogenerated electrons rather than from the oxidation of water by the holes. These results are in agreement with Nakamura *et al.*, who revealed and assigned O-O stretching of a surface peroxo species to identify Ti-OOH as a primary intermediate from the  $\text{O}_2$  photoreduction.<sup>22</sup> Robertson *et al.*, however, reported that the formation of hydroxyl radicals for the photocatalytic process could be preferable through the water oxidation at the valence band rather than through the oxygen reduction at the conduction band.<sup>6,23</sup> Based on the identification of these intermediates, a mechanism for the photocatalytic formation of hydroperoxide has previously been proposed (Scheme 1).<sup>22,24</sup> In this mechanism, the photogenerated conduction band electrons reduce  $\text{Ti}^{4+}$  at the surface that

adsorbs  $\text{H}_2\text{O}$ , then molecular oxygen attacks immediately to form superperoxo  $\text{TiOO}\cdot$ . This superperoxo is reduced to peroxo  $\text{Ti}(\text{O}_2)$ , which is equivalent to the hydroperoxide  $\text{Ti-OOH}$  when it is protonated.

**Scheme 1** Proposed mechanism for the photocatalytic formation of hydroperoxides. (Copyright 2003 American Chemical Society.)



Furthermore, an increase in the intensities of the OH and OD stretching bands is observed after illumination which may be assigned either to the stretching modes of Ti-OH formed upon illumination or to the OH stretching vibration of adsorbed water molecules which in turn increases the hydrophilicity of the  $\text{TiO}_2$  surface. Hashimoto *et al.* reported that during UV irradiation not only the photocatalytic reactions take place on the surface but also the photoinduced hydrophilicity resulting from the separation and diffusion of photogenerated electrons and holes occurring on the surface of  $\text{TiO}_2$ .<sup>3</sup> As shown in Fig. 3, at low concentrations of  $\text{H}_2\text{O}$  ( $\text{H}_2\text{O}\% < \text{D}_2\text{O}\%$ ), the reduction of the OH band with the simultaneous increase in the OD stretching band in the dark revealed that the deuteride ions have a stronger adsorption affinity than the hydroxyl ions. Furthermore, it can be clearly observed that the photoinduced hydrophilicity of the  $\text{TiO}_2$  surfaces which was explained by an increase in the amount of hydroxyl groups is readily induced upon UV light irradiation in the presence of  $\text{O}_2$ . These results can be largely attributed to either an increase in the number of surface OH groups or to an increased adsorption of water molecules on the  $\text{TiO}_2$  surface.

Several mechanisms suggested that the photoinduced holes play a crucial role in the photoinduced hydrophilicity conversion. It was thus proposed that the photogenerated holes produced in the bulk of  $\text{TiO}_2$  diffuse to the surface where they are trapped at lattice oxygen sites. The trapped holes are consumed by reaction with the  $\text{TiO}_2$  itself creating oxygen vacancies,<sup>25</sup> or by breaking the bond between the lattice titanium and oxygen ions upon the coordination of water molecules at the titanium site.<sup>10</sup> Subsequently the water

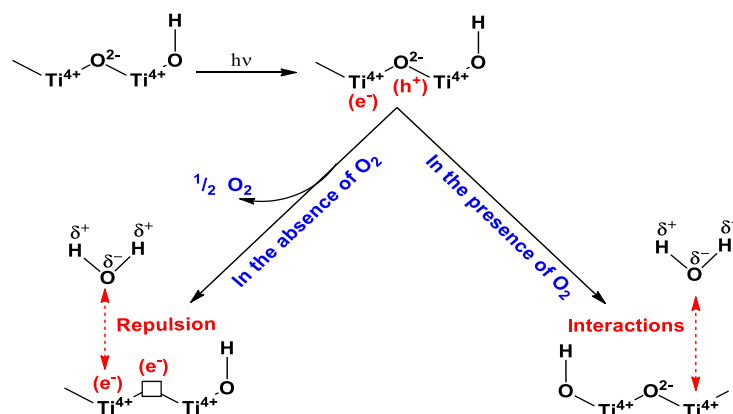
molecule dissociates in an oxygen vacancy or releases proton for charge compensation to produce new OH groups. As shown in Fig. 5, however, an isotopic exchange between deuteride ions and hydroxyl groups takes place on the TiO<sub>2</sub> surface in the dark according to eqn 3. After 6 h of irradiation even during a prolonged time in the dark, however, no isotopic exchange was detected between hydroxyl groups and deuteride ions. From this result we suggest that the increase of OH and OD stretching groups under irradiation is most likely caused by adsorption of H<sub>2</sub>O and D<sub>2</sub>O molecules, respectively, and not by the generation of hydroxyl groups. There have been several reports supporting our suggestion that water molecules strongly adsorb onto the TiO<sub>2</sub> surface under UV illumination. Nosaka *et al.* reported that the increase in the amount of adsorbed water on the TiO<sub>2</sub> surface after UV light irradiation was observed by <sup>1</sup>H NMR spectroscopy.<sup>26</sup> Another study by Uosaki *et al.* using SFG spectroscopy confirmed that the UV illumination increased not only the amount of adsorbed water but also the order of the adsorbed water on the TiO<sub>2</sub> surface.<sup>27</sup> Although the mechanism for the H<sub>2</sub>O/UV light interactions still remains uncertain, it seems that the particle network during UV light irradiation might be responsible for the enhancement of water adsorption on a TiO<sub>2</sub> particle film due to a new distribution of the particles. Wang *et al.* revealed the fact that under UV(A) illumination the total exposed TiO<sub>2</sub> surface increases due to the de-aggregation of particles agglomerates which was explained by assuming that part of the absorbed light energy is converted non-adiabatically into heat which is subsequently used to break the bonds between the particles thus producing additional surface area for the photocatalytic process.<sup>17,28</sup> One of the first ATR-FTIR studies that focused on the adsorption phenomena in aqueous solution was performed by Mendive *et al.*, who combined experimental data and theoretical calculations to demonstrate that the water molecule can fill the space in between the particles which was demonstrated by the increase in the IR band corresponding to the bending mode of water.<sup>29</sup>

We propose that UV irradiation leads to an increase in the amount of adsorbed water by thermal processes with hydrophilicity effects simultaneously taking place on the TiO<sub>2</sub> surface. Moreover, as shown in Fig. 4, the results clearly indicate that the presence of O<sub>2</sub> is necessary to enhance the photoadsorption of H<sub>2</sub>O and D<sub>2</sub>O on TiO<sub>2</sub> surfaces during UV(A) irradiation. This confirms that the adsorption of water and D<sub>2</sub>O to TiO<sub>2</sub> surfaces is



caused by a photoinduced charge transfer process in presence of molecular oxygen. Takeuchi *et al.*<sup>30</sup> proposed a mechanism which revealed that when TiO<sub>2</sub> surfaces were irradiated with UV light in the absence of O<sub>2</sub>, the electrons trapped on the Ti<sup>3+</sup> sites were not scavenged by O<sub>2</sub> and the holes trapped on the TiO<sub>2</sub> surface were immediately consumed to oxidize the lattice oxygen, resulting in the formation of oxygen vacancies. Such photoreduced TiO<sub>2</sub> surfaces can behave as negatively charged surfaces. Thus, water molecules could hardly adsorb on the photoreduced surfaces due to repulsive effects (Scheme 2). On the other hand, when the TiO<sub>2</sub> surfaces are irradiated in the presence of O<sub>2</sub>, the surface trapped electrons are scavenged by O<sub>2</sub> and the photoreduced surfaces are immediately oxidized. In this way, the TiO<sub>2</sub> surface is very likely interacting with water molecules due to interaction effects resulting in an increase in the amount of adsorbed water. The results of this investigation indicate that the photoinduced hydrophilic effect is achieved by an increase in the amount of adsorbed H<sub>2</sub>O molecules and this phenomenon occurs not only by a thermal process but also by a photoinduced charge transfer process.

**Scheme 2** Interaction model of adsorbed water during UV(A) light irradiation in the absence and presence of O<sub>2</sub> molecules.



## 2.6 Conclusions

The behaviour of adsorbed H<sub>2</sub>O and D<sub>2</sub>O in photocatalytic processes and in photoinduced hydrophilicity on TiO<sub>2</sub> surfaces has been addressed using ATR-FTIR spectroscopy. This study made it possible, to investigate adsorption processes at the TiO<sub>2</sub>/aqueous solution interface, quantitatively and *in situ*. It was shown that the photocatalytic reduction of O<sub>2</sub> at the anatase surface leads to the formation of hydroperoxo groups as demonstrated by a FTIR band at 3483 cm<sup>-1</sup>. Adsorption of H<sub>2</sub>O with different

ratios of D<sub>2</sub>O on TiO<sub>2</sub> revealed that the deuteride ions exhibit stronger adsorption ability than hydroxyl ions resulting in an isotopic exchange reaction which takes place in the dark. Upon illumination with UV light in the presence of O<sub>2</sub> both OH and OD groups are formed, which in turn increase the hydrophilicity of the TiO<sub>2</sub> surface. In contrast, when the solution was saturated with argon or nitrogen, no formation of OH and OD groups was detected and the hydrophilicity was strongly inhibited. The increase in the amount of OH and OD groups is suggested to be caused by photoadsorption of H<sub>2</sub>O and D<sub>2</sub>O due to deaggregation of the pre-existing network of particles rather than by dissociative water and D<sub>2</sub>O adsorption at surficial oxygen vacancies. Finally, it is concluded that the role of oxygen during UV irradiation is very crucial for the presence of both the photoinduced hydrophilic as well as the photocatalytic response.

## 2.7 Acknowledgements

Belhadj H. gratefully acknowledges a scholarship from the Deutscher Akademischer Austauschdienst (DAAD) providing the financial support to perform his Ph.D. studies in Germany. The present study was performed within the Project “Establishment of the Laboratory ‘Photoactive Nanocomposite Materials’” No. 14.Z50.31.0016 supported by a Mega-grant of the Government of the Russian Federation.

## 2.8 References

- 1 M. R. Hoffmann, S. T. Martin, W. Choi, and D. W. Bahnemann, *Chem. Rev.*, 1995, **95**, 69–96.
- 2 J. Tschirch, R. Dillert, D. Bahnemann, B. Proft, A. Biedermann and B. Goer, *Res. Chem. Intermed.*, 2008, **34**, 381–392.
- 3 M. Miyauchi, A. Nakajima, T. Watanabe and K. Hashimoto, *Chem. Mater.*, 2002, **14**, 2812–2816.
- 4 J. Xu, N. Sahai, C. M. Eggleston and M. a. a. Schoonen, *Earth Planet. Sci. Lett.*, 2013, **363**, 156–167.
- 5 T. Hirakawa and Y. Nosaka, *Langmuir*, 2002, **18**, 3247–3254.
- 6 P. K. J. Robertson, D. W. Bahnemann, L. a. Lawton and E. Bellu, *Appl. Catal. B Environ.*, 2011, **108–109**, 1–5.
- 7 R. Wang, K. Hashimoto, A. Fujishima, M. Chikuni, E. Kojima, A. Kitamura, M. Shimohigoshi and T. Watanabe, *Adv. Mater.*, 1998, **10**, 135–138.
- 8 L. Zhang, R. Dillert, D. Bahnemann and M. Vormoor, *Energy Environ. Sci.*, 2012, **5**, 7491.

- 9 L. M. Liu, P. Crawford and P. Hu, *Prog. Surf. Sci.*, 2009, **84**, 155–176.
- 10 N. Sakai, A. Fujishima, T. Watanabe and K. Hashimoto, *J. Phys. Chem. B*, 2003, **107**, 1028–1035.
- 11 T. Zubkov, D. Stahl, T. L. Thompson, D. Panayotov, O. Diwald and J. T. Yates, *J. Phys. Chem. B*, 2005, **109**, 15454–15462.
- 12 H. Irie and K. Hashimoto, *Environmental Photochemistry Part II*, 2005, vol. 2M.
- 13 K. Hashimoto, H. Irie and A. Fujishima, *Jpn. J. Appl. Phys.*, 2005, **44**, 8269–8285.
- 14 G. Munuera, A. R. González-Elipe, J. Soria and J. Sanz, *J. Chem. Soc. Faraday Trans. 1 Phys. Chem. Condens. Phases*, 1980, **76**, 1535.
- 15 M. Takeuchi, K. Sakamoto, G. Martra, S. Coluccia and M. Anpo, *J. Phys. Chem. B*, 2005, **109**, 15422–15428.
- 16 C. Wang, C. Böttcher, D. W. Bahnemann and J. K. Dohrmann, *J. Mater. Chem.*, 2003, **13**, 2322–2329.
- 17 C. Wang, R. Pagel, J. K. Dohrmann and D. W. Bahnemann, *Comptes Rendus Chim.*, 2006, **9**, 761–773.
- 18 C. Y. Wang, R. Pagel, D. W. Bahnemann and J. K. Dohrmann, *J. Phys. Chem. B*, 2004, **108**, 14082–14092.
- 19 S. J. Hug and B. Sulzberger, *Langmuir*, 1994, **10**, 3587–3597.
- 20 C. B. Mendive, T. Bredow, A. Feldhoff, M. a Blesa and D. Bahnemann, *Phys. Chem. Chem. Phys.*, 2009, **11**, 1794–808.
- 21 J. C. Duplan, L. Mahi and J. L. Brunet, *Chem. Phys. Lett.*, 2005, **413**, 400–403.
- 22 R. Nakamura, A. Imanishi, K. Murakoshi and Y. Nakato, *J. Am. Chem. Soc.*, 2003, **125**, 7443–50.
- 23 L. A. Lawton, P. K. J. Robertson, B. J. P. A. Cornish, I. L. Marr and M. Jaspars, *J. Catal.*, 2003, **213**, 109–113.
- 24 G. Mattioli, F. Filippone and A. A. Bonapasta, *J. Am. Chem. Soc.*, 2006, **128**, 13772–13780.
- 25 R. Wang, K. Hashimoto, A. Fujishima, M. Chikuni, E. Kojima, A. Kitamura, M. Shimohigoshi and T. Watanabe, *Nature*, 1997, **388**, 431–432.
- 26 A. Y. Nosaka, E. Kojima, T. Fujiwara, H. Yagi, H. Akutsu and Y. Nosaka, *J. Phys. Chem. B*, 2003, **107**, 12042–12044.
- 27 K. Uosaki, T. Yano and S. Nihonyanagi, *J. Phys. Chem. B*, 2004, **108**, 19086–19088.
- 28 J. Schneider, M. Matsuoka, M. Takeuchi, J. Zhang, Y. Horiuchi, M. Anpo and D. W. Bahnemann, *Chem. Rev.*, 2014, **114**, 9919–9986.
- 29 C. B. Mendive, D. Hansmann, T. Bredow and D. Bahnemann, *J. Phys. Chem. C*, 2011, **115**, 19676–19685.
- 30 M. Takeuchi, G. Martra, S. Coluccia and M. Anpo, *J. Phys. Chem. C*, 2007, **111**, 9811–9817.

## 2.9 Supplementary Information

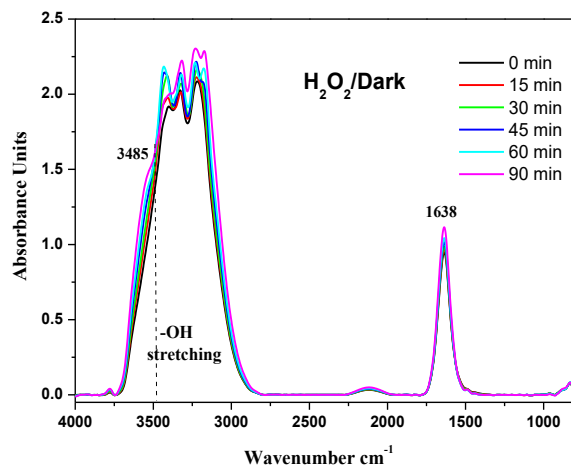


**Figure S1.** Spectrum of adsorption of H<sub>2</sub>O<sub>2</sub> in the dark at different times

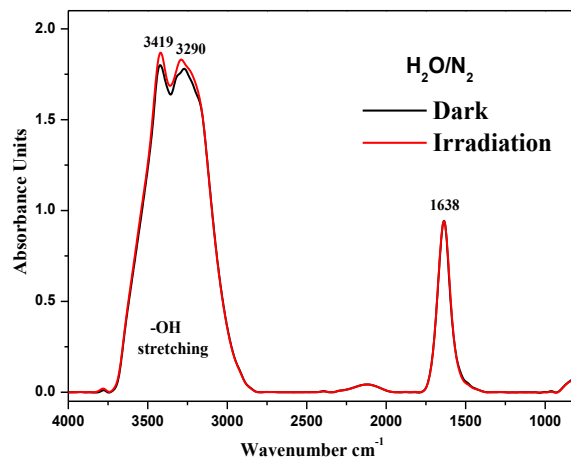


**Figure S2.** Adsorption of H<sub>2</sub>O in the presence N<sub>2</sub> in the dark and under UV(A) illumination

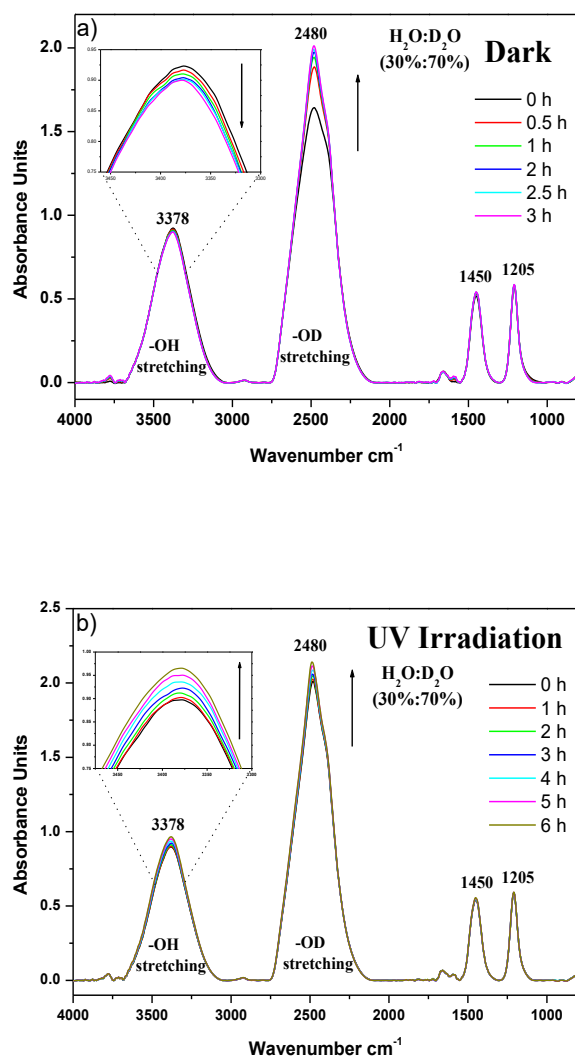


**Figure S3.** Time evolution of the ATR-FTIR spectra of an adsorbed mixture of  $\text{H}_2\text{O}:\text{D}_2\text{O}$  (30%:70%) in the presence of  $\text{O}_2$  on  $\text{TiO}_2$  a) in the dark for 3 h, b) under 6 h of UV(A) illumination.



## Chapter 3

### ***In Situ* ATR-FTIR Investigation of the Effects of H<sub>2</sub>O and D<sub>2</sub>O Adsorption on the TiO<sub>2</sub> Surface**

H. Belhadj<sup>a</sup>, Y. AlSalka<sup>a</sup>, P. K. J. Robertson<sup>b</sup> and D. Bahnemann<sup>a,c</sup>

<sup>a</sup>Institut für Technische Chemie, Leibniz Universität Hannover, Callinstraße 3, D-30167 Hannover, Germany.

<sup>b</sup>Centre for the Theory and Application of Catalysis (CenTACat), School of Chemistry and Chemical Engineering, Queen's University Belfast, Stranmillis Road, Belfast, BT9 5AG, UK.

<sup>c</sup>Laboratory "Photoactive Nanocomposite Materials", Saint-Petersburg State University, Ulyanovskaya str. 1, Peterhof, Saint-Petersburg, 198504 Russia.

Published in ECS Transactions, 75 (50) (2017) 101-113.

DOI: 10.1149/07550.0101ecst

### 3 *In situ* ATR-FTIR Investigation of the Effects of H<sub>2</sub>O and D<sub>2</sub>O Adsorption on the TiO<sub>2</sub> surface

#### 3.1 Abstract

We have investigated the behavior of H<sub>2</sub>O and D<sub>2</sub>O adsorption on TiO<sub>2</sub> surfaces in the dark and under UV irradiation using *in situ* ATR-FTIR spectroscopy. The influence of an electron scavenger (oxygen) and a hole scavenger (ethanol) on the hydroxyl group and/or hydration water behavior on the TiO<sub>2</sub> surface were also investigated. Adsorption of H<sub>2</sub>O–D<sub>2</sub>O mixtures revealed an isotopic exchange reaction occurring in the dark onto the surface of the TiO<sub>2</sub> material. Under UV(A) irradiation, the quantity of both OH and OD groups was found to be increased by the presence of molecular oxygen. On the other hand, the ATR-FTIR study of the ethanol adsorption in H<sub>2</sub>O and D<sub>2</sub>O revealed a stronger adsorption capacity for ethanol compared to both H<sub>2</sub>O and D<sub>2</sub>O resulting in molecular and dissociative adsorption of ethanol on the TiO<sub>2</sub> surface. When the system was subsequently illuminated with UV(A) light, the surface becomes enriched with adsorbed water. Different possible mechanisms and hypotheses are discussed in terms of the effect of UV irradiation on the TiO<sub>2</sub> particle network for the photocatalytic reaction and photoinduced hydrophilicity.

#### 3.2 Introduction

Photocatalysis and Photoinduced Hydrophilicity have attracted significant attention due to their potential applications in environmental protection [1]. Surface OH groups on TiO<sub>2</sub> materials have been assumed to play important roles in both photocatalytic reactions and photoinduced hydrophilicity [2]. Adsorbed species such as water, substrate and molecular oxygen, however, are expected to affect the hydroxyl group behavior on the TiO<sub>2</sub> surface, which play a major role in the charge transfer and trapping reactions occurring at the TiO<sub>2</sub>/water interface under UV (A) irradiation. In oxygenated systems the photogenerated electron reacts with molecular oxygen producing superoxide anion radicals, while the photogenerated holes are either trapped by the surface hydroxyl group or/and water molecules forming reactive hydroxyl radicals or they initiate the direct oxidation of an adsorbed organic donor [3]. It was reported, however, that during UV irradiation not only did the photocatalytic reactions take place on the surface but the



photoinduced hydrophilicity also occurred due to the separation and diffusion of photogenerated electrons and holes occurring at the TiO<sub>2</sub>/water interface [4]. Additionally, a competitive reaction in aqueous solutions, would take place during UV irradiation between direct oxidation and indirect oxidation of organic molecules due to the different adsorption behaviors of substrates [5]. Alternatively, during UV irradiation the particle network of the TiO<sub>2</sub> material could play a significant role in the absorption of light and adsorption of species [6]. Thus, special attention has been focused on the particle network during photocatalytic reactions and therefore, several mechanisms regarding the effect of UV(A) light on the particle network have been suggested such as the Antenna mechanism and deaggregation concept [1,6]. Although the interfacial substrate/TiO<sub>2</sub> interactions have been extensively studied, the effect of water and oxygen adsorption, together with the associated hydroxyl groups during UV irradiation are, however, still not completely understood for both photocatalytic reactions and photoinduced hydrophilicity. In this study, Attenuated Total Reflectance-FTIR spectroscopy, was used for an *in-situ* mechanistic investigation at the water/TiO<sub>2</sub> interface. The adsorption behavior of H<sub>2</sub>O and D<sub>2</sub>O on the TiO<sub>2</sub> surface was investigated in the absence and in the presence of both an electron scavenger (oxygen) and a hole scavenger (ethanol). Several mechanisms considering the interaction of UV(A) light and the hydroxyl groups formation or/and hydration water on the TiO<sub>2</sub> surface have been addressed. This work, therefore, provides new insight into the mechanistic aspects of photoinduced hydrophilicity and photocatalytic reactions on TiO<sub>2</sub> surfaces.

### 3.3 Experimental

#### 3.3.1 Materials

TiO<sub>2</sub> (Hombikat UV100, 100% anatase) was kindly supplied by Sachtleben Chemie. Ethanol ( $\geq 99.8\%$ ) was purchased from ROTH. The Deuterium oxide (D<sub>2</sub>O) (99.9 atom% D) were purchased from Sigma Aldrich. Deionized water (H<sub>2</sub>O) was supplied from a Millipore Mill-Q system with a resistivity equal to 18.2  $\Omega$  cm at 25 °C.

#### 2.3.2 ATR-FTIR Measurements

Attenuated total reflection Fourier transformed infrared (ATR-FTIR) *in-situ* spectra were recorded employing an IFS 66 BRUKER instrument equipped with an internal

reflection element 45° ZnSe crystal and a deuterated triglycine sulfate (DTGS) detector. A thin anatase layer was deposited on the ZnSe ATR crystal ( $2.3 \text{ g m}^{-2}$  and 1-3  $\mu\text{m}$  thick) [7]. Prior to starting the irradiation experiments, spectra of adsorption of  $\text{H}_2\text{O}$  and  $\text{D}_2\text{O}$  on the  $\text{TiO}_2$  material were monitored in the dark. The spectrum of the  $\text{TiO}_2$ -coated crystal were taken as background and used as the blank for the subsequent measurements. When the last spectrum of each experiment had been recorded, the UV(A) lamp was turned on and another sequence of spectra were recorded.

For the ethanol experiments, 18 ml of circulating 30 vol% aqueous ethanol solution was employed at a flow rate of approximately  $4 \text{ ml min}^{-1}$ . These experiments were started by pumping the background water/ $\text{D}_2\text{O}$  (12.6 ml) through the flow cell at a flow rate of  $4 \text{ ml min}^{-1}$ , and allowing the  $\text{TiO}_2$  deposit to equilibrate with the background solution. One spectrum was used as blank to subtract the signals of the water/ $\text{D}_2\text{O}$ , the pure solution of ethanol (5.4 ml) was subsequently added to the aqueous solution. A new set of spectra were then collected in the dark. Prior to illumination, the last spectrum of the ethanol solution was recorded in the dark with the  $\text{TiO}_2$  layer being subtracted, and another spectra was collected during UV irradiation.

The interferometer and the infrared light path in the spectrometer were constantly purged with argon and nitrogen to avoid  $\text{H}_2\text{O}$  and  $\text{CO}_2$  contamination. The spectra were recorded with 300 scans at  $4 \text{ cm}^{-1}$  resolution and analyzed using OPUS version 6.5 software. Irradiation of samples with UV(A) light was carried out using an LED lamp (Model LED-Driver, THORLABS) emitting UV light (365 nm). The distance from the UV lamp to the surface of the test solution was kept 30 cm on which the intensity of UV(A) light was of  $1.0 \text{ mWcm}^{-2}$  as measured by UV radiometer (Dr. Honle GmbH, Martinsried, Germany).

### 3.4 Results and Discussion

#### 3.4.1 Adsorption of $\text{H}_2\text{O}$ and $\text{D}_2\text{O}$ on $\text{TiO}_2$

Figure 1 shows the ATR-FTIR spectra of  $\text{H}_2\text{O}$ – $\text{D}_2\text{O}$  mixtures adsorbed on the surface of  $\text{TiO}_2$  in the dark. The IR spectrum of the adsorbed water on  $\text{TiO}_2$  is represented by a strong IR absorbance of an O–H stretching band in the region between  $3700$  and  $2850 \text{ cm}^{-1}$  and a bending mode of  $\delta$  (H–O–H) at  $1638 \text{ cm}^{-1}$  which is assigned to undissociated water molecules. When  $\text{D}_2\text{O}$  was used instead of water, all the bands that correspond to the

adsorbed water on  $\text{TiO}_2$  surface were shifted to lower frequency with exchanging H for D, resulting an O–D stretching band in the region between  $2750\text{--}2050\text{ cm}^{-1}$  and  $\delta$  (D–O–D) bending band at  $1205\text{ cm}^{-1}$ .

It can be clearly seen from these spectra that the intensity of the band in the OH-stretching region decreased gradually with increasing the loading of  $\text{D}_2\text{O}$ . The peak of the isotopologue HDO bending band centred at  $1450\text{ cm}^{-1}$  was formed and increased by increasing the concentration of  $\text{H}_2\text{O}$  in  $\text{D}_2\text{O}$  until it approached equimolar proportions [8], and this then decreased again with further increases in the quantities of  $\text{H}_2\text{O}$  in  $\text{D}_2\text{O}$  (Fig. 1 inset).

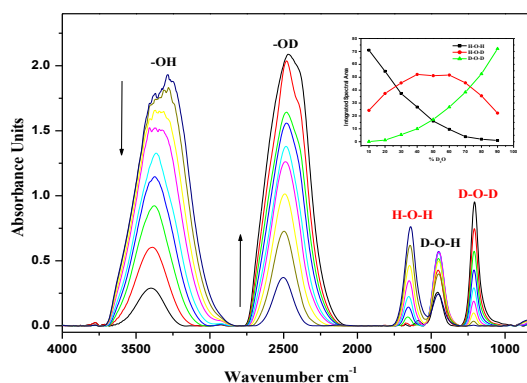


**Figure 1.** ATR–FTIR spectra of  $\text{D}_2\text{O}$ – $\text{H}_2\text{O}$  mixtures with different concentrations adsorbed on  $\text{TiO}_2$  in the dark. (Copyright 2015 Royal Society of Chemistry.)

Adsorbed  $\text{D}_2\text{O}$  molecules on  $\text{TiO}_2$  surfaces are expected to affect the behavior of hydroxyl groups, thus a series of experiments for water adsorption with different ratios of  $\text{D}_2\text{O}$  were performed before and after UV irradiation in the presence of oxygen. Figure 2 shows the time evolution of the intensity of the integrated spectral areas of the OH and OD stretching groups before and after UV(A) irradiation with different ratios ( $\text{H}_2\text{O}:\text{D}_2\text{O}$ ). As can be clearly seen, in the dark, at low concentrations of  $\text{H}_2\text{O}$  ( $\text{H}_2\text{O}\% < \text{D}_2\text{O}\%$ ), a strong decrease in the amount of OH stretching was observed. Simultaneously, the amount of OD stretching groups adsorbed on  $\text{TiO}_2$  increased during this period until the system reached equilibrium. In contrast, at higher concentrations of  $\text{H}_2\text{O}$  ( $\text{H}_2\text{O}\% > \text{D}_2\text{O}\%$ ), both OH and OD stretching bands increased. Interestingly, at an equimolar mixture of 50%  $\text{H}_2\text{O}$  and  $\text{D}_2\text{O}$ , a decrease in intensity of OH stretching with a simultaneous increase in the OD stretching could be observed in the dark. These results suggest that the deuteride ions

show a stronger adsorption ability in the dark than hydroxyl ions at the surface of the TiO<sub>2</sub> material. Thus, the deuteride ions could lead to an isotopic exchange process by replacing the hydroxyl groups adsorbed on the TiO<sub>2</sub> surface (reaction 1) [9]:

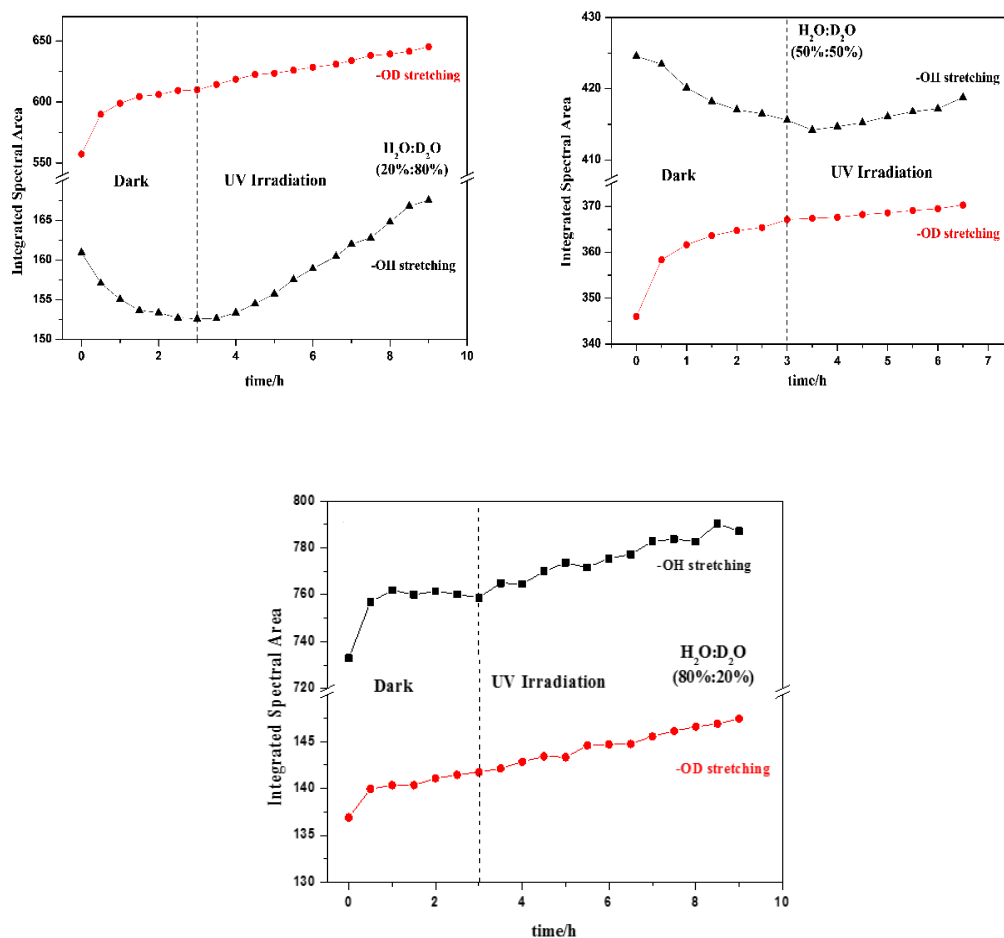
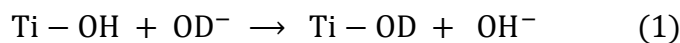


**Figure 2.** Time evolution of the intensity of the integrated spectral areas of the OH and OD stretching groups before and after UV(A) irradiation with different ratios (H<sub>2</sub>O:D<sub>2</sub>O). (Copyright 2015 Royal Society of Chemistry.)

When the system was subsequently illuminated with UV(A) light in presence of oxygen, the amount of OH and OD group stretching increased almost immediately. These results indicate that UV irradiation leads to an increase in the number of surface OH groups which in turn increases the hydrophylicity of the TiO<sub>2</sub> surface. These results, however, might be attributed to either an increase in the number of surface OH groups by the formation of new OH and OD groups on the surface or by increasing the amount of

H<sub>2</sub>O and D<sub>2</sub>O molecules chemisorbed on the TiO<sub>2</sub> surface. Several mechanisms have been discussed to explain photoinduced hydrophilicity on TiO<sub>2</sub> surface. Hashimoto *et al.* reported that the increase in the amount of OH groups was believed to be caused by dissociative adsorption of water in vacancies resulting two kinds of hydroxyl groups on the surface i.e., bridging and terminal hydroxyl groups [4]. Another mechanism was proposed by Yates *et al.*, who demonstrated that under UV light irradiation the decomposition of organic contaminants can take place leading to the creation of superhydrophilic surfaces [10].

Figure 3 shows the time evolution of the intensity of the integrated spectral areas of the OH and OD stretching groups before and after UV irradiation at prolonged time periods. As can be clearly seen, an isotopic exchange between deuteride ions and hydroxyl groups have been achieved in the dark. Interestingly, after 6 h of UV irradiation, however, no isotopic exchange was detected between hydroxyl groups and deuteride ions during a prolonged time in the dark. From this result, we suggest that the increase of OH and OD stretching groups under irradiation is most likely caused by adsorption of H<sub>2</sub>O and D<sub>2</sub>O molecules, respectively, and not by the generation of hydroxyl groups.

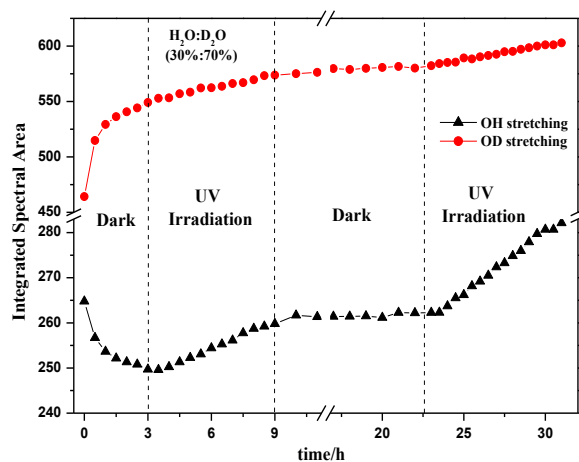
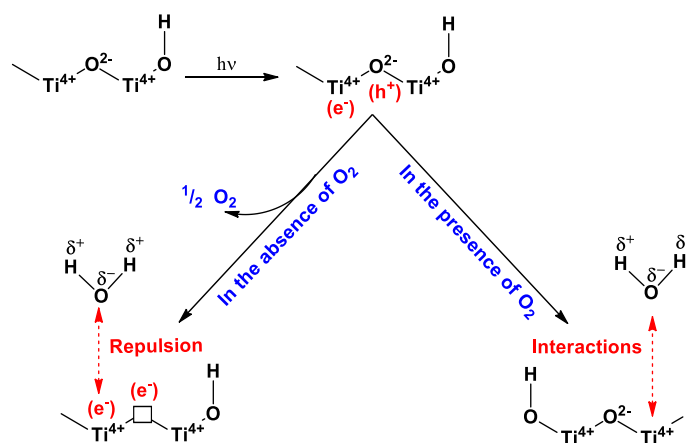


**Figure 3.** Time evolution of the intensity of the integrated spectral areas of OH and OD stretching groups before and after UV(A) irradiation with prolonged time (Alternately). (Copyright 2015 Royal Society of Chemistry.)

In order to elucidate the mechanism of the adsorption of H<sub>2</sub>O and D<sub>2</sub>O, the effect of oxygen on the OH and OD group behavior on the TiO<sub>2</sub> surface have been investigated. The integrated intensity of the OH and OD stretching groups increased significantly upon illumination in the presence of molecular oxygen. By contrast, when the sample was purged with nitrogen or argon, no increase in the OH and/or OD stretching group was observed (Figure are not shown). These results clearly indicate that the presence of O<sub>2</sub> is necessary to enhance the photoadsorption of H<sub>2</sub>O and D<sub>2</sub>O on TiO<sub>2</sub> surfaces during UV(A) irradiation. Our results confirm the critical influence of oxygen on adsorption behavior, resulting in an increase the adsorption of H<sub>2</sub>O and D<sub>2</sub>O on TiO<sub>2</sub> surfaces which is most likely caused by a photoinduced charge transfer process [9]. Takeuchi *et al.* proposed that when TiO<sub>2</sub> surfaces were irradiated with UV light in the absence of O<sub>2</sub>, the electrons trapped on the Ti<sup>3+</sup> sites were not scavenged by O<sub>2</sub> and the holes trapped on the TiO<sub>2</sub> surface were immediately consumed to oxidize the lattice oxygen, resulting in the formation of oxygen vacancies. Such photoreduced TiO<sub>2</sub> surfaces can behave as negatively charged surfaces. Thus, water molecules hardly adsorb on the photoreduced surfaces due to repulsive effects (Scheme 1) [11].

**Scheme 1** Interaction model of adsorbed water during UV(A) light irradiation in the absence and presence of O<sub>2</sub> molecules. (Copyright 2015 Royal Society of Chemistry.)



### 3.4.2 Adsorption of ethanol in H<sub>2</sub>O and D<sub>2</sub>O on TiO<sub>2</sub>

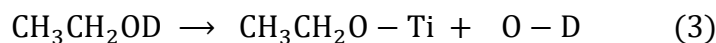
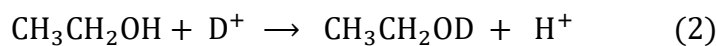
Figure 4 and 5 show the time evolution of the spectra of adsorbed ethanol on TiO<sub>2</sub> in H<sub>2</sub>O a) and D<sub>2</sub>O b) respectively, in the dark and under UV(A) irradiation in the presence of O<sub>2</sub>. The adsorption of ethanol (30 vol%) and water on TiO<sub>2</sub> were performed in the dark with molecular ratios of 12% and 88% respectively. As shown in figure 4, the adsorption of ethanol on TiO<sub>2</sub> produces several positive absorption bands in the region 3000-2750 cm<sup>-1</sup> and 1470-1250 cm<sup>-1</sup> which are assigned to different types of CH vibration of on both CH<sub>2</sub> and CH<sub>3</sub> groups [12,13]. The two most prominent peaks of the adsorbed ethanol appeared at 1043 cm<sup>-1</sup> and 1085 cm<sup>-1</sup> which are assigned to the symmetric and asymmetric stretching frequencies of the CO stretching modes [14]. Since water and D<sub>2</sub>O were used as the background and over subtraction occurred, a broad negative band assigned to band bending  $\delta$  (H–O–H)/ $\delta$  (D–O–D) and hydroxyl group stretching OH/OD were observed.

It can clearly be seen from figure 4a that in the dark the typical bands of adsorbed ethanol increased. Simultaneously, the negative band corresponding to the water adsorption decreased. Even though the molecular ratio of ethanol was very low (12%) compared to water and D<sub>2</sub>O (88%), a similar desorption behavior of D<sub>2</sub>O, was observed during the dark period. This phenomenon is clearly due to the stronger adsorption of ethanol on the TiO<sub>2</sub> surface compared to water resulting in desorption of water and D<sub>2</sub>O molecules. It has previously been reported that alcohol and water adsorb competitively on the oxide surface both molecularly and dissociatively, with the formation of surface hydroxyl and methoxy groups [15]. As shown in Fig. 4b unlike the case of water, the typical bands of adsorbed ethanol, as well as the band centered at 3395 cm<sup>-1</sup> which is assigned to the OH group of ethanol have increased. These results indicate clearly the adsorption of molecular ethanol on the TiO<sub>2</sub> surface. Simultaneously, a new band at 949 cm<sup>-1</sup> was observed, which increased during the adsorption of ethanol in the dark. This band has previously been assigned in the literature to OD band bending of deuterated ethanol, Et(OD) [16].

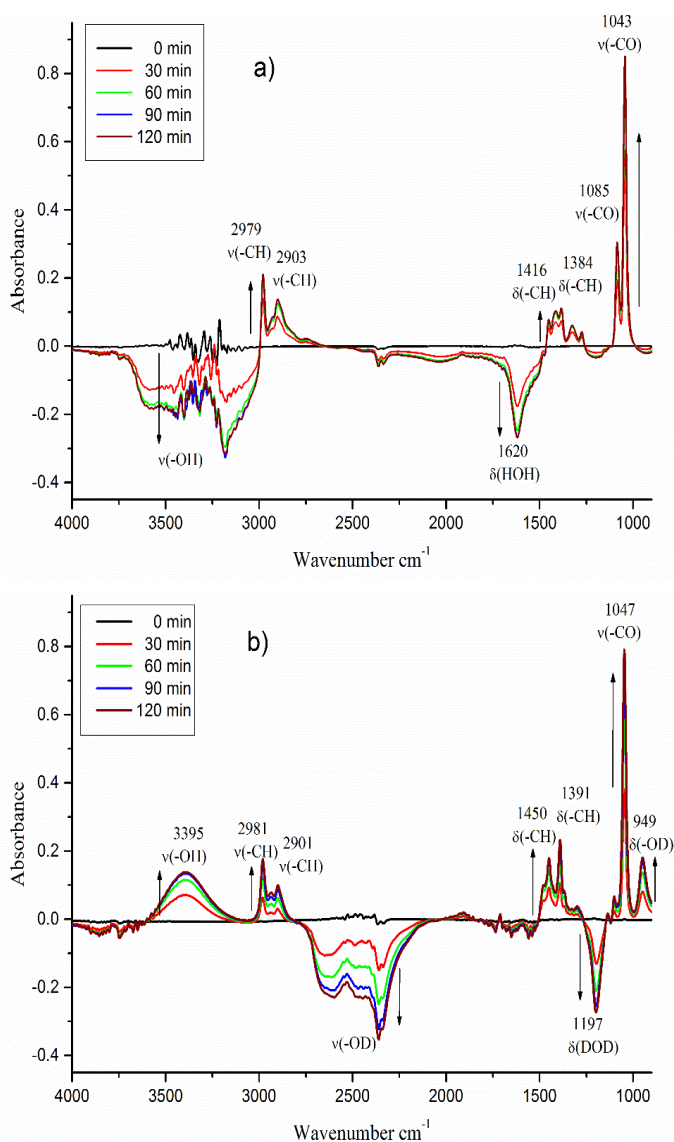
Interestingly, no isotopic exchange was detected in the region 3000-3600 cm<sup>-1</sup> although the adsorption of ethanol occurred in D<sub>2</sub>O. This result also confirmed that molecular ethanol was adsorbed on the TiO<sub>2</sub> surface. It has also been reported that, ethanol dissociates on TiO<sub>2</sub> resulting in sorbed ethoxide groups atop of Lewis acidic Ti<sup>4+</sup> centers (monodentate) or between two Ti<sup>4+</sup> centers (bidentate), while the H from the alcohol

associates with a neighboring basic surface O to form an OH group [17]. The increasing band bending of OD at  $949\text{ cm}^{-1}$  (Fig.4b), indicated the dissociation of deuterated ethanol on the  $\text{TiO}_2$  surface resulting ethoxide at  $\text{Ti}^{4+}$  and the D at a neighboring basic surface.

According to ref. [18] and [15], the proposed dissociation and isotopic exchange reaction of ethanol in the heavy water ( $\text{D}_2\text{O}$ ) are as follows:



From this result, we suggest that in the dark, ethanol can adsorb on  $\text{TiO}_2$  surface in both, molecular and dissociation forms.

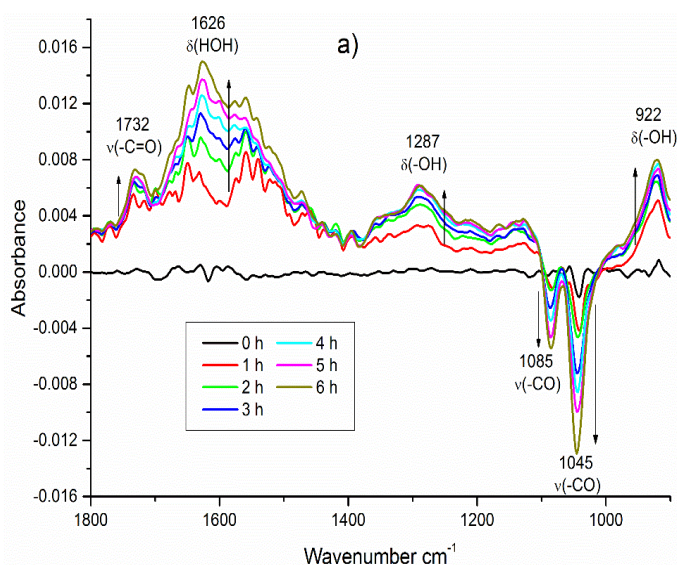


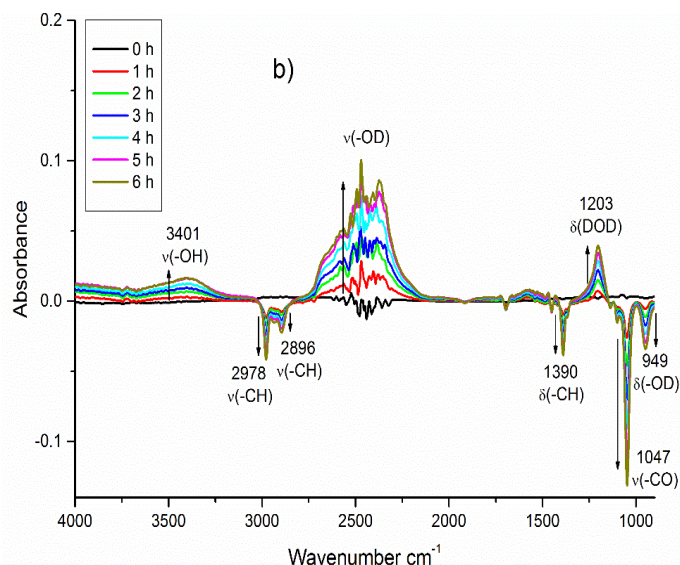
**Figure 4.** Time evolution of the ATR-FTIR spectra of adsorbed ethanol on  $\text{TiO}_2$  in  $\text{H}_2\text{O}$  a) and  $\text{D}_2\text{O}$  b) in the dark.



Figure 5 shows the time evolution of the ATR-FTIR spectra (1800-800  $\text{cm}^{-1}$ ) of adsorbed ethanol on  $\text{TiO}_2$  in  $\text{H}_2\text{O}$  a) and  $\text{D}_2\text{O}$  b) under UV irradiation in the presence of  $\text{O}_2$ . As can be seen clearly under UV irradiation, the typical bands of adsorbed ethanol solutions have decreased in  $\text{H}_2\text{O}$  and  $\text{D}_2\text{O}$ . A strong decrease in the intensities of the two prominent peaks of the adsorbed ethanol at 1047  $\text{cm}^{-1}$  (CO) and 1085  $\text{cm}^{-1}$  (C-C) decreased in  $\text{H}_2\text{O}$  as well as in  $\text{D}_2\text{O}$  where the intensities were much higher than in water. Additionally, the bands in the 1740-1710  $\text{cm}^{-1}$  and 1600-1520  $\text{cm}^{-1}$  regions, which were assigned respectively to carbonyl and carboxylate groups increased gradually. These results indicate that the ethanol was photocatalytically oxidized resulting in the formation of acetaldehyde and acetic acid as photoproducts [17,13].

Interestingly, the typical band of water and  $\text{D}_2\text{O}$  increased when the system was performed under UV irradiation (Figure 5b). This result can tentatively be explained either by photoinduced charge transfer process or by the formation of water as an intermediate product. Lin *et al.* proposed mechanism pathways of the formation of  $\text{CH}_3\text{CO}_{\text{ad}}$ ,  $\text{CO}_2$ , and  $\text{H}_2\text{O}$  as photoproducts in the presence of  $\text{O}_2$  during the oxidation of ethanol [19,20]. Although, it is well known that the ethanol can be easily adsorbed onto  $\text{TiO}_2$  surfaces, however the adsorption mechanism of water and  $\text{D}_2\text{O}$  on  $\text{TiO}_2$  surfaces are still unclear.





**Figure 5.** Time evolution of the ATR–FTIR spectra ( $1800\text{--}800\text{ cm}^{-1}$ ) of adsorbed ethanol on  $\text{TiO}_2$  in  $\text{H}_2\text{O}$  a) and  $\text{D}_2\text{O}$  b) under UV irradiation in the presence of  $\text{O}_2$ .

In order to clarify the main factors affecting the adsorption of water during UV illumination, the effect of  $\text{O}_2$  has been investigated. Figure 6 shows the evolution of the adsorbed ethanol spectra ( $1800\text{--}900\text{ cm}^{-1}$ ) under UV irradiation in the absence of  $\text{O}_2$  in water a) and  $\text{D}_2\text{O}$  b). In the dark, the adsorption behavior of ethanol in water and  $\text{D}_2\text{O}$  was observed in the IR spectrum (Figure not shown) which were similar to those reported in figure 4.

Under UV irradiation, the typical bands of adsorbed ethanol decreased in water and  $\text{D}_2\text{O}$  (figure 6). In the meantime, the increase of the intensities of carbonyl and carboxylate groups was observed, which is similar to the observation in the presence of oxygen. As expected, the shifting of the background during oxidation of ethanol was observed. The upward baseline shift during irradiation was interpreted as transient and persistent diffuse reflectance infrared signals due to the accumulation of free electrons at the conduction band of  $\text{TiO}_2$  particles upon irradiation, where the baseline IR absorption for  $\text{TiO}_2$  rises immediately upon UV irradiation [21]. Similar results were reported by Highfield *et al.*, who clearly observed the direct hole oxidation of the adsorbed ethanol molecules by photoinduced holes ( $\text{h}^+$ ) at the valence band of  $\text{TiO}_2$  [17]. Interestingly, although the photocatalytic system occurred in the absence of  $\text{O}_2$ , a similar behavior of the adsorption of water and  $\text{D}_2\text{O}$  has been observed. Additionally, when  $\text{D}_2\text{O}$  was used instead of water, no formation of  $\text{H}_2\text{O}$  was detected in presence and absence of  $\text{O}_2$  respectively, in figure

5b and figure 6b. This result would exclude the possibility that the adsorption of water and D<sub>2</sub>O in presence of ethanol resulted either from photoinduced charge transfer process or from adsorption of water formed as product.

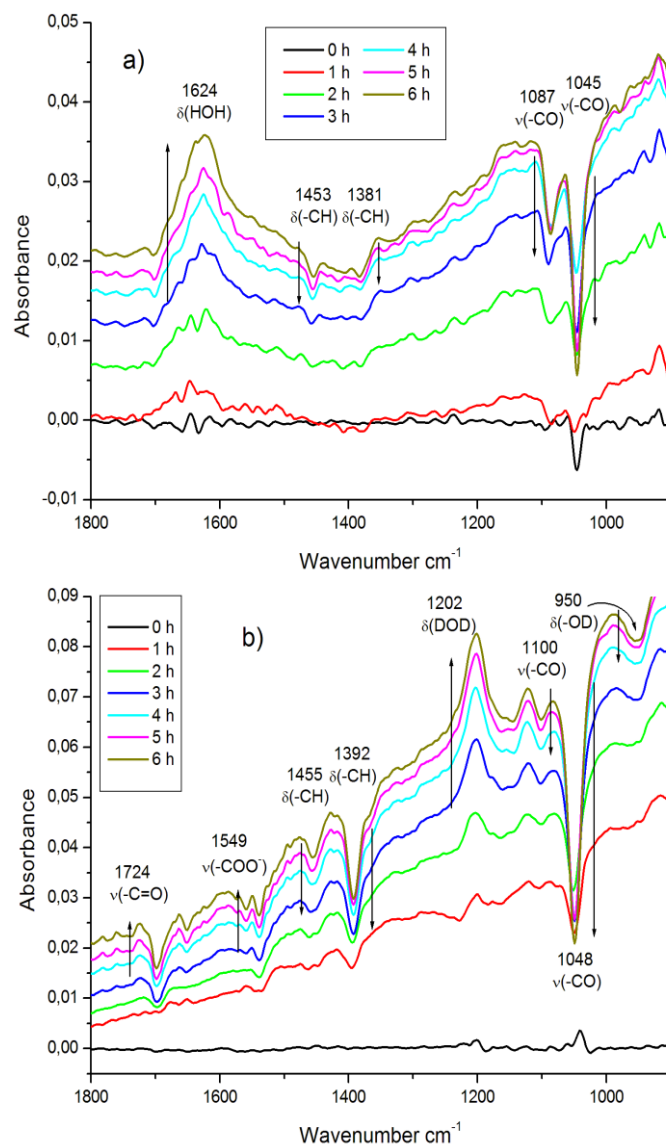
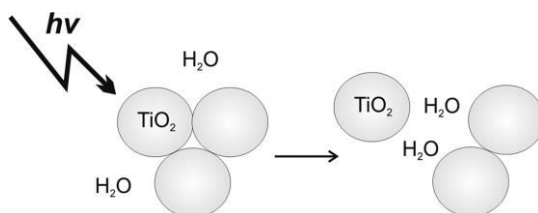


**Figure 6.** Time evolution of the ATR-FTIR spectra of adsorbed ethanol on TiO<sub>2</sub> in H<sub>2</sub>O a) and D<sub>2</sub>O b) in the absence of O<sub>2</sub>.

Considering the effect of UV light on TiO<sub>2</sub> particles, however it seems that the particle network resulting under UV light irradiation might be responsible for the enhancement of water adsorption on TiO<sub>2</sub> particles due to a new distribution of the particles.

Several interpretations of the mechanism of the UV-induced hydrophilicity have been reported in the literature which can explain the behavior of water adsorption. Yates *et al.*, reported that only under UV light illumination could the decomposition of organic contaminants take place leading to the generation of hydrophilic surfaces [10]. On the other hand, Wang *et al.* found that the total TiO<sub>2</sub> exposed surface increased under UV(A) illumination leading to an increase in the surface area due to de-aggregation of particle agglomerates which in turn enhanced the photonic efficiency [6]. The same mechanism was considered by Mendive *et al.* who demonstrated that due to de-aggregation of particle the water molecule could fill the space between the particles (Scheme 2), which was demonstrated by the increase in the IR band corresponding to the bending mode of water [22]. In other studies, Thermal chemistry showed that there were mainly two reaction channels for ethanol desorption which lead to the suggestion of a mechanism involving the creation of new adsorption sites for water adsorption by means of a photothermal-desorption of adsorbed ethanol molecules [15]. The behavior of the preadsorption of water on the thermal desorption reaction of ethoxy has been reported by Gamble *et al.* [23]. From these results we suggest that the adsorption of water and D<sub>2</sub>O are most likely to occur via photothermic rather than photoelectronic processes.

**Scheme 2.** Proposed Mechanism of TiO<sub>2</sub> Nanoparticle Layer Expansion (Copyright 2011 American Chemical Society.)



Based on the hypotheses reported in the literature, i.e., the de-aggregation concept, super-hydrophilicity phenomena and photo-induced removal of impurities, we suggest that the adsorption of H<sub>2</sub>O and D<sub>2</sub>O molecules on TiO<sub>2</sub> surfaces during UV light irradiation occurred not only by photoinduced charge transfer processes (photoinduced adsorption/desorption and photocatalytic reaction) but also by thermal processes (thermal desorption and de-aggregation of particle).

### 3.5 Conclusions

The behavior of adsorbed H<sub>2</sub>O and D<sub>2</sub>O in photocatalytic processes and in photoinduced hydrophilicity on TiO<sub>2</sub> surfaces has been studied in the presence and absence electron (O<sub>2</sub>) and holes (ethanol) scavenger. Adsorption of H<sub>2</sub>O with different ratios of D<sub>2</sub>O on TiO<sub>2</sub> revealed different isotopic exchange reactions, which take place in the dark. Upon illumination with UV light in the presence of O<sub>2</sub>, both OH and OD groups are formed leading to increase the hydrophilicity of the TiO<sub>2</sub> surface. The increase in the amount of OH and OD groups is suggested to be caused by photoinduced charge transfer allowing the adsorption of H<sub>2</sub>O and D<sub>2</sub>O onto the TiO<sub>2</sub> surface. The FTIR spectra of ethanol in the dark shows the coexistence of ethanol adsorption both, in molecular and in dissociation forms. Under UV(A) illumination the typical EtOH bands decreased on the surface while the adsorption of water and D<sub>2</sub>O increased. Several mechanisms reported in the literature can explain this behavior, such as replacement of surface impurities that are photocatalytically destroyed, exchange of adsorbed water molecules by thermal desorption of ethanol and increase of hydroxylation by augmentation of surface area due to the deaggregation of particles agglomerates.

### 3.6 Acknowledgements

Belhadj H. gratefully acknowledges a scholarship from the Deutscher Akademischer Austauschdienst (DAAD) providing the financial support to perform his Ph.D. studies in Germany. The present study was performed within the Project “Establishment of the Laboratory ‘Photoactive Nanocomposite Materials’” No. 14.Z50.31.0016 supported by a Mega-grant of the Government of the Russian Federation.

### 3.7 References

- 1 J. Schneider, M. Matsuoka, M. Takeuchi, J. Zhang, Y. Horiuchi, M. Anpo and D. W. Bahnemann, *Chem. Rev.*, 2014, **114**, 9919–9986.
- 2 L. M. Liu, P. Crawford and P. Hu, *Prog. Surf. Sci.*, 2009, **84**, 155–176.
- 3 T. Hirakawa and Y. Nosaka, *Langmuir*, 2002, **18**, 3247–3254.
- 4 H. Irie, K. Hashimoto, *Environmental Photochemistry Part II*, 2005, vol. 2M.
- 5 P. K. J. Robertson, D. W. Bahnemann, J. M. C. Robertson and F. Wood, in *Environmental Photochemistry Part II*, Springer-Verlag, Berlin/Heidelberg, 2005,

- vol. 2, pp. 367–423.
- 6 C. Wang, R. Pagel, J. K. Dohrmann and D. W. Bahnemann, *Comptes Rendus Chim.*, 2006, **9**, 761–773.
  - 7 S. J. Hug and B. Sulzberger, *Langmuir*, 1994, **10**, 3587–3597.
  - 8 J. C. Duplan, L. Mahi and J. L. Brunet, *Chem. Phys. Lett.*, 2005, 413, 400–403.
  - 9 H. Belhadj, A. Hakki, P. K. J. Robertson and D. W. Bahnemann, *Phys. Chem. Chem. Phys.*, 2015, **17**, 22940–22946.
  - 10 T. Zubkov, D. Stahl, T. L. Thompson, D. Panayotov, O. Diwald and J. T. Yates, *J. Phys. Chem. B*, 2005, **109**, 15454–15462.
  - 11 M. Takeuchi, G. Martra, S. Coluccia and M. Anpo, *J. Phys. Chem. C*, 2007, **111**, 9811–9817.
  - 12 J. Tan, L. Yang, Q. Kang and Q. Cai, *Anal. Lett.*, 2011, **44**, 1114–1125.
  - 13 Z. Yu and S. S. C. Chuang, *J. Catal.*, 2007, **246**, 118–126.
  - 14 S. Corsetti, F. M. Zehentbauer, D. McGloin and J. Kiefer, *Fuel*, 2015, **141**, 136–142.
  - 15 Z. Ma, Q. Guo, X. Mao, Z. Ren, X. Wang, C. Xu, W. Yang, D. Dai, C. Zhou, H. Fan and X. Yang, *J. Phys. Chem. C*, 2013, **117**, 10336–10344.
  - 16 A. V. Stuart and G. B. B. M. Sutherland, *J. Chem. Phys.*, 1956, **24**, 559–570.
  - 17 D. Gong, V. P. Subramaniam, J. G. Highfield, Y. Tang, Y. Lai and Z. Chen, *ACS Catal.*, 2011, **1**, 864–871.
  - 18 Y. Wu, Y. Li and Q. Zhuang, *J. Photochem. Photobiol. A Chem.*, 1991, **62**, 261–267.
  - 19 W.-C. Wu, C.-C. Chuang and J.-L. Lin, *J. Phys. Chem. B*, 2000, **104**, 8719–8724.
  - 20 C. A. Walenta, S. L. Kollmannsberger, J. Kiermaier, A. Winbauer, M. Tschurl and U. Heiz, *Phys. Chem. Chem. Phys.*, 2015, **17**, 22809–22814.
  - 21 S. H. Szczepankiewicz, a J. Colussi and M. R. Hoffmann, *J. Phys. Chem. B*, 2000, **104**, 9842–9850.
  - 22 C. B. Mendive, D. Hansmann, T. Bredow and D. Bahnemann, *J. Phys. Chem. C*, 2011, **115**, 19676–19685.
  - 23 L. Gamble, L. S. Jung and C. T. Campbell, *Surf. Sci.*, 1996, **348**, 1–16.

## Chapter 4

### **Pathways of the Photocatalytic Reaction of Acetate in H<sub>2</sub>O and D<sub>2</sub>O: A Combined EPR and ATR-FTIR Study**

Hamza Belhadj<sup>a,\*</sup>, Stephanie Melchers<sup>a</sup>, Peter K. J. Robertson<sup>b</sup> and Detlef W. Bahnemann<sup>a,c,\*</sup>

<sup>a</sup>Institut für Technische Chemie, Leibniz Universität Hannover, Callinstraße 3, D-30167 Hannover, Germany.

<sup>b</sup>Centre for the Theory and Application of Catalysis (CenTACat), School of Chemistry and Chemical Engineering, Queen's University Belfast, Stranmillis Road, Belfast, BT9 5AG, UK.

<sup>c</sup>Laboratory “Photoactive Nanocomposite Materials”, Saint-Petersburg State University, Ulyanovskaya str. 1, Peterhof, Saint-Petersburg, 198504 Russia.

Published in Journal of Catalysis, 344 (2016) 831–840.

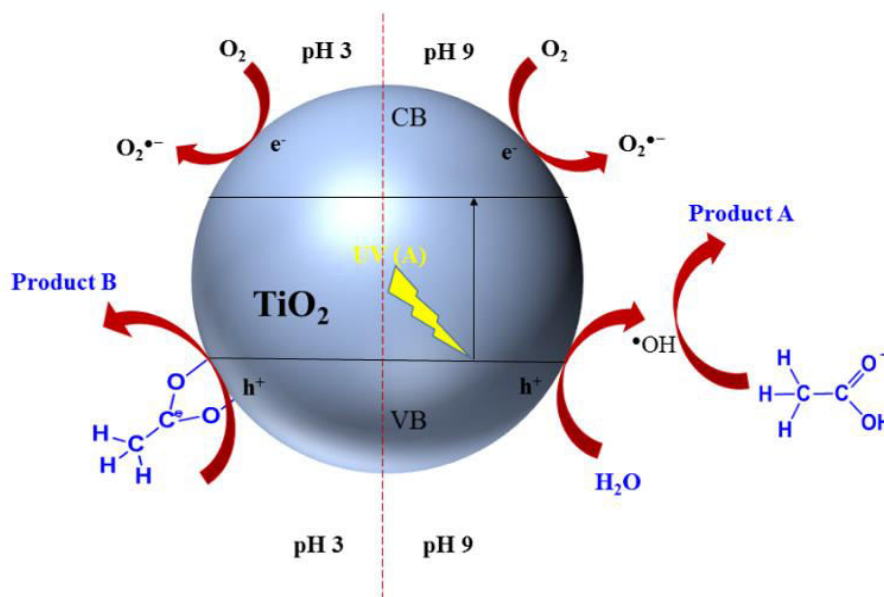
DOI: 10.1016/j.jcat.2016.08.006.

## 4 Pathways of the Photocatalytic Reaction of Acetate in H<sub>2</sub>O and D<sub>2</sub>O: A Combined EPR and ATR-FTIR Study

### 4.1 Abstract

The adsorption and photocatalytic degradation of acetate on TiO<sub>2</sub> surfaces was investigated in H<sub>2</sub>O and D<sub>2</sub>O by ATR-FTIR and EPR Spectroscopy respectively. These studies were carried out in the dark and under UV(A) illumination to gain additional insights into the adsorption behaviour with the identification of paramagnetic species formed during the oxidation of acetate. Isotopic exchange during the adsorption of D<sub>2</sub>O on TiO<sub>2</sub> surface led to different interactions between the adsorbate and OD groups. At different pH levels, several surface complexes of acetate can be formed such as monodentate, or bidentates. Under UV(A) irradiation of TiO<sub>2</sub> aqueous suspensions, the formation of hydroxyl and methoxy radicals evidenced as the corresponding spin-adducts, were found to dominate in alkaline and acidic suspensions respectively. Two possible pathways for the oxidation of acetate have been suggested at different pH levels in solution in terms of the source of the spin adduct formed. These proposed pathways were found to be in good agreement with ATR-FTIR and EPR results.

**Keywords:** TiO<sub>2</sub>, Acetate, Adsorption, D<sub>2</sub>O, pH, Photocatalysis, *In-situ* ATR-FTIR, EPR spin trapping.





## 4.2 Introduction

Titanium dioxide, ( $\text{TiO}_2$ ), is an effective photocatalyst for the degradation of a broad range of organic pollutants [1]. The photocatalytic oxidation processes of organic pollutants is initiated by the formation of valence band holes ( $\text{h}^+_{\text{vb}}$ ) and conduction band electrons ( $\text{e}^-_{\text{cb}}$ ) which are formed in a  $\text{TiO}_2$  particle upon ultra band gap illumination. Consequently, the  $\text{TiO}_2$  particles act as electron donors and electron acceptors for molecules in the surrounding medium. For example, the holes may react with water and/or hydroxyl ions to form hydroxyl radicals, while the excited electrons react with molecular oxygen to form superoxide radicals and hydrogen peroxide [2]. It was previously reported that the oxidation of organic pollutants on the surface of  $\text{TiO}_2$  proceeds via two pathways [3]. One pathway involves photogenerated holes that oxidize adsorbed pollutant species directly. In the second pathway, pollutants are oxidized indirectly by free radicals produced at the  $\text{TiO}_2$  surface.

Acetic acid/acetate has been used as the model pollutant by many research groups for the study of fundamental photocatalytic mechanisms. In oxygen free conditions, Muggli *et al*, reported that the photocatalytic decomposition of acetic acid on  $\text{TiO}_2$  resulted in the formation of  $\text{CO}_2$ , with  $\text{CH}_4$ , and  $\text{C}_2\text{H}_6$ , as intermediate products [4,5]. In aerated aqueous solution, Carraway *et al*, have shown that acetate is rapidly photooxidized on  $\text{ZnO}$  colloids to give formate and glyoxylate, as intermediate products which serve as effective electron donors on illuminated  $\text{ZnO}$  surfaces [6]. In another study, it was reported that during photocatalytic oxidation of acetic acid on platinized  $\text{TiO}_2$ , the methyl radical could be formed via two reaction pathways [4]. It was reported that in the presence of oxygen the photocatalytic degradation of acetate in a suspension of  $\text{TiO}_2$  both the holes and hydroxyl radicals acted as oxidising species and it was suggested that two types of reactions may be responsible for the  $\text{TiO}_2$  mediated photodegradation of acetate:[6]

- (i) direct hole oxidation of adsorbed acetic acid/acetate molecules by photoinduced holes ( $\text{h}^+$ ) at the valence band of  $\text{TiO}_2$  semiconductor, or/and
- (ii) indirect oxidation via hydroxyl radicals or other reactive oxygen species such as superoxide radicals and hydrogen peroxide.

In contrast, the adsorption of substrates was also one of the most important determinants for the photocatalytic degradation process. Robertson *et al*. suggested that

the direct charge transfer to organic molecules required that the scavenging molecules were adsorbed on the TiO<sub>2</sub> surface prior to the adsorption of the photon [3]. Furthermore, the adsorption behaviour of organic molecules was different during UV illumination [7]. Mendive *et al.* reported that the deaggregation of particles agglomerates occurred during UV irradiation resulting in an greater available surface area which in turn enhanced the photonic efficiency [8]. Adsorbed species such as water or molecular oxygen, together with the influence of pH are also expected to affect the degradation pathway on TiO<sub>2</sub> surface but their overall influences have yet to be clearly determined.

For a better understanding of the interfacial acetate/TiO<sub>2</sub> interactions, we have studied the adsorption of acetate on anatase surfaces (UV100) in H<sub>2</sub>O and D<sub>2</sub>O, as well as the formation of reactive oxygen species (ROS) using attenuated total reflection Fourier transform infrared (ATR-FTIR) and electron paramagnetic resonance (EPR) spectroscopy. This paper considers the effect of pH in terms of the adsorption behaviour of acetate on TiO<sub>2</sub> surfaces as well as the formation of primary intermediate radicals before and after UV(A) irradiation in order to provide further insight into the interfacial reaction mechanism of acetate decomposition during UV irradiation.

### 4.3 Experimental section

#### 4.3.1 Materials

TiO<sub>2</sub> (Hombikat UV100, 100% anatase) was kindly supplied by Sachtleben Chemie. Sodium acetate trihydrate ( $\geq 99.5\%$ ) was purchased from ROTH. The spin traps 5,5-dimethyl-1-pyrroline-N-oxide (DMPO) and Deuterium oxide (D<sub>2</sub>O) (99.9 atom% D) were purchased from Sigma Aldrich. Deionized water (H<sub>2</sub>O) was supplied from a Millipore Mill-Q system with a resistivity equal to 18.2  $\Omega$  cm at 25 °C. pH adjustments and measurements were performed using a Metrohm 691 model pH-meter using 0.5 mol L<sup>-1</sup> of HNO<sub>3</sub> or NaOH.

#### 4.3.2 ATR-FTIR Spectroscopic Measurements

##### 4.3.2.1 Preparation of TiO<sub>2</sub> film on the ATR-FTIR Crystal

Initially, an aqueous suspension of TiO<sub>2</sub> at a concentration of 5 g l<sup>-1</sup> was prepared and sonicated for 15 min in an ultrasonic cleaning bath. An aliquot of 400  $\mu$ L of the TiO<sub>2</sub>

suspension was placed on the surface of the ZnSe ATR crystal and this small volume was simply spread by balancing the unit manually. The suspension was then dried by storing the crystal in a semi-opened desiccator at room temperature. Prior to deposition of the TiO<sub>2</sub> films, the ZnSe surfaces (area = 6.8 mm×72 mm) were cleaned by polishing with 1 mm diamond paste (Metadi II, polishing grade) and rinsed with methanol and deionised water. The coverage of the final dry layer of particles obtained was 2.3 g m<sup>-2</sup> and the layer appeared to be very homogeneous under visual inspection. In the original preparation by Hug *et al*, Atomic Force Microscopy (AFM) measurements of layers with coverage of 2.3 g m<sup>-2</sup> yielded a thickness of 1-3 μm [9]. The final resulting layers of particles remained stable over the entire course of the experiment. Thus, it was assumed that the effective path lengths at all wavelengths remained unchanged.

#### 4.3.2.2 ATR FTIR measurement

The ATR-FTIR spectra of the TiO<sub>2</sub> samples were monitored by a FTIR spectrometer (IFS 66 BRUKER) equipped with an internal reflection element 45° ZnSe crystal and a deuterated triglycine sulfate (DTGS) detector. The interferometer and the infrared light path in the spectrometer were constantly purged with Argon and nitrogen to avoid H<sub>2</sub>O and CO<sub>2</sub> contamination. The spectra were recorded with 300 scans at 4 cm<sup>-1</sup> resolution and analyzed using OPUS version 6.5 software.

Irradiation of samples with UV(A) light were carried out using an LED lamp (Model LED-Driver, THORLABS) emitting UV light (365 nm). The distance from the UV lamp to the surface of the test solution was kept 30 cm on which the intensity of UV(A) light was of 1.0 mWcm<sup>-2</sup> as measured by UV radiometer (Dr. Honle GmbH, Martinsried, Germany). In order to observe the interaction between water/deuterium oxide and acetate at TiO<sub>2</sub>/aqueous solution interface, a first infrared spectrum was taken as a reference background. Prior to starting the irradiation experiments, spectra of adsorption of acetate (10<sup>-1</sup> M) with H<sub>2</sub>O or D<sub>2</sub>O on the TiO<sub>2</sub> were monitored in the dark. When the last spectrum of each experiment had been recorded in the dark, the UV(A) lamp was turned on and another sequence of spectra was recorded.

### 4.3.3 EPR measurement

EPR spectra were recorded at room temperature on a MiniScope X-band EPR spectrometer (MS400 Magnettech GmbH, Germany) operating at 9.41 GHz field modulation. The acquisition parameters were as follows: centre field: 335.4086 mT, sweep time 60 s, number of points: 4096, number of scan: 1, modulation amplitude: 0.2 mT, power: 10 mW, gain: 5. The experimental EPR spectra acquisition and simulation was carried out using MiniScope and Winsim 2002 software.

The samples for EPR measurements were prepared as follows:  $\text{TiO}_2$  ( $1\text{g L}^{-1}$ ) was suspended in water or  $\text{D}_2\text{O}$  with concentration of acetate ( $10^{-3}\text{ M}$ ). The solution (10 ml) was stirred for at least 30 min in the dark to allow equilibration of the system. Before the measurement, 1 mL of  $10^{-3}\text{ M}$  acetate was introduced into the eppendorf tube and then 200  $\mu\text{L}$  of 20 mM of DMPO was immediately added to the solution. The tube was shaken by hand to ensure homogenization of the sample. Subsequently, approximately 500  $\mu\text{L}$  of this sample was immediately transferred into quartz flat cell cuvette (FZK 160-7 $\times$ 0.3) designed for EPR analysis. The samples were irradiated directly in the EPR spectrometer microwave cavity by a spot UV-light (LC8, Hamamatsu, 200 W super-quiet mercury-xenon lamp) through the quartz window of the cell for the experiments.

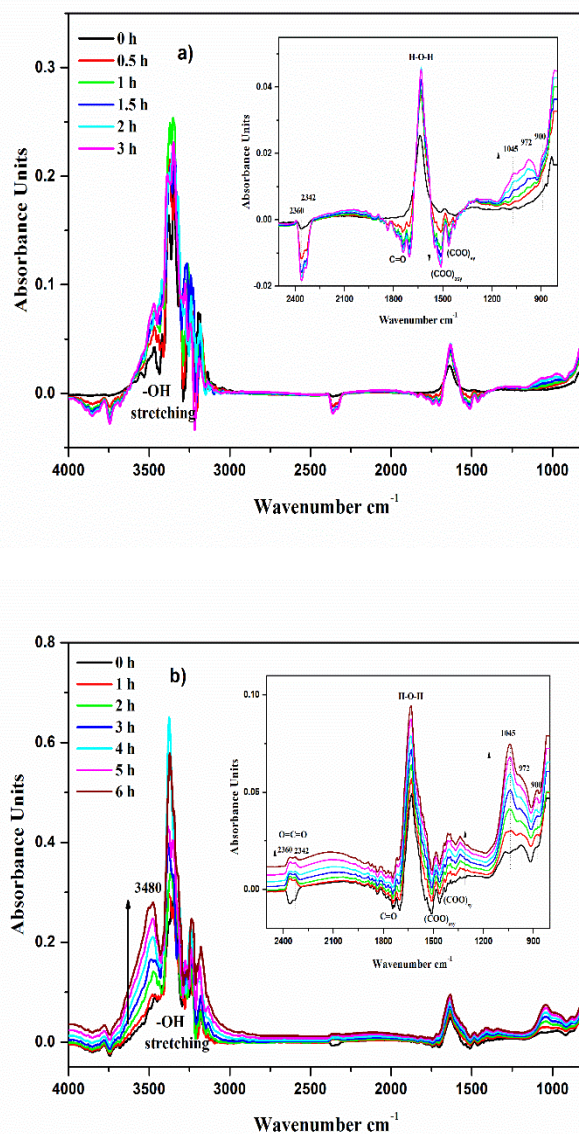
## 4.4 Results

### 4.4.1 ATR-FTIR study

#### 4.4.1.1 Adsorption of acetate in $\text{H}_2\text{O}$ and $\text{D}_2\text{O}$ on $\text{TiO}_2$

Fig. 1 and 2 show the time evolution of the spectra of adsorbed acetate on  $\text{TiO}_2$  in  $\text{H}_2\text{O}$  (pH 6.0) and  $\text{D}_2\text{O}$  (pD 6.4) [10] respectively in the dark (a) and under UV(A) irradiation (b). The inserted figures show the time evolution of the ATR-FTIR spectral region at  $2500\text{-}800\text{ cm}^{-1}$  (Fig.1) and  $2000\text{-}800\text{ cm}^{-1}$  (Fig.2) where typical bands assigned to acetate anions can be clearly observed. The two most prominent peaks of the adsorbed acetate at  $1450\text{-}1400$  and  $1600\text{-}1545\text{ cm}^{-1}$  are the symmetric and asymmetric stretching frequencies of the carboxylate ion ( $\nu_{\text{sy}}\text{ COO}$  and  $\nu_{\text{asy}}\text{ COO}$ ) respectively [11]. Since the first infrared spectrum (water and acetate) was used as the background, a negative band of water bending mode was observed. The carbonyl zone was also observed from 1700 to

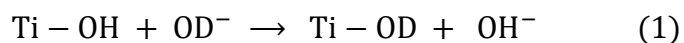
1500  $\text{cm}^{-1}$ , and included C=O and O–C=O stretching modes [12]. However, these bands are obscured by relatively strong negative  $\delta_{\text{HOH}}$  at 1638  $\text{cm}^{-1}$  which are very similar to those obtained by other workers [13],[14]. The bands at 1045  $\text{cm}^{-1}$  have previously been assigned in the literature to rocking  $\text{CH}_3$  vibrations[15,16] whereas the bands at 925-975 and 900  $\text{cm}^{-1}$  can be assigned, respectively to C-C and OH bending [11,17,12].



**Fig. 1.** Time evolution of the ATR–FTIR spectra of adsorbed acetate in the presence of  $\text{O}_2$  on  $\text{TiO}_2$  at pH 6.0 a) in the dark for 3 h, b) under 6 h of UV(A) illumination.

On the other hand the adsorption of  $\text{H}_2\text{O}$  and  $\text{D}_2\text{O}$  take place on the  $\text{TiO}_2$  surface which is represented by strong IR absorbance of the OH stretching ( $3000\text{-}3600\text{ cm}^{-1}$ ) and OD

stretching regions (2300-2700). In addition the bands at  $1638\text{ cm}^{-1}$  and  $1205\text{ cm}^{-1}$  can be assigned to the molecular bending modes of  $\text{H}_2\text{O } \delta$  (H–O–H) and  $\text{D}_2\text{O } \delta$  (D–O–D), respectively. It can be clearly seen from figure (Fig. 1a) that in the dark typical bands of adsorbed water as well as the band centred at  $1045\text{ cm}^{-1}$ , which is assigned to the  $\text{CH}_3$  group, have increased. A strong decrease in the intensities of carboxylate group, however, have also been detected. This negative band indicates the decrease in the IR intensity ( $I$ ) with respect to  $I_0$  due to the background subtraction [18,14,19]. The band observed at  $2360$  and  $2342\text{ cm}^{-1}$  was assigned to the  $\text{CO}_2$  group which decreased due to the desorption of molecular  $\text{CO}_2$  contamination [8]. When  $\text{D}_2\text{O}$  was used instead of water, the shifting of  $\text{D}_2\text{O}$  band bending at  $1205\text{ cm}^{-1}$  revealed the same vibrational bands that corresponded to the symmetric and antisymmetric  $\nu$  ( $\text{COO}^-$ ) stretching vibrations (Fig. 2a). Furthermore, the intensity of the band of  $\text{D}_2\text{O}$  adsorption (OD stretching, D–O–D bending) also increased. Surprisingly, unlike the case of water adsorption, the intensity of the band assigned to  $\text{CH}_3$  at  $1045\text{ cm}^{-1}$  and OH bending at  $900\text{ cm}^{-1}$  gradually decreased during the dark period. These results indicate that adsorption of  $\text{D}_2\text{O}$  on  $\text{TiO}_2$  surfaces clearly affects the behaviour of acetate adsorption. Additionally, it is obvious from the spectra that the intensity of the OH-stretching band centred at  $3269\text{ cm}^{-1}$  decreased gradually in the dark (Fig. 2a). Our previous study reported that in the dark the deuterated ion showed a stronger adsorption than hydroxyl ions on the surface of  $\text{TiO}_2$ , resulting in an isotopic exchange by replacing hydroxyl groups adsorbed on the  $\text{TiO}_2$  surface (reaction 1) with OD groups [20].



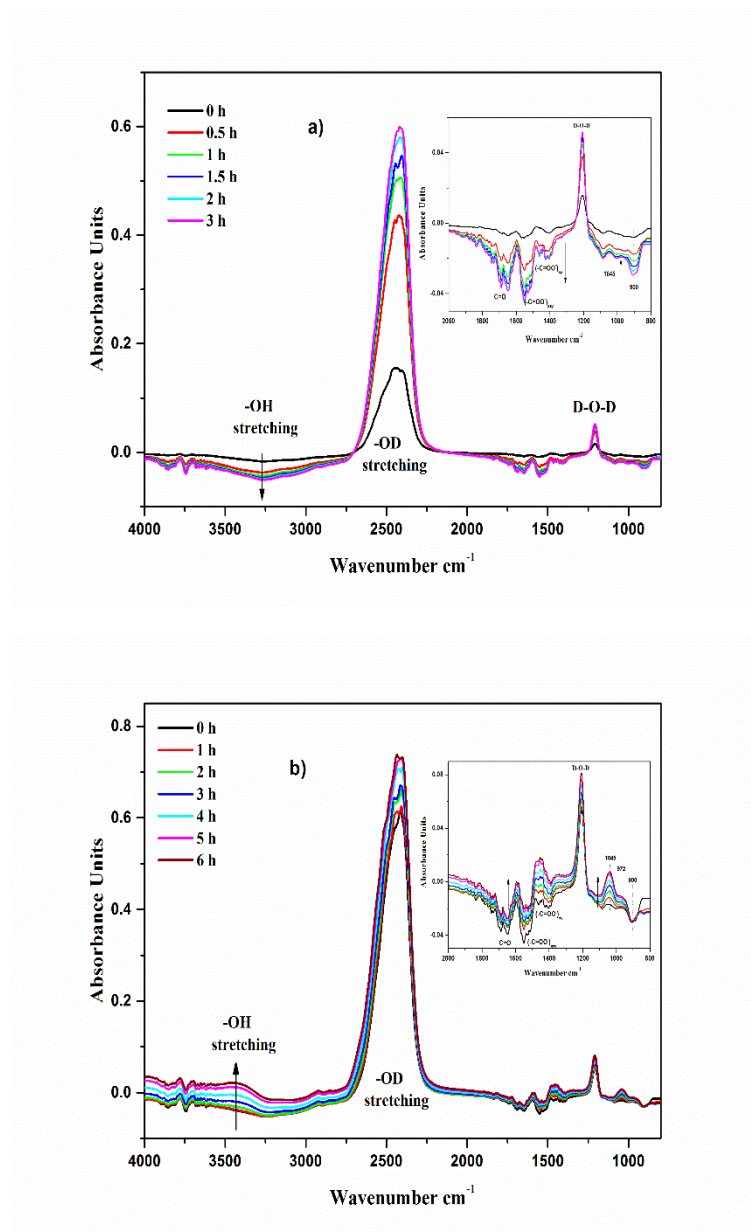


**Fig. 2.** Time evolution of the ATR-FTIR spectra of adsorbed acetate in D<sub>2</sub>O in the presence of O<sub>2</sub> on TiO<sub>2</sub> at pD 6.4 a) in the dark for 3 h, b) under 6 h of UV(A) illumination.

When the system was subsequently illuminated with UV(A) light in presence of oxygen, the intensity of the typical bands assigned to the acetate anions in H<sub>2</sub>O (Fig. 1b) and D<sub>2</sub>O (Fig. 2b) increased. The upward baseline shift following irradiation was interpreted as transient and persistent diffuse reflectance infrared signals due to the population of conduction band electrons upon irradiation of TiO<sub>2</sub> particles, where the baseline IR absorption for TiO<sub>2</sub> rises immediately upon UV irradiation [21,14].

Meanwhile, the band at  $1045\text{ cm}^{-1}$  assigned to the  $\text{CH}_3$  rocking vibration increased and appeared to be stronger in water than in  $\text{D}_2\text{O}$ , with a shoulder at  $972\text{ cm}^{-1}$  which could be assigned to the C-C band. Interestingly, although the interferometer was constantly purged with argon and nitrogen to avoid  $\text{H}_2\text{O}$  and  $\text{CO}_2$  contamination, the intensity of the band assigned to  $\text{CO}_2$  increased during UV(A) illumination. Furthermore in the region of OH stretching (Fig. 1b), an increase of the band at  $3480\text{ cm}^{-1}$  was observed which could be assigned to the formation of  $\text{H}_2\text{O}_2$  [20]. Conversely, as shown in Fig. 2b, the OH stretching band increased and shifted towards a higher wavenumber ( $3480\text{ cm}^{-1}$ ) during UV(A) irradiation. These indicate the formation of these band can be attributed to photocatalytically generated  $\text{CO}_2$  and  $\text{H}_2\text{O}_2$  as photoproducts.

#### 4.4.1.2 Effect of pH

Figs. 3 and 4 show the evolution of the adsorbed acetate spectra in the dark a) and under UV(A) irradiation b) over time at pH 3 and 9 respectively. The pH values of the solution during UV (A) irradiation have been recorded (Table S1, Supplementary Information). In the IR spectrum, a similar adsorption behaviour with respect to the water band was observed in the dark. In contrast, the behaviour of acetate adsorption depended strongly on the solution pH. At pH 3 the band centred at  $1066\text{ cm}^{-1}$  which includes the  $\text{CH}_3$  vibration, showed a higher intensity compared to that observed at pH 9 where the band shifted and centred with a lower intensity at  $964\text{ cm}^{-1}$  (Fig. 4a). The shifting of the absorption maximum with lower intensity can be explained by the interaction of the carboxylate ions with protons resulting in a small OH bending band at  $900\text{ cm}^{-1}$ .



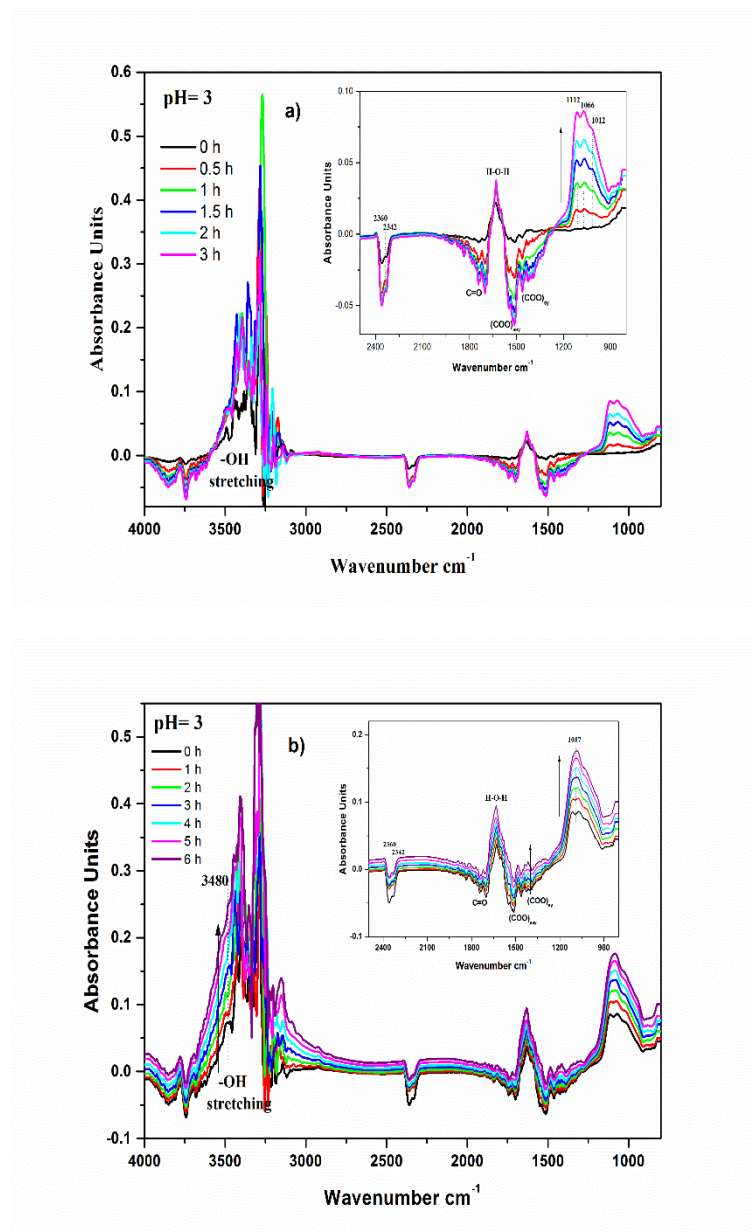


**Fig. 3.** Time evolution of the ATR-FTIR spectra of adsorbed acetate in the presence of  $O_2$  on  $TiO_2$  at pH 3, a) in the dark for 3 h, b) under 6 h of UV(A) illumination.

The spectral development of acetate adsorption under UV illumination at pH 3 and 9 are shown in Figs. 3b and 4b, respectively. The symmetric and asymmetric stretching vibrations of carboxylate ions increased during UV irradiation. As can be seen clearly in the region of OH stretching the band at  $3480\text{ cm}^{-1}$  assigned to Ti-OOH also increased during UV irradiation in acid and alkaline solutions. The behaviour of the  $CO_2$  bands at  $2360$  and  $2342\text{ cm}^{-1}$ , however, are clearly different. It is worth noting that at pH 6 (Fig.

1b) and pH 9 (Fig. 4b) the CO<sub>2</sub> band increased while at lower pH (Fig. 3b) the band decreased during UV(A) illumination. These results indicate that the photocatalytic reactions on the TiO<sub>2</sub> surfaces are different and depend strongly on the solution pH.

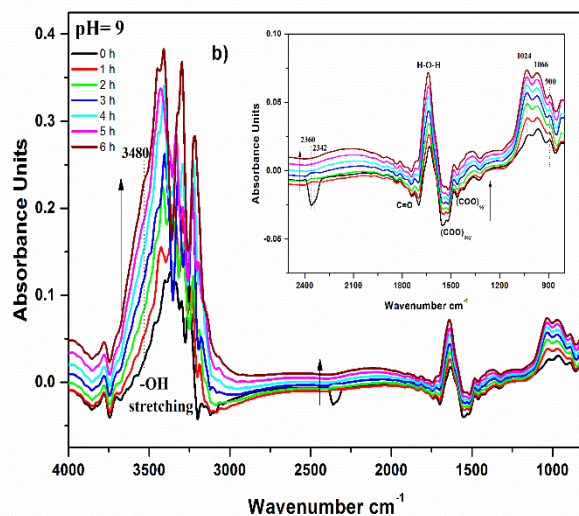
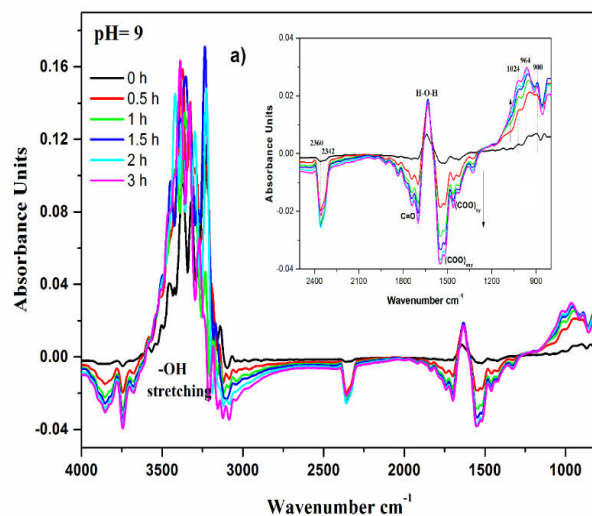
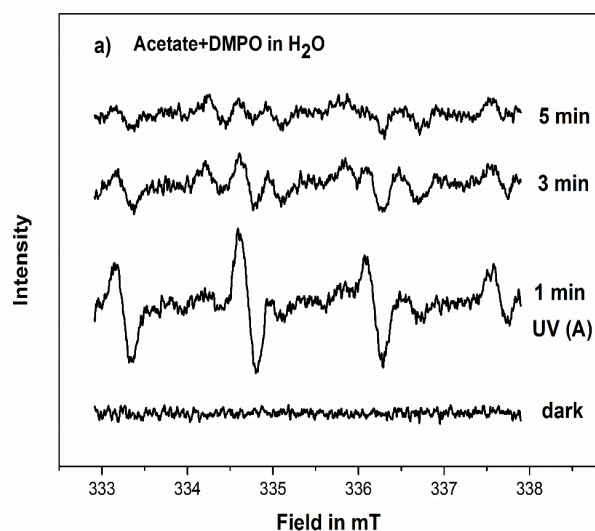


**Fig. 4.** Time evolution of the ATR-FTIR spectra of adsorbed acetate in the presence of O<sub>2</sub> on TiO<sub>2</sub> at pH 9, a) in the dark for 3 h, b) under 6 h of UV(A) illumination.

## 4.4.2 EPR study

### 4.4.2.1 EPR spin-trapping studies of radicals generated

The EPR spin-trap technique was employed using DMPO as a spin-trapping agent to probe the nature of the reactive oxygen species generated during the degradation of acetate in the presence of molecular oxygen. Fig. 5 shows the time course EPR spectra monitored by DMPO (spin-trap) at pH 6.0 in water (a) and pD 6.4 in D<sub>2</sub>O (b) before and after UV(A) irradiation. As shown in Fig. 5, no EPR signals were observed in H<sub>2</sub>O and D<sub>2</sub>O when the reaction was performed in the dark. In contrast, under UV irradiation the photoexcitation of acetate (10<sup>-3</sup>M) in TiO<sub>2</sub> aqueous suspensions in the presence of DMPO spin trap leads to the production of a four-line of EPR signal (with approximate intensities 1:2:2:1) in both H<sub>2</sub>O and D<sub>2</sub>O. The quartet peak intensity of the DMPO adduct with a 1:2:2:1 intensity in H<sub>2</sub>O as well as in D<sub>2</sub>O were virtually identical (Fig. 5b). The hyperfine parameters for the two DMPO adducts are:  $a_N = 1.477$  mT,  $a_H = 1.485$  mT,  $g = 2.0057$ ; for the DMPO-OH adducts these are  $a_N = 1.477$  mT,  $a_H = 1.485$  mT,  $g = 2.0057$ . The DMPO-OH or DMPO-OD adducts are detailed in Fig. S1, (Supplementary Information). To take into account the presence of isotopic exchange ( $\text{Ti-OH} + \text{OD}^- \rightarrow \text{Ti-OD} + \text{OH}^-$ ) before UV(A) illumination, leads to the suggestion that these quartet peaks are assigned to a DMPO-OD adduct, which can be formed by oxidation of the D<sub>2</sub>O or OD group [22]. It can be clearly observed, however, that after 1 min irradiation the intensity of the peaks gradually decreased.



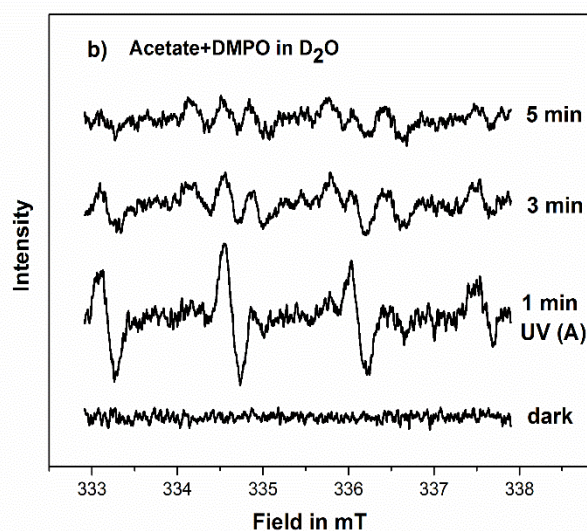


**Fig. 5.** DMPO spin-trapping EPR spectra in the dark and under UV(A) irradiation at pH 6.0 in water (a) DMPO-OH ( $a_N = 1.477$  mT,  $a_H = 1.485$  mT;  $g = 2.0057$ ) and pD 6.4 in D<sub>2</sub>O (b) DMPO-OD ( $a_N = 1.477$  mT,  $a_H = 1.485$  mT;  $g = 2.0057$ ).

Fig. 6 shows the EPR spectra observed during the photocatalytic reaction at pH 9 (Fig. 6a) and pH 3 (Fig. 6b). As can be seen in the dark, such signals were not detected at either pH 9 or pH 3. When the sample was exposed to UV(A) irradiation at pH 9, however, four characteristic peaks of the DMPO-OH• adduct were observed with a maximum intensity after 3 min of irradiation which exhibits a hyperfine splitting constant  $a_N = 1.475$  mT,  $a_H = 1.481$  mT and  $g$ -value = 2.0057 (Fig. S2, Supplementary Information). After that the EPR signal of DMPO-OH• completely decayed towards zero with continued UV irradiation (Fig. 6a). In contrast, at pH 3 (Fig. 6b), several peaks are formed. Due to spin-spin interactions these characteristic peaks might be assigned to a mixture of spin adducts of DMPO-•OOH/O<sub>2</sub>•<sup>-</sup> [23,24] and DMPO-OCH<sub>3</sub> spin-adducts [25]. Brezova' *et al* reported that the DMPO-•OOH/O<sub>2</sub>•<sup>-</sup> spin adducts have very low stability and are converted to DMPO-OH• in aqueous media [26]. The simulation analysis of the experimental EPR spectra (Fig. S3, Supplementary Information) revealed the interaction of EPR signals attributed to DMPO-OH ( $a_N = 1.475$  mT,  $a_H = 1.475$  mT;  $g = 2.0057$ ) and DMPO-OCH<sub>3</sub> ( $a_N = 1.452$  mT,  $a_H = 1.091$  mT ;  $a_H^\gamma = 0.121$  mT;  $g = 2.0057$ ). The EPR spectrum corresponding to the DMPO-OH• are clearly observed. Therefore, the other-line EPR signal is most likely to be attributed to the DMPO-OCH<sub>3</sub> spin-adducts, which

increased during the first 3 min of UV(A) irradiation. The hyperfine splitting constants of the methoxy radicals (DMPO-OCH<sub>3</sub>) are similar to those reported by Zhu *et al.*[27] (Table S2, Supplementary Information). Furthermore, it was reported that methyl radicals may react immediately with molecular oxygen resulting in the generation of peroxomethyl radicals serving as a source of •DMPO–OCH<sub>3</sub> spin-adducts [26, 28]. Time dependent EPR spectra show that after 3 min of irradiation the signal intensity of the DMPO-OH and DMPO–OCH<sub>3</sub> adducts decrease during oxidation of acetate. These results clearly show the existence of different radical intermediates representing respectively, spin adducts of DMPO-OH• and DMPO-OCH<sub>3</sub> at pH 9 and pH 3, which would provide new insight into the mechanism of oxidation of acetate at different pH levels.

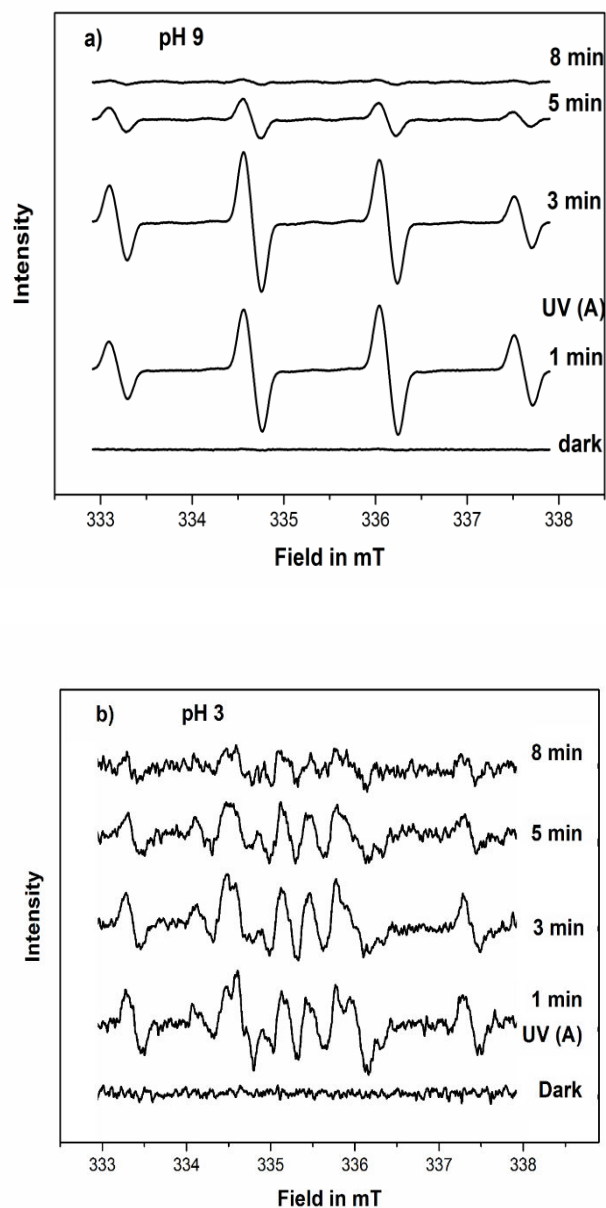


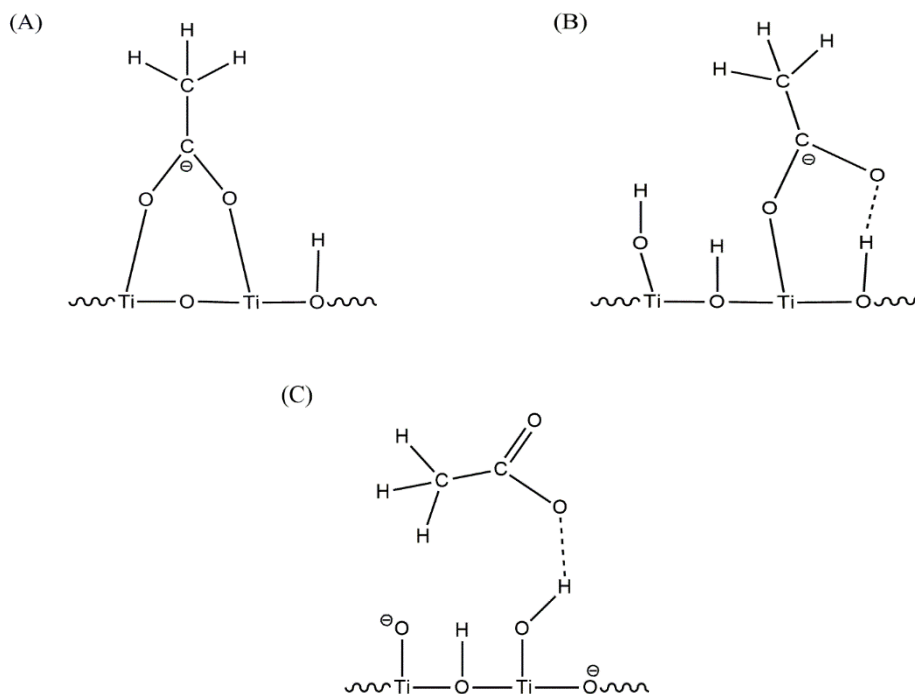
**Fig. 6.** DMPO spin-trapping EPR spectra in the dark and under UV(A) irradiation at pH 9 (a) DMPO-OH ( $a_N = 1.475$  mT,  $a_H = 1.481$  mT;  $g = 2.0057$ ) and pH 3 (b) DMPO-OH adducts ( $a_N = 1.475$  mT,  $a_H = 1.475$  mT;  $g = 2.0057$ ) and DMPO-OCH<sub>3</sub> adducts ( $a_N = 1.452$  mT,  $a_H = 1.091$  mT;  $a_H^\gamma = 0.121$  mT;  $g = 2.0057$ ).

#### 4.5 Discussion

The photocatalytic activity for the decomposition of acetate depends strongly on two factors: the adsorption behaviour of acetate on TiO<sub>2</sub> surface and the effect of reactive oxygen species formed as part of the process. Therefore, it is important to elucidate the

adsorption behaviour of acetate before and after UV(A) irradiation. As shown in Figs. 1 and 2, the spectrum of acetate adsorbed in the dark in H<sub>2</sub>O and D<sub>2</sub>O on TiO<sub>2</sub> is characterized by two strongly negative bands at 1450–1400 and 1600–1545 cm<sup>-1</sup>, which can be assigned to symmetric  $\nu_{\text{sy}}$  (COO<sup>-</sup>) and asymmetric  $\nu_{\text{asy}}$  (COO<sup>-</sup>) stretching vibrations, respectively. It is important to consider, however, that during the adsorption of acetate the adsorption of H<sub>2</sub>O and D<sub>2</sub>O yielded positive peaks (Figs. 1 and 2). Guan *et al.* remarked upon a competitive reaction between the adsorption of water and organic compounds, which was dominated by the water adsorption because of the surface acidity [29]. On the other hand, Rotzinger *et al.* have reported that the adsorption of acetate on TiO<sub>2</sub> surface led to a specific reversible interaction of the carboxylate group with the TiO<sub>2</sub> surface [12]. Three different possibilities for the adsorption of carboxylate groups on TiO<sub>2</sub> surfaces have been proposed [12,30,31]: (i) As a bidentate structure, where both oxygen atoms bind to the same Ti atom. (ii) As monodentate replacing the basic OH group at the surface. (iii) As bidentate structure (bridging carboxylate) involving the carboxyl group and two Ti centres from the surface. The behaviour of acetate adsorption, however, is strongly influenced by the solution pH [30]. As can be seen clearly at pH 3 (Fig. 3a), the band centred at 1066 cm<sup>-1</sup> which includes the CH<sub>3</sub> vibration increased in the dark compared to at pH 9 where the band shifted and centred with a lower intensity at 964 cm<sup>-1</sup> (Fig. 4a). These results indicate that at pH < pH<sub>zpc</sub> the interaction of TiO<sub>2</sub> with anions are favoured resulting in the formation of a bidentate structure involving two distinct Ti atoms (Scheme 1A). Recent theoretical work by Thornton *et al.* [32] has shown that the adsorption of acetic acid on anatase TiO<sub>2</sub> is more likely to be a bidentate structure. Nevertheless, as can be seen from the ATR-FTIR spectra in D<sub>2</sub>O at neutral (pH ≈ pH<sub>zpc</sub>), isotopic exchange (reaction 1) had a clear effect on the behaviour of adsorbed acetate, where the intensity of OH bending at 900 cm<sup>-1</sup> decreased and ultimately disappeared in the dark (Fig. 2a). The disappearance of this band would suggest an interaction between the carboxylate and OD group resulting in a reduction of the amount of OH bending (Scheme S1, Supplementary Information). These results indicate that at pH values next to the pH<sub>zpc</sub>, the acetate preferentially adsorbs on the positively charged anatase in the monodentate structure. This is facilitated by the presence of the hydrogen atom, which interacts with OH groups in the vicinity and these interactions are less intense due to the

weakly charged surface (Scheme 1B). Whereas at higher pH (Fig. 4a), the negative charged surface repulse the negative charged acetate anions resulting weak bonds such as hydrogen bonds or dipole-dipole interactions. (Scheme 1C).



**Scheme 1.** Schematic representation for the adsorption of acetate on anatase surface (UV100) in the dark at  $\text{pH} < \text{pH}_{\text{zpc}}$  (A),  $\text{pH} \approx \text{pH}_{\text{zpc}}$  (B),  $\text{pH} > \text{pH}_{\text{zpc}}$  (C).

Upon UV(A) irradiation an excited electron and positive hole are formed. The electron and hole may migrate to the catalyst surface where they can participate in redox reactions with adsorbed species. As can be seen in figs. 1b and 2b, the typical bands of adsorbed acetate as well as the bands of  $\text{H}_2\text{O}$  and  $\text{D}_2\text{O}$  adsorption have increased during UV irradiation. Wang et al. revealed the fact that under UV(A) illumination the total exposed  $\text{TiO}_2$  surface increases due to the de-aggregation of particles agglomerates which was explained by assuming that part of the absorbed light energy is converted non-adiabatically into heat which is subsequently used to break the bonds between the particles thus producing additional surface area for the photocatalytic process [7]. Recently, we have shown that the excitation of  $\text{TiO}_2$  by UV light leads to an increase in the amount of adsorbed  $\text{H}_2\text{O}$  and  $\text{D}_2\text{O}$  in presence of oxygen by a photoinduced charge transfer process [20]. From this point of view the adsorption behaviour of acetate as well as the adsorption of intermediates formed during UV irradiation needs to be taken into account. This

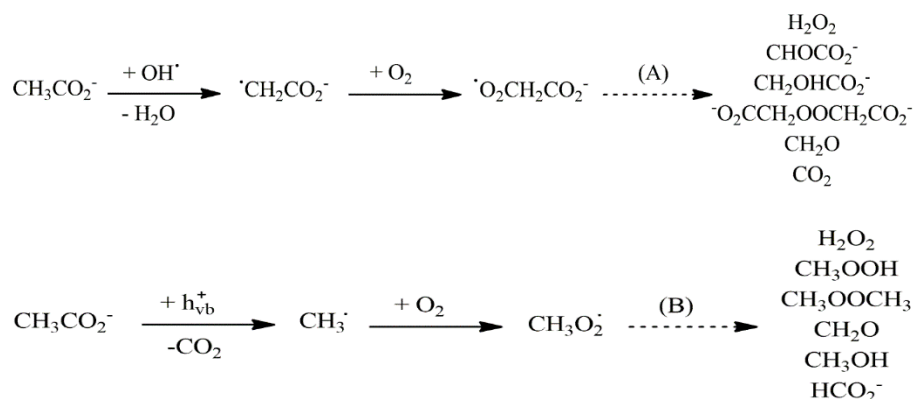


assumption was confirmed by increasing again the typical bands of adsorbed acetate during UV (A) illumination (Fig. 1b). As shown in Fig. 2b, unlike the case of water, at  $900\text{ cm}^{-1}$  no increase of OH bending band have been detected in  $\text{D}_2\text{O}$  (Fig. 2b). This fact may interpreted as a new rearrangement of acetate adsorption resulting in the shift of OD band bending to lower frequency ( $< 800\text{ cm}^{-1}$ ). Thus, the formation of OH band bending was not possible anymore as schematically illustrated in Fig. 2b. Furthermore the intensity of the band of  $\text{CH}_3$  formed at  $1045\text{ cm}^{-1}$  is lower in  $\text{D}_2\text{O}$  compared in  $\text{H}_2\text{O}$  during UV irradiation. These results indicate a specific interaction of  $\text{D}_2\text{O}$  or /and OD group with intermediates on the  $\text{TiO}_2$  surface during the degradation of acetate.

The effect of pH revealed the formation of the  $\text{CO}_2$  bands at  $2360$  and  $2342\text{ cm}^{-1}$  as well as the  $\text{H}_2\text{O}_2$  band at  $3480\text{ cm}^{-1}$  at  $\text{pH} > \text{pH}_{\text{zpc}}$ , (Figs. 1b and 4b), which can be considered as evidence for such adsorption intermediates being formed during oxidation of acetate. Interestingly, no formation of the  $\text{CO}_2$  band was observed at pH 3 (Fig. 3b). From these results we suggest that the pathway for the degradation of acetate during UV irradiation is different and related to the pH of the solution. It was reported that the degradation rates of acetic acid depend strongly on the pH of the suspension. Carraway *et al.*, reported that on acidic suspensions, formate and formaldehyde have been detected as the only products of the photocatalytic oxidation of acetate, while in alkaline suspensions, the main products are glycolate and formate accompanied by smaller amounts of glyoxylate and formaldehyde [6].

The EPR investigation showed that in alkaline suspensions, upon photoexcitation of  $\text{TiO}_2$  in water, hydroxyl radicals are formed and this was confirmed by the addition of DMPO into the suspensions. This resulted in a significant increase of the DMPO–OH adduct EPR intensity (Fig. 6a). In contrast at lower pH levels, (pH 3) the signal intensity of hydroxyl radicals was negligible compared to that at pH 9 (Fig. 6b). These results suggest that at pH 9 the degradation of acetate mainly occurred by indirect oxidation via hydroxyl radical attack. Thus, the decrease of pH values of the solution only at pH 9 during UV(A) irradiation (Table S1, Supplementary Information) indicate that in alkaline solution the hydroxyl radicals are being predominately formed by oxidation of hydroxyl ions in the water layer adsorbed on  $\text{TiO}_2$  surfaces. On the other hand, Schuchmann *et al.*, have reported that the hydroxyl radicals attack acetate ions primarily at the methyl group.

The radicals that are subsequently formed react quickly with molecular oxygen leading to the formation of different products (Scheme 2A) [33,34]. The existence of  $\text{CO}_2$  and  $\text{H}_2\text{O}_2$  as products was confirmed at pH 9 by means of *in situ* ATR-FTIR spectroscopy (Fig. 4b). As can be seen clearly at pH 3, a new spin adduct of DMPO-OCH<sub>3</sub> has been also detected which was confirmed by Spin Fit simulations (Fig. S3, Supplementary Information). Fig. 6b clearly shows that UV excitation of  $\text{TiO}_2$  leads to an increase in the typical signal of methoxy radicals (DMPO-OCH<sub>3</sub>;  $a_{\text{N}} = 1.452$  mT,  $a_{\text{H}} = 1.091$  mT;  $a_{\text{H}^\gamma} = 0.121$  mT;  $g = 2.0057$ ). This observation makes clear that the oxidation of acetate at pH 3 occurs mainly through direct oxidation by the hole ( $\text{h}^+$ ) resulting in the well-known Kolbe decarboxylation with the formation of methyl radicals. Different products are then formed when these methyl radicals react with oxygen [26]. As expected at pH 3, no formation of  $\text{CO}_2$  has been detected by ATR-FTIR spectroscopy (Fig. 3b), which confirms the validity of the proposed mechanism (Scheme 2B). In general, it is obvious from these results that the adsorption behaviour of acetate as well as the adsorption of water on  $\text{TiO}_2$  surfaces play a vital role for the trapping of photogenerated charge carriers upon UV(A) irradiation, which is strongly dependent on the pH of the suspension.



**Scheme 2.** Proposed mechanism for the photocatalytic reaction of acetate at pH 9 (A) and pH 3 (B).

#### 4.6 Conclusion

As an *in-situ* technique, ATR-FTIR studies provide important evidence of the adsorption behaviour of acetate on  $\text{TiO}_2$  surfaces before and after UV(A) irradiation. The experimental results have shown that the interaction of acetate with the  $\text{TiO}_2$  surface depends strongly on the pH of the suspension. Under acidic pH conditions, the formation

of a bidentate structure involving two distinct Ti atoms is favoured due to the interaction of TiO<sub>2</sub> with anions. At pH values next to the p*H*<sub>zpc</sub>, the acetate preferentially adsorbs on the positively charged anatase in the monodentate structure. UV(A) irradiation of TiO<sub>2</sub> in the presence of molecular O<sub>2</sub> lead to the formation of H<sub>2</sub>O<sub>2</sub> and CO<sub>2</sub> as photoproducts in alkaline solutions, whereas in acidic solution, the only product of H<sub>2</sub>O<sub>2</sub> was detected. Results of the EPR study indicate that the degradation of acetate at pH 9 mainly occurred by indirect oxidation via hydroxyl radical attack whereas at pH 3 the degradation of acetate occurs via direct oxidation of surface-bound acetate by valence band holes.

#### 4.7 Acknowledgements

Belhadj H. gratefully acknowledges a scholarship from the Deutscher Akademischer Austauschdienst (DAAD) providing the financial support to perform his Ph.D. studies in Germany. The present study was performed within the Project “Establishment of the Laboratory ‘Photoactive Nanocomposite Materials’ No. 14.Z50.31.0016 supported by a Mega-grant of the Government of the Russian Federation. This work was partially funded by the German Federal Ministry of Education and Research (contract no. 13N13350, PureBau – Untersuchung von Werkstoffsystemen Für photokatalytisch hocheffiziente Baustoffe-Teilvorhaben: Oberflächenchemie der Photokatalysatoren und der Werkstoffe).

#### 4.8 References

- [1] M.R. Hoffmann, S.T. Martin, W. Choi, D.W. Bahnemann, Environmental Applications of Semiconductor Photocatalysis, *Chem. Rev.* 95 (1995) 69–96. doi:10.1021/cr00033a004.
- [2] T. Hirakawa, Y. Nosaka, Properties of O<sub>2</sub><sup>•-</sup> and OH<sup>•</sup> Formed in TiO<sub>2</sub> aqueous suspensions by photocatalytic reaction and the influence of H<sub>2</sub>O<sub>2</sub> and some ions, *Langmuir*. 18 (2002) 3247–3254. doi:10.1021/la015685a.
- [3] P.K.J. Robertson, D.W. Bahnemann, J.M.C. Robertson, F. Wood, Photocatalytic Detoxification of Water and Air, in: *Environ. Photochem. Part II*, Springer-Verlag, Berlin/Heidelberg, 2005: pp. 367–423. doi:10.1007/b138189.
- [4] D.S. Muggli, J.L. Falconer, Parallel Pathways for Photocatalytic Decomposition of Acetic Acid on TiO<sub>2</sub>, *J. Catal.* 187 (1999) 230–237. doi:10.1006/jcat.1999.2594.
- [5] D.S. Muggli, S. a Keyser, J.L. Falconer, Photocatalytic decomposition of acetic acid on TiO<sub>2</sub>, *Catal. Letters*. 55 (1998) 129–132.
- [6] E.R. Carraway, a J. Hoffman, M.R. Hoffmann, Photocatalytic oxidation of organic acids on quantum-sized semiconductor colloids., *Environ. Sci. Technol.* 28 (1994) 786–93. doi:10.1021/es00054a007.

- [7] C. Wang, R. Pagel, J.K. Dohrmann, D.W. Bahnemann, Antenna mechanism and deaggregation concept: novel mechanistic principles for photocatalysis, *Comptes Rendus Chim.* 9 (2006) 761–773. doi:10.1016/j.crci.2005.02.053.
- [8] C.B. Mendive, D. Hansmann, T. Bredow, D. Bahnemann, New insights into the mechanism of TiO<sub>2</sub> photocatalysis: Thermal processes beyond the electron-hole creation, *J. Phys. Chem. C.* 115 (2011) 19676–19685. doi:10.1021/jp112243q.
- [9] S.J. Hug, B. Sulzberger, In situ Fourier Transform Infrared Spectroscopic Evidence for the Formation of Several Different Surface Complexes of Oxalate on TiO<sub>2</sub> in the Aqueous Phase, *Langmuir.* 10 (1994) 3587–3597. doi:10.1021/la00022a036.
- [10] A. Krężel, W. Bal, A formula for correlating pK<sub>a</sub> values determined in D<sub>2</sub>O and H<sub>2</sub>O, *J. Inorg. Biochem.* 98 (2004) 161–166. doi:10.1016/j.jinorgbio.2003.10.001.
- [11] J.-J. Max, C. Chapados, Infrared Spectroscopy of Aqueous Carboxylic Acids: Comparison between Different Acids and Their Salts, *J. Phys. Chem. A.* 108 (2004) 3324–3337. doi:10.1021/jp036401t.
- [12] F.P. Rotzinger, J.M. Kesselman-Truttman, S.J. Hug, V. Shklover, M. Grätzel, Structure and Vibrational Spectrum of Formate and Acetate Adsorbed from Aqueous Solution onto the TiO<sub>2</sub> Rutile (110) Surface, *J. Phys. Chem. B.* 108 (2004) 5004–5017. doi:10.1021/jp0360974.
- [13] F. Guzman, S.S.C. Chuang, Tracing the reaction steps involving oxygen and IR observable species in ethanol photocatalytic oxidation on TiO<sub>2</sub>, *J. Am. Chem. Soc.* 132 (2010) 1502–1503. doi:10.1021/ja907256x.
- [14] D. Gong, V.P. Subramaniam, J.G. Highfield, Y. Tang, Y. Lai, Z. Chen, In situ mechanistic investigation at the liquid/solid interface by attenuated total reflectance FTIR: Ethanol photo-oxidation over pristine and platinumized TiO<sub>2</sub> (P25), *ACS Catal.* 1 (2011) 864–871. doi:10.1021/cs200063q.
- [15] L.H. Jones, Infrared Spectra and Structure of the Crystalline Sodium Acetate Complexes of U(VI), Np(VI), Pu(VI), and Am(VI). A Comparison of Metal-Oxygen Bond Distance and Bond Force Constant in this Series, *J. Chem. Phys.* 23 (1955) 2105. doi:10.1063/1.1740675.
- [16] K. Ito, H.J. Bernstein, the Vibrational Spectra of the Formate, Acetate, and Oxalate Ions, *Can. J. Chem.* 34 (1956) 170–178. doi:10.1139/v56-021.
- [17] J. Coates, Interpretation of Infrared Spectra, A Practical Approach, *Encycl. Anal. Chem.* (2000) 10815–10837. doi:10.1002/9780470027318.
- [18] A.R. Almeida, J. a. Moulijn, G. Mul, In situ ATR-FTIR study on the selective photo-oxidation of cyclohexane over anatase TiO<sub>2</sub>, *J. Phys. Chem. C.* 112 (2008) 1552–1561. doi:10.1021/jp077143t.
- [19] J.M. Kesselman-Truttman, S.J. Hug, Photodegradation of 4,4'-bis(2-sulfostyryl)biphenyl (DSBP) on metal glides followed by in situ ATR-FTIR spectroscopy, *Environ. Sci. Technol.* 33 (1999) 3171–3176. doi: 10.1021/es981226t
- [20] H. Belhadj, A. Hakki, P.K.J. Robertson, D.W. Bahnemann, In situ ATR-FTIR study of H<sub>2</sub>O and D<sub>2</sub>O adsorption on TiO<sub>2</sub> under UV irradiation, *Phys. Chem. Chem. Phys.* 17 (2015) 22940–22946. doi:10.1039/C5CP03947A.
- [21] S.H. Szczepankiewicz, a J. Colussi, M.R. Hoffmann, Infrared Spectra of Photoinduced

- Species on Hydroxylated Titania Surfaces, *J. Phys. Chem. B.* 104 (2000) 9842–9850. doi:10.1021/jp0007890.
- [22] K. Makino, T. Hagiwara, A. Murakami, A mini review: Fundamental aspects of spin trapping with DMPO, *Int. J. Radiat. Appl. Instrumentation. Part. 37* (1991) 657–665. doi:10.1016/1359-0197(91)90164-W.
- [23] H. Fu, L. Zhang, S. Zhang, Y. Zhu, J. Zhao, Electron spin resonance spin-trapping detection of radical intermediates in N-doped TiO<sub>2</sub>-assisted photodegradation of 4-chlorophenol., *J. Phys. Chem. B.* 110 (2006) 3061–5. doi:10.1021/jp055279q.
- [24] M. Polovka, EPR spectroscopy: A tool to characterize stability and antioxidant properties of foods, *J. Food Nutr. Res.* 45 (2006) 1–11.
- [25] D. Dvoranová, Z. Barbieriková, V. Brezová, Radical Intermediates in Photoinduced Reactions on TiO<sub>2</sub> (An EPR Spin Trapping Study), *Molecules.* 19 (2014) 17279–17304. doi:10.3390/molecules191117279.
- [26] V. Brezová, S. Gabčová, D. Dvoranová, A. Staško, Reactive oxygen species produced upon photoexcitation of sunscreens containing titanium dioxide (an EPR study), *J. Photochem. Photobiol. B Biol.* 79 (2005) 121–134. doi:10.1016/j.jphotobiol.2004.12.006.
- [27] B.-Z. Zhu, H.-T. Zhao, B. Kalyanaraman, J. Liu, G.-Q. Shan, Y.-G. Du, B. Frei, Mechanism of metal-independent decomposition of organic hydroperoxides and formation of alkoxyl radicals by halogenated quinones, *Proc. Natl. Acad. Sci.* 104 (2007) 3698–3702. doi:10.1073/pnas.0605527104.
- [28] A. Marchaj, D.G. Kelley, A.B. Bakac, J.H. Espenson, Kinetics of the Reactions Between Alkyl Radicals and Molecular Oxygen in Aqueous Solution, *J. Phys. Chem.* 95 (1991) 4440–4441.
- [29] K. Guan, Relationship between photocatalytic activity, hydrophilicity and self-cleaning effect of TiO<sub>2</sub>/SiO<sub>2</sub> films, *Surf. Coatings Technol.* 191 (2005) 155–160. doi:10.1016/j.surfcoat.2004.02.022.
- [30] S.J. Hug, D. Bahnemann, Infrared spectra of oxalate, malonate and succinate adsorbed on the aqueous surface of rutile, anatase and lepidocrocite measured with in situ ATR-FTIR, *J. Electron Spectros. Relat. Phenomena.* 150 (2006) 208–219. doi:10.1016/j.elspec.2005.05.006.
- [31] M.F. Atitar, H. Belhadj, R. Dillert, D.W. Bahnem, The Relevance of ATR-FTIR Spectroscopy in Semiconductor Photocatalysis, in: *Emerg. Pollut. Environ. - Curr. Furth. Implic., InTech*, 2015. doi:10.5772/60887.
- [32] D.C. Grinter, M. Nicotra, G. Thornton, Acetic Acid Adsorption on Anatase TiO<sub>2</sub> (101), *J. Phys. Chem. C.* 116 (2012) 11643–11651. doi:10.1021/jp303514g.
- [33] H.Z. and C. von S. Man Nien Schuchmann, Acetate Peroxyl Radicals, O<sub>2</sub>CH<sub>2</sub>C0: A Study on the  $\gamma$ -Radiolysis and Pulse Radiolysis of Acetate in Oxygenated Aqueous Solutions, *Zeitschrift Für Naturforsch.* 40b (1985) 1015–1022. [http://inis.iaea.org/search/search.aspx?orig\\_q=RN:17081730](http://inis.iaea.org/search/search.aspx?orig_q=RN:17081730).
- [34] H.-P. Schuchmann, C. von Sonntag, Methylperoxyl radicals: a study of the  $\gamma$ -radiolysis of methane in oxygenated aqueous solutions, *Zeitschrift Für Naturforsch.* 39b (1984) 217–221. doi:10.1515/znb-1984-0217.

## 4.9 Supplementary Information

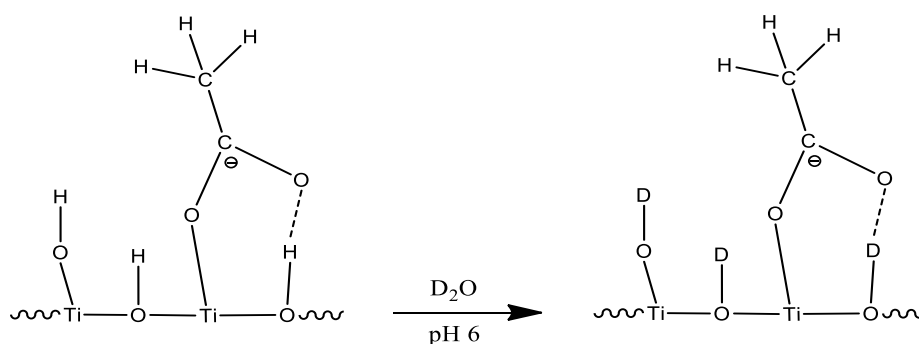
**Table S1.** Time evolution of the pH values of the solution at different pH during UV (A) irradiation.

Time (h)	0	1	2	3	4	5	6
pH $\approx$ pH <sub>zpc</sub>	6.04	6.04	6.04	6.02	6.02	6.00	6.00
pH < pH <sub>zpc</sub>	3.00	2.98	2.87	2.82	2.80	2.80	2.80
pH > pH <sub>zpc</sub>	9.00	7.75	7.50	7.44	7.42	7.41	7.41

**Table S2.** Hyperfine splitting constants of DMPO spin adducts.

Spin-Adduct	Hyperfine Coupling Constants (mT) This study			Hyperfine Coupling Constants (mT) literature			Reference
	$a_N$	$a_H$	$a_{H^\gamma}$	$a_N$	$a_H$	$a_{H^\gamma}$	
DMPO-OH	1.477	1.485	-	1.49	1.49	-	K. Makino <i>et al.</i> [1]
DMPO-OD	1.477	1.485	-	1.49	1.49	-	K. Makino <i>et al.</i> [1]
DMPO-OCH <sub>3</sub>	1.452	1.091	0.121	1.45	1.07	0.132	B. Zhu <i>et al.</i> [2]

Hyperfine coupling constants in Gauss (1 G = 0.1 mT).



**Scheme S1.** Schematic representation for the adsorption of acetate on anatase surface (UV100) in D<sub>2</sub>O in the dark at pH 6.

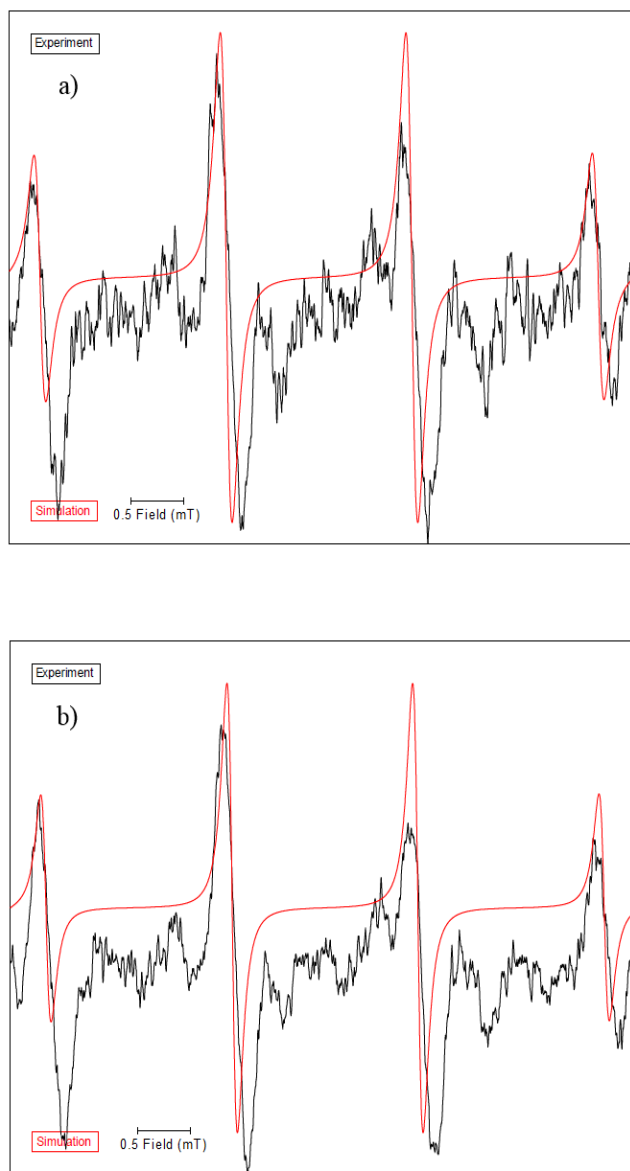


**Fig. S1.** Experimental (black) and simulated (red) EPR spectra measured after 1 min of continuous UV irradiation in the presence of spin trapping agent DMPO. Catalyst loading, 1 g L<sup>-1</sup>; acetate (10<sup>-3</sup>M); DMPO (20 mM); pH 6. The simulation represents EPR signal of the DMPO-OH adducts ( $a_N = 1.477$  mT,  $a_H = 1.485$  mT;  $g = 2.0057$ ) in H<sub>2</sub>O a) and DMPO-OD adducts ( $a_N = 1.477$  mT,  $a_H = 1.485$  mT;  $g = 2.0057$ ) in D<sub>2</sub>O b).

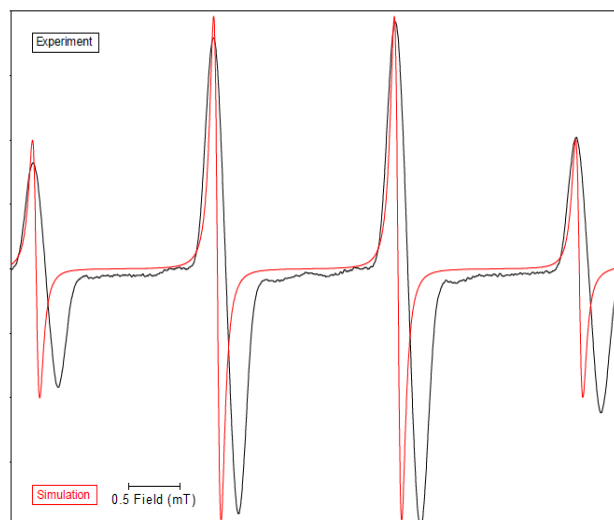


**Fig. S2.** Experimental (black) and simulated (red) EPR spectra measured after 1 min of continuous UV irradiation in the presence of spin trapping agent DMPO. Catalyst loading,  $1 \text{ g L}^{-1}$ ; acetate ( $10^{-3} \text{ M}$ ); DMPO (20 mM); pH 9. The simulation represents EPR signal of the DMPO–OH adducts ( $a_{\text{N}} = 1.475 \text{ mT}$ ,  $a_{\text{H}} = 1.481 \text{ mT}$ ;  $g = 2.0057$ ).

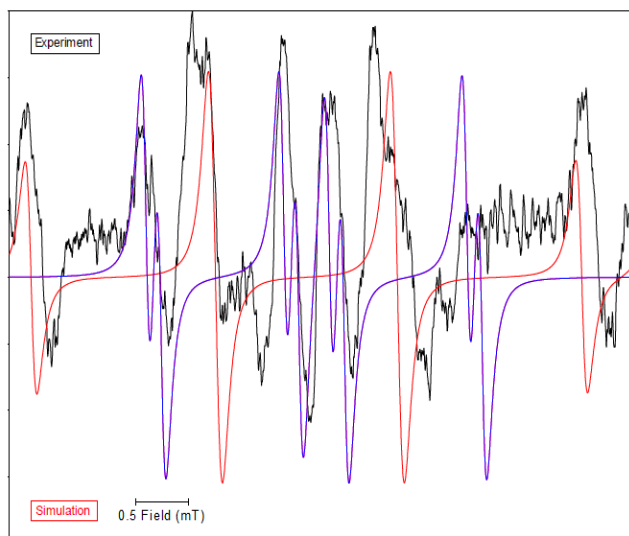


**Fig. S3:** Experimental (black) and simulated (red, blue) EPR spectra measured after 1 min of continuous UV irradiation in the presence of spin trapping agent DMPO. Catalyst loading,  $1 \text{ g l}^{-1}$ ; acetate ( $10^{-3} \text{ M}$ ); DMPO (20 mM); pH 3. The simulation represents a linear combination of DMPO–OH adducts (red:  $a_{\text{N}} = 1.475 \text{ mT}$ ,  $a_{\text{H}} = 1.475 \text{ mT}$ ;  $g = 2.0057$ ) and DMPO–OCH<sub>3</sub> adducts (blue:  $a_{\text{N}} = 1.452 \text{ mT}$ ,  $a_{\text{H}} = 1.091 \text{ mT}$ ;  $a_{\text{H}}^{\gamma} = 0.121 \text{ mT}$ ;  $g = 2.0057$ ).



**References**

- [1] K. Makino, T. Hagiwara, A. Murakami, A mini review: Fundamental aspects of spin trapping with DMPO, *Int. J. Radiat. Appl. Instrumentation. Part. 37* (1991) 657–665. doi:10.1016/1359-0197(91)90164-W.
- [2] B.-Z. Zhu, H.-T. Zhao, B. Kalyanaraman, J. Liu, G.-Q. Shan, Y.-G. Du, B. Frei, Mechanism of metal-independent decomposition of organic hydroperoxides and formation of alkoxy radicals by halogenated quinones, *Proc. Natl. Acad. Sci.* 104 (2007) 3698–3702. doi:10.1073/pnas.0605527104.



## Chapter 5

### **Mechanisms of Simultaneous Hydrogen Production and Formaldehyde Oxidation in H<sub>2</sub>O and D<sub>2</sub>O over Platinized TiO<sub>2</sub>**

Hamza Belhadj<sup>\*,†</sup>, Saher Hamid<sup>†</sup>, Peter K. J. Robertson<sup>‡</sup> and Detlef W. Bahnemann<sup>\*,†,§</sup>

<sup>†</sup>Institut für Technische Chemie, Leibniz Universität Hannover, Callinstraße 3, D-30167 Hannover, Germany

<sup>‡</sup>Sustainable Energy Research Centre, School of Chemistry and Chemical Engineering, Queen's University Belfast, Stranmillis Road, Belfast, BT9 5AG, UK.

<sup>§</sup>Laboratory "Photoactive Nanocomposite Materials", Saint-Petersburg State University, Ulyanovskaya str. 1, Peterhof, Saint-Petersburg, 198504 Russia

Published in ACS Catalysis, 7 (2017) 4753–4758.

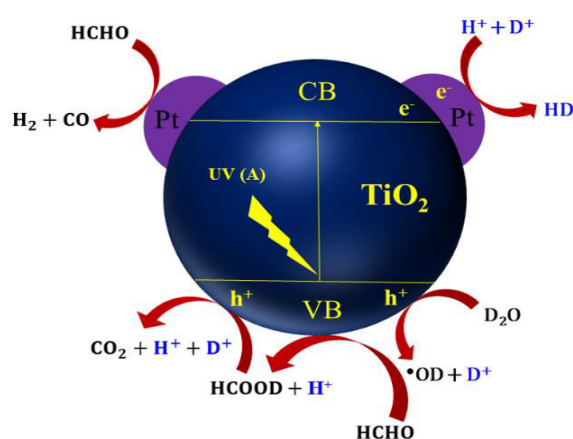
DOI: 10.1021/acscatal.7b01312

## 5. Mechanisms of Simultaneous Hydrogen Production and Formaldehyde Oxidation in H<sub>2</sub>O and D<sub>2</sub>O over Platinized TiO<sub>2</sub>

### 5.1 ABSTRACT

The simultaneous photocatalytic degradation of formaldehyde and hydrogen evolution on platinized TiO<sub>2</sub> have been investigated employing different H<sub>2</sub>O-D<sub>2</sub>O mixtures under oxygen free conditions using quadrupole mass spectrometry (QMS) and attenuated total reflection Fourier transform infrared spectroscopy (ATR-FTIR). The main reaction products obtained from the photocatalytic oxidation of 20% formaldehyde were hydrogen and carbon dioxide. The ratio of evolved H<sub>2</sub> to CO<sub>2</sub> was to 2/1. The HD gas yield was found to be dependent on the solvent and was maximized in a H<sub>2</sub>O/D<sub>2</sub>O mixture (20%/80%). The study of the solvent isotope effect on the degradation of formaldehyde indicates that the mineralization rate of formaldehyde (CO<sub>2</sub>) decreases considerably when the concentration of D<sub>2</sub>O is increased. On the basis of the ATR-FTIR data, the formaldehyde in D<sub>2</sub>O is gradually converted to deuterated formic acid during UV irradiation, which was confirmed by different band shifting. An additional FTIR band at 2050 cm<sup>-1</sup> assigned to CO was detected and was found to increase during UV irradiation due to the adsorption of molecular CO on Pt/TiO<sub>2</sub>. The results of these investigations showed that the molecular hydrogen is mainly produced by the reduction of two protons originating from water and formaldehyde. A detailed mechanism for the simultaneous hydrogen production and formaldehyde oxidation in D<sub>2</sub>O is also presented.

**KEYWORDS:** *Pt/TiO<sub>2</sub>, hydrogen production, D<sub>2</sub>O, formaldehyde, photocatalytic reaction.*



## 5.2 INTRODUCTION

Simultaneous production of hydrogen with degradation of organic pollutants has been a subject of intense global research interest, since it could address the issues of both energy sustainability and environmental remediation at the same time.<sup>1,2</sup> In both applications, photocatalytic reactions are initiated by exciting electrons from the valence band (VB) to the conduction band (CB) at the TiO<sub>2</sub>/water interface or in the bulk of the TiO<sub>2</sub> particles following UV irradiation. Although both applications are based on the same photoinduced charge transfer occurring on TiO<sub>2</sub> particles, sacrificial agents play a significant role as electron donor/acceptors for photocatalytic degradation reactions and hydrogen production. The photocatalytic degradation process involves the formation of reactive oxygen species (ROS), which can oxidize and degrade organic compounds. In this case, trapped electrons are readily scavenged by adsorbed molecular oxygen, which is essential to achieve the mineralization under aerated conditions. On the other hand, photocatalytic hydrogen production takes place under oxygen-free conditions which is achieved by photogenerated electrons, provided that their energy is sufficient to reduce protons to hydrogen molecules.<sup>3</sup> In other words, the photocatalytic degradation of pollutants is initiated by a single electron transfer, whereas the hydrogen production is carried out via a two electron transfer process. To achieve dual-function photocatalysis, the photocatalyst TiO<sub>2</sub> should be able to oxidize organic substrates with protons as an electron acceptor.

A large variety of organic compounds, such as methanol, ethanol, acetic acid and acetaldehyde, have been used as sacrificial reagents which provide an efficient electron/hole separation due to the fact that they react irreversibly with photogenerated holes, resulting in higher quantum efficiencies.<sup>3,4</sup> Indeed, the photogenerated holes either can react with surface Ti–OH groups, adsorbed water producing •OH radicals, or might be transferred directly to adsorbed organic molecules. Different studies have demonstrated that the continued addition of electron donors (sacrificial agents) is required for effective hydrogen production at the semiconductor conduction band with a consequential simultaneous degradation of the electron donating agent, such as an organic substrate, via a valence band reaction.<sup>5,6</sup> Since the competitive reactions may take place between the adsorption of water and organic compounds on TiO<sub>2</sub> surfaces, the primary events and the source of molecular hydrogen formed during the oxidation of organic molecules have not

yet been clearly determined. In order to get a better understanding of the reaction mechanisms under aqueous conditions, a simple system is advantageous; therefore, formaldehyde has been chosen as a model pollutant.

In this work, details of the mechanism of the photocatalytic hydrogen evolution on platinized TiO<sub>2</sub> from aqueous formaldehyde solutions in different concentrations of D<sub>2</sub>O have been investigated. The effect and the role of D<sub>2</sub>O adsorption on the photocatalytic activity have been considered. Particular attention is focused on the mechanisms of hydrogen production to determine whether the origin of the evolved molecular hydrogen is from water or formaldehyde. The photocatalytic degradation mechanism of formaldehyde in D<sub>2</sub>O was elucidated on the basis of the QMS spectrometer and further confirmed by ATR-FTIR spectroscopy data.

### **5.3 EXPERIMENTAL SECTION**

#### **5.3.1 Materials**

Platinized TiO<sub>2</sub> photocatalyst powders (1 wt% Pt) were kindly supplied by H.C. Starck. Formaldehyde solution (37 wt. % in H<sub>2</sub>O) and deuterium oxide (D<sub>2</sub>O) (99.9 atom% D) were purchased from Sigma-Aldrich. Deionized water (H<sub>2</sub>O) was supplied from a Millipore Mill-Q system with a resistivity equal to 18.2 Ω cm at 25 °C.

#### **5.3.2 Photocatalytic Activity Measurements**

##### **5.3.2.1 Quadrupole Mass Spectrometer**

The photocatalytic reactions were carried out in an experimental setup consisting of a gas supply, a mass flow controller, a 100 cm<sup>3</sup> double jacket Duran and/or a quartz glass reactor with inlets and outlets, and a quadrupole mass spectrometer (QMS) for gas analysis (Hiden HPR-20). The system was continuously purged with argon as the carrier gas, the Ar flow was controlled by a mass flow controller (MFC) as schematically shown in Figure 1.<sup>6</sup>

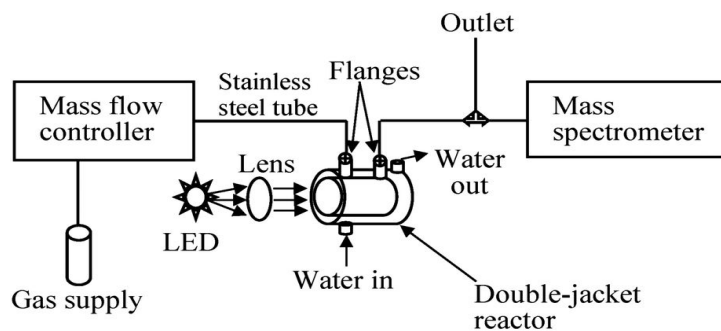


**Figure 1.** Experimental setup for the measurement of the photocatalytic H<sub>2</sub> and CO<sub>2</sub> evolution. (Copyright 2014 Royal Society of Chemistry).

In a typical run, 0.05 g of the photocatalyst Pt/TiO<sub>2</sub> was suspended in 50 mL of an aqueous 20% formaldehyde solution by sonication. The suspension was transferred into the photoreactor and purged with Ar for 30 min to remove dissolved O<sub>2</sub>. Afterward, the reactor was connected to the mass flow controller and to the Q/C capillary sampling inlet of the QMS through metal flanges and adapters. To remove the air in the headspace of the reactor, an Ar gas stream was continuously flowed through the reactor before irradiation, until no traces of molecular oxygen or nitrogen could be detected by the QMS. The Ar gas flow rate through the reactor was kept constant at 10 cm<sup>3</sup> min<sup>-1</sup> during the photocatalytic experiments. The inlet flow rate/gas consumption by the QMS was 1 cm<sup>3</sup> min<sup>-1</sup> and the excess gas was directed toward the exhaust. The sampling rate of the QMS was in the millisecond time range, thus allowing a fast tracking of the reaction. After stabilization of the system background, the reactor was irradiated from the outside using a xenon lamp (light intensity 30 mW cm<sup>-2</sup>). For quantitative analysis of H<sub>2</sub> and CO<sub>2</sub>, the QMS was calibrated employing standard diluted H<sub>2</sub> and CO<sub>2</sub>, respectively, in Ar (Linde Gas, Germany).

### 5.3.2.2 ATR-FTIR Spectroscopy

Initially, an aqueous suspension of platinumized TiO<sub>2</sub> at a concentration of 5 g L<sup>-1</sup> was prepared and sonicated for 15 min in an ultrasonic cleaning bath. An aliquot of 400 μL of the TiO<sub>2</sub> suspension was placed on the surface of the ZnSe ATR crystal and this small volume was simply spread by balancing the unit manually. The suspension was then evaporated to dryness by storing the crystal in a semiopened desiccator at room temperature. Prior to deposition of the TiO<sub>2</sub> films, the ZnSe surfaces (area = 6.8 mm×72 mm) were cleaned by polishing with 1 mm diamond paste (Metadi II, polishing grade)

and rinsed with methanol and deionized water. The coverage of the final dry layer of particles obtained was  $2.3 \text{ g m}^{-2}$  and the layer appeared to be very homogeneous under visual inspection. In the original preparation by Hug *et al*, Atomic Force Microscopy (AFM) measurements of layers with coverage of  $2.3 \text{ g m}^{-2}$  yielded a thickness of 1-3  $\mu\text{m}$ .<sup>7</sup> The final resulting layers of particles remained stable over the entire course of the experiment. Thus, it was assumed that the effective path lengths at all wavelengths remained unchanged.

The ATR-FTIR spectra of the  $\text{TiO}_2$  samples were monitored by a FTIR spectrometer (IFS 66 BRUKER) equipped with an internal reflection element  $45^\circ$  ZnSe crystal and a deuterated triglycine sulfate (DTGS) detector. The interferometer and the infrared light path in the spectrometer were constantly purged with argon and nitrogen to avoid  $\text{H}_2\text{O}$  and  $\text{CO}_2$  contamination. The spectra were recorded with 300 scans at  $4 \text{ cm}^{-1}$  resolution and analyzed using OPUS version 6.5 software. Irradiation of samples with UV(A) light were carried out using an LED lamp (Model LED-Driver, THORLABS) emitting UV light (365 nm). The distance from the UV lamp to the surface of the test solution was kept at 30 cm in which the intensity of UV(A) light was  $1.0 \text{ mWcm}^{-2}$  as measured by a UV radiometer (Dr. Honle GmbH, Martinsried, Germany).

## 5.4 RESULTS

The photocatalytic reactions of formaldehyde were examined by the quadrupole mass spectrometer (QMS) and attenuated total reflection Fourier transform infrared spectroscopy (ATR-FTIR). The QMS experimental setup shown in Figure 1 allowed in line monitoring of the entire course of the reaction with the advantage of simultaneously detecting several gaseous compounds formed during the photocatalytic reaction. Figure 2 shows the time course of the photocatalytic  $\text{H}_2$  and  $\text{CO}_2$  evolution from photooxidation of a 20 vol% formaldehyde in aqueous solution at pH 3.2. Before UV illumination was started, the time course of the investigated gaseous compounds was monitored in the dark for 60 min until their signals became stable. Typical results of QMS analysis in the photocatalytic reaction revealed that after the light was switched on, evolved gases such  $\text{H}_2$  and  $\text{CO}_2$  were observed and reached the region with different constant evolution rates. The  $\text{H}_2$  and  $\text{CO}_2$  evolution rates were determined from the difference between the baseline



(at the end) and the average of all measuring points obtained in the middle part of the curve (steady state region). In addition to the evolution of H<sub>2</sub> and CO<sub>2</sub>, traces of CO gas were also detected with constant evolution rates (Table S1. in the Supporting Information). Additionally, as shown in Figure 2, the evolution rates of H<sub>2</sub> and CO<sub>2</sub> gas were observed to be regular and steady during the oxidation of formaldehyde within a period of 6 h. However, the amount of evolved molecular hydrogen was found to be more than double that of the quantity of CO<sub>2</sub> generated. The rates for H<sub>2</sub> and CO<sub>2</sub> evolution were determined to be 54 and 24 μmol h<sup>-1</sup>, respectively. It was assumed that the photocatalytic oxidation of formaldehyde occurred according to Eq. (1), where the ratio of evolved H<sub>2</sub> to CO<sub>2</sub> is 2/1.

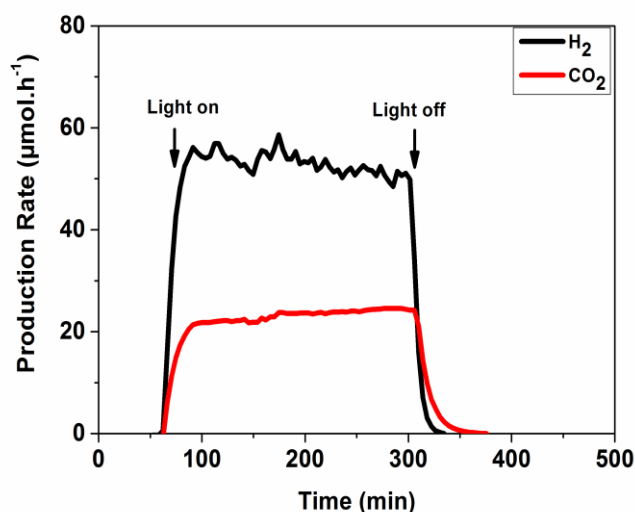
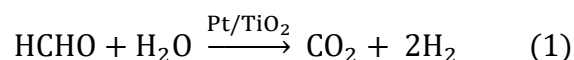


**Figure 2.** Photocatalytic H<sub>2</sub> and CO<sub>2</sub> evolution on platinized TiO<sub>2</sub> from 20 vol% formaldehyde solution. Condition: 0.5 gL<sup>-1</sup> Pt/TiO<sub>2</sub>, 50 mL suspensions, and UV illumination employing a xenon lamp (light intensity 30 mW cm<sup>-2</sup>).

In order to understand the mechanism of the photocatalytic degradation of formaldehyde as well as to identify the origin of the evolved hydrogen gas, a series of photocatalytic degradations of formaldehyde on platinized TiO<sub>2</sub> were performed for 6 h under UV irradiation at different concentrations of D<sub>2</sub>O. Table 1 shows the photocatalytic of H<sub>2</sub>, D<sub>2</sub> and HD gas evolution from a 20 vol% aqueous formaldehyde solution in

different concentrations of D<sub>2</sub>O. The evolution of H<sub>2</sub>, D<sub>2</sub> and HD gas were detected by mass spectrometry (QMS).

**Table 1.** Photocatalytic Evolution of H<sub>2</sub>, D<sub>2</sub> and HD on Platinized TiO<sub>2</sub> from 20 vol% formaldehyde solution<sup>a</sup>

<b>Experiments</b>	<b>H<sub>2</sub></b> (a.u.)	<b>D<sub>2</sub></b> (a.u.)	<b>HD</b> (a.u.)
0% D <sub>2</sub> O	2.2	0	0
20% D <sub>2</sub> O	1.7	0.002	0.1
40% D <sub>2</sub> O	1.4	0.01	0.3
60% D <sub>2</sub> O	0.9	0.03	0.4
80% D <sub>2</sub> O	0.2	0.2	0.6

<sup>a</sup>Condition: 0.5 gL<sup>-1</sup> Pt/TiO<sub>2</sub>, 50 mL suspensions, and UV illumination employing xenon lamp (light intensity 30 mW cm<sup>-2</sup>).

It is clearly seen from table 1 that the photocatalytic H<sub>2</sub> evolution significantly decreased with increasing D<sub>2</sub>O concentration. At the same time, the amount of HD and D<sub>2</sub> increased. Additionally, the amount of evolved HD was found to be rather high in comparison to D<sub>2</sub>. The typical time courses of the photocatalytic H<sub>2</sub>, HD and D<sub>2</sub> evolution rates from aqueous formaldehyde in H<sub>2</sub>O-D<sub>2</sub>O mixture (20%:80%) is shown in Figure 3. It is clearly seen that the signal of the appropriate gaseous compound increased directly after the lamp was switched on. Then the evolved gases, such as H<sub>2</sub>, D<sub>2</sub> and HD reached their peaks with different constant evolution rates. When the light was switched off, the gas evolution rate rapidly decreased reaching the baseline of the corresponding compounds in the system. Interestingly, although the photocatalytic reaction was performed in 80% of D<sub>2</sub>O, the increases of evolved HD were much higher than those of D<sub>2</sub> gas. These results clearly show the effect of solvent in the formation of molecular hydrogen during photocatalytic oxidation of formaldehyde.

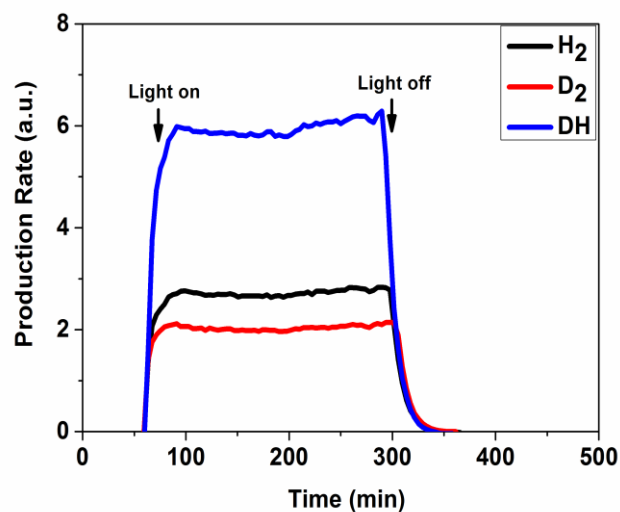


**Figure 3.** Photocatalytic H<sub>2</sub>, D<sub>2</sub> and HD evolution in H<sub>2</sub>O/D<sub>2</sub>O mixture (20%/80%) on platinized TiO<sub>2</sub> from 20 vol% formaldehyde solution. Conditions: 0.5 gL<sup>-1</sup> Pt/TiO<sub>2</sub>, 50 mL suspensions, and UV illumination employing a xenon lamp (light intensity 30 mW cm<sup>-2</sup>).

Furthermore, D<sub>2</sub>O is expected to have an influence on the photocatalytic mineralization rate of formaldehyde on platinized TiO<sub>2</sub> under UV irradiation which occurs simultaneously with the isotopic hydrogen evolution as shown in table 1. Figure 4 shows the photocatalytic evolution rate of CO<sub>2</sub> in H<sub>2</sub>O at different concentrations of D<sub>2</sub>O on Pt/TiO<sub>2</sub>. It is obvious from Figure 4 that the constant evolution rates of CO<sub>2</sub> have decreased gradually by increasing the concentration of D<sub>2</sub>O. The formation of CO<sub>2</sub> confirms the complete mineralization of formaldehyde through the oxidation of intermediates. The mineralization rate of formaldehyde (CO<sub>2</sub>), however, was significantly reduced when the photocatalytic reaction was conducted in the D<sub>2</sub>O solvent. On the basis of these results, we suggest that the adsorption of H<sub>2</sub>O/D<sub>2</sub>O plays a crucial role in photocatalytic reactions which may act as electron donors and electron acceptors for simultaneous hydrogen production and formaldehyde oxidation over platinized TiO<sub>2</sub>.

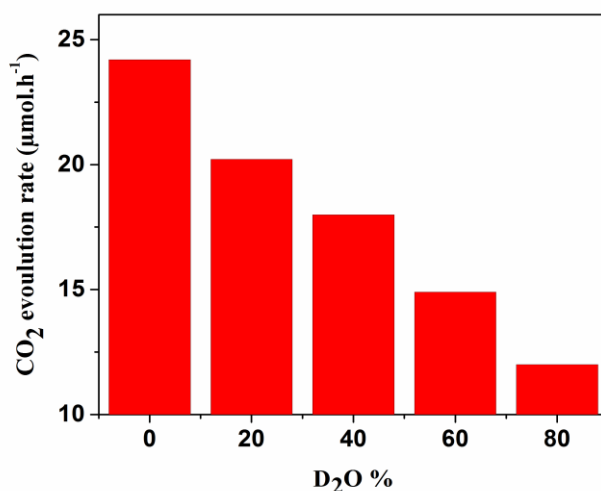
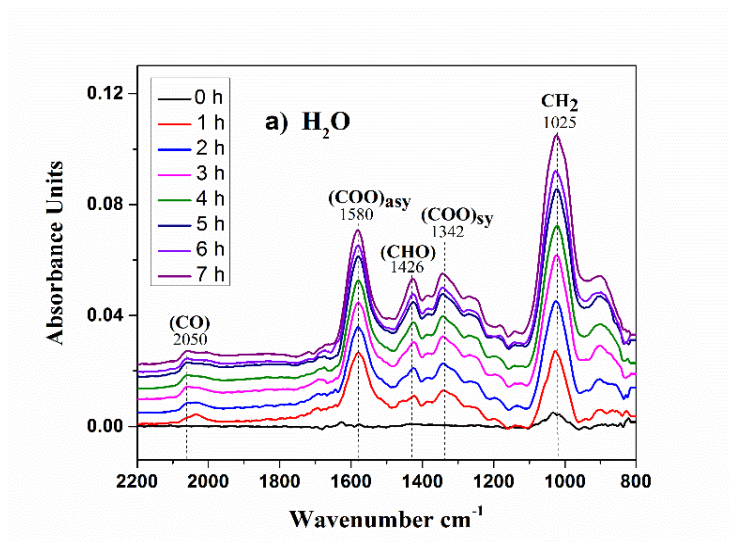


**Figure 4.** Photocatalytic CO<sub>2</sub> evolution rates in H<sub>2</sub>O with different concentrations of D<sub>2</sub>O on platinized TiO<sub>2</sub> from 20 vol% formaldehyde solution. Conditions: 0.5 gL<sup>-1</sup> Pt/TiO<sub>2</sub>, 50 mL suspensions, and UV illumination employing a xenon lamp (light intensity 30 mWcm<sup>-2</sup>).

For a better understanding of the reaction mechanism of this process at the platinized TiO<sub>2</sub>/aqueous solution interface, the adsorption behavior of formaldehyde on TiO<sub>2</sub> surfaces under UV irradiation was investigated by *in situ* ATR-FTIR spectroscopy. The time evolution of the adsorbed 20% formaldehyde spectra on Pt/TiO<sub>2</sub> at pH 3.2 were performed in the dark for 2 h in pure water (a) and H<sub>2</sub>O–D<sub>2</sub>O mixture (20%:80%) (b), (Figure S1. in the Supporting Information). The FTIR spectra are reported in absorbance units, with subtraction of the spectrum of pure H<sub>2</sub>O (D<sub>2</sub>O) as background. The spectrum of formaldehyde adsorption shows different IR absorbances at 1025, 1248, 1435 and 2912 cm<sup>-1</sup> which are assigned to different types of CH<sub>2</sub> vibrations<sup>8,9,10</sup> (Figure S1a). When D<sub>2</sub>O was used instead of pure water as a background, the typical bands assigned to formaldehyde were also observed (Figure S1 b). Since the concentration of 20 vol% aqueous formaldehyde solution was prepared in water, the bands at 3400 cm<sup>-1</sup> and 1450 cm<sup>-1</sup> were observed and assigned respectively to the OH stretching mode band of water and the isotopologue HDO bending band at 1450 cm<sup>-1</sup> where the band attributed to the scissor modes of the CH<sub>2</sub> at 1435 cm<sup>-1</sup> overlapped.<sup>11</sup>

Prior to UV(A) irradiation, the spectrum of formaldehyde adsorption under dark conditions was taken as reference background spectrum. Figure 5. shows the time evolution of the FTIR spectra recorded during the photocatalytic decomposition 20%

formaldehyde in pure water (a) and H<sub>2</sub>O/D<sub>2</sub>O mixture (20%:80%) (b), respectively. The most striking feature here was the initially rapid upward shift in the baseline which was interpreted as transient and persistent diffuse reflectance infrared signals due to the population of conduction band electrons upon irradiation of TiO<sub>2</sub> particles.<sup>12</sup> Furthermore, it can be clearly seen from Fig. 5a that during UV(A) illumination the formation of new bands at 1580, 1426 and 1342 cm<sup>-1</sup> corresponding to  $\nu_{\text{asym}}(\text{COO}^-)$ ,  $\delta(\text{CHO})$  and  $\nu_{\text{sym}}(\text{COO}^-)$ , respectively were observed.<sup>13</sup> The bands detected at 2050 cm<sup>-1</sup> during UV irradiation have previously been assigned in the literature to CO on Pt in the “on-top” position.<sup>14,15</sup> Surprisingly, unlike the case of pure water, the band at 1426 cm<sup>-1</sup> assigned to  $\delta(\text{CHO})$  was shifted to a lower frequency (1415 cm<sup>-1</sup>), whereas the bands at 1580 cm<sup>-1</sup> and 1342 cm<sup>-1</sup>, assigned to asymmetric  $\nu_{\text{asym}}(\text{COO}^-)$  and symmetric  $\nu_{\text{sym}}(\text{COO}^-)$  stretching vibrations, shifted to higher values at 1590 cm<sup>-1</sup> and 1348 cm<sup>-1</sup> respectively (Fig. 5b). Furthermore, two bands observed at 1730 and 1668 cm<sup>-1</sup> were assigned to carbonyl groups with different vibration modes i.e., C=O, O-C=O.<sup>13,16</sup> As can be seen in Figure 5, the appearance of new bands can be considered as evidence for such adsorption intermediates being formed during oxidation of formaldehyde which can most likely be attributed to photocatalytically generated formate/formic acid. These results indicate that the photocatalytic reactions and the behavior of formate/formic acid formed, however, are strongly influenced by deuterated water (D<sub>2</sub>O).



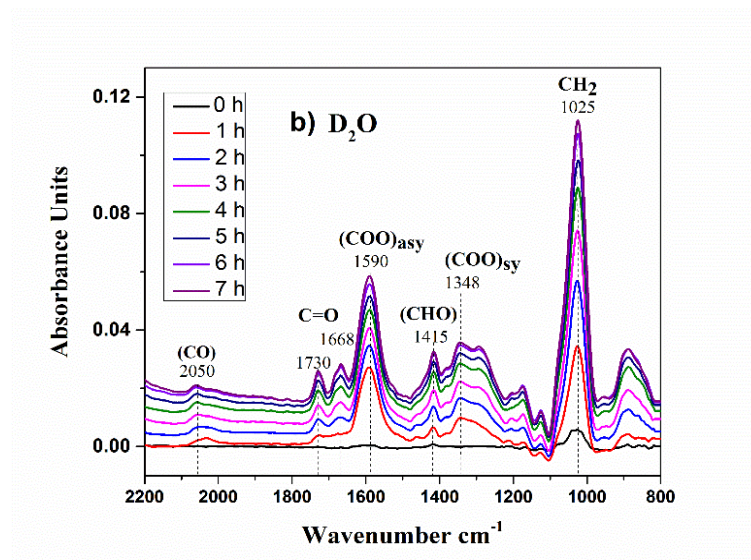
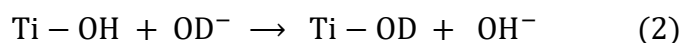


**Figure 5.** Time evolution of the ATR–FTIR spectra of adsorbed formaldehyde (a) in pure water and (b) in H<sub>2</sub>O–D<sub>2</sub>O mixture (20%/80%) on platinumized TiO<sub>2</sub> under 7 h of UV(A) illumination.

## 5.5 DISCUSSION

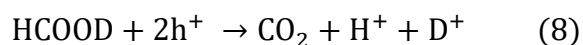
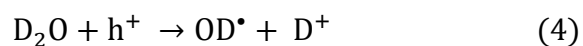
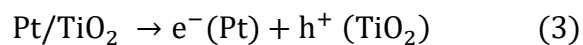
The photocatalytic hydrogen production over platinumized TiO<sub>2</sub> during oxidation of formaldehyde was examined by the quadrupole mass spectrometry (QMS). It is well known that formaldehyde acts as an electron donor or a so-called sacrificial reagent for the photocatalytic H<sub>2</sub> production at the surface of Pt/TiO<sub>2</sub>. It is obvious from Figure 2 that the amount of evolved molecular hydrogen was 2 times higher than that of the quantity of CO<sub>2</sub> that was generated. The ratio of H<sub>2</sub> to CO<sub>2</sub> that was evolved was found to be 2/1 (eq. 1). It was reported that the photocatalytic activity of H<sub>2</sub> production depends strongly on a range of experimental parameters including platinum deposition, catalyst concentration, pH and concentration of formaldehyde.<sup>17</sup> The effect of water adsorption, however, was expected in photocatalytic reactions which could use protons as electron acceptors for hydrogen production reactions. Isotopic studies show that different gases were evolved, namely H<sub>2</sub>, HD, and D<sub>2</sub>, which were formed during UV irradiation of the photocatalyst (Table 1). These results clearly indicate the effect of solvent (D<sub>2</sub>O) in molecular hydrogen formation during the photocatalytic oxidation of formaldehyde. Interestingly, although the concentration of D<sub>2</sub>O was higher (80%), the intensity of the signal assigned to HD increased and showed a maximum intensity during UV(A) illumination in comparison to

the signal of D<sub>2</sub> (Figure 3). These results confirm that during photocatalytic oxidation of formaldehyde the protons from water molecule were involved as electron acceptors to produce molecular hydrogen. The adsorption of D<sub>2</sub>O was also found to play a role in the photocatalytic degradation of formaldehyde. As shown in Figure 4, the evolution rate of CO<sub>2</sub> produced during UV irradiation was found to be maximized in pure water, and then decreased with the addition of increasing levels of D<sub>2</sub>O. In our previous study we reported that the isotopic exchange during D<sub>2</sub>O adsorption takes place on the surface of the photocatalyst in the dark by replacing hydroxyl groups adsorbed on the TiO<sub>2</sub> surface (eq 2).<sup>11</sup>

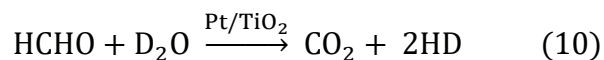


Thus, under UV illumination, the photogenerated valence band holes could oxidize the deuteride ions adsorbed at the surface forming •OD radicals. Since the isotopic exchange reaction occurred on the catalyst surface, the kinetic isotopic effect was expected during the photocatalytic reaction. The first primary kinetic solvent isotope effect on a photocatalytic oxidation reaction was reported by Cunningham *et al.*<sup>18</sup> This behavior was confirmed by Robertson *et al.* who also proposed that the photocatalytic reactions take place on the catalyst surface rather than in the bulk of the solution.<sup>19</sup> As shown in Figure 4, the reduced rate of photocatalytic activity was clearly observed in the presence of D<sub>2</sub>O. This result again confirms the role of the solvent as an electron donor which is involved in the photocatalytic oxidation of formaldehyde. Robertson *et al.* proposed that the reduced rate of photocatalytic degradation may have been due to •OD radicals having a lower oxidation potential in comparison to •OH radicals.<sup>20</sup> It was reported however, that both holes and hydroxyl radicals acted as oxidizing species both directly and indirectly, for the degradation of formaldehyde.<sup>17</sup> Although the formation of CO<sub>2</sub> confirmed the complete mineralization of formaldehyde as the final oxidation, primary intermediate products were however generated during the photocatalytic process. *In-situ* ATR-FTIR studies of the photocatalytic reaction of formaldehyde revealed the formation of new bands of carboxylate groups at 1580 cm<sup>-1</sup> and 1342 cm<sup>-1</sup> which were assigned to the asymmetric  $\nu_{\text{asym}}$  (COO<sup>-</sup>) and symmetric  $\nu_{\text{sym}}$  (COO<sup>-</sup>) stretching vibrations of formate adsorption (Figure 5a). Sun *et al.* reported that the formaldehyde molecules could be adsorbed to the hydroxyl groups on the TiO<sub>2</sub> surface via hydrogen bonding. Under UV

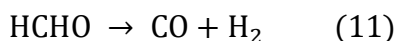
irradiation, however, the adsorbed formaldehyde rapidly converted to the formate species and adsorbed through the bridging bidentate structure.<sup>21</sup> Interestingly, when a H<sub>2</sub>O/D<sub>2</sub>O mixture (20%/80%) was used instead of pure water, the band at 1426 cm<sup>-1</sup> assigned to  $\delta$  (CHO) shifted to a lower frequency (1415 cm<sup>-1</sup>) while the carboxylate band shifted to higher frequency (Figure 5b). Surprisingly, unlike the case of water, different vibration modes of carbonyl groups were observed at 1730 cm<sup>-1</sup> and 1668 cm<sup>-1</sup> (Figure 5b). Taking into account, that the p*K*<sub>a</sub> value in D<sub>2</sub>O should be higher than that in H<sub>2</sub>O, the protonation of formic acid becomes more favorable in D<sub>2</sub>O.<sup>22</sup> From these results we suggest that in the presence of D<sub>2</sub>O the formaldehyde was most likely gradually converted to deuterated formic acid (HCOOD) during the photocatalytic reaction. It is worth noting that, a competitive reaction between the adsorption of H<sub>2</sub>O/D<sub>2</sub>O and formate/formic acid may occur during photooxidation of formaldehyde. On the basis of findings by Medlin *et al.* the adsorption of water induces the dissociation of formic acid to formate on the Pt/TiO<sub>2</sub> surface. These transformations can have an important influence on elementary reaction steps and the rate of photocatalytic decomposition of formic acid on Pt/TiO<sub>2</sub>.<sup>23</sup> Our previous work revealed, however, that the isotopic exchange leads to a new constructive interaction between the adsorbate/intermediate and the OD group.<sup>24,25</sup> Due to the kinetic solvent isotope effect, we suggest that the oxidation of formaldehyde mainly occurs directly by •OD radicals resulting in deuterated formic acid (HCOOD) as an adsorbed intermediate. Subsequently, the deuterated formic acid adsorbed reacts through direct oxidation by valence band holes (photo-Kolbe reaction). Simultaneously, the photogenerated electrons reduce H<sup>+</sup> and D<sup>+</sup> originally coming from formaldehyde and D<sub>2</sub>O to form molecular HD. The details of the proposed mechanism of simultaneous hydrogen production and formaldehyde oxidation in the presence of D<sub>2</sub>O are presented in Eqs. (3–10):







Moreover, the band observed at  $2050 \text{ cm}^{-1}$  during UV irradiation was assigned to the CO adsorbed on Pt in the “on-top” position.<sup>14</sup> Two different sources for CO gas formation can be explained by decarbonylation of formaldehyde or/and dehydration of formic acid.<sup>26,27</sup> Since the evolution rate of  $\text{H}_2$  ( $54 \mu\text{mol h}^{-1}$ ) was more than twice that of  $\text{CO}_2$  ( $24 \mu\text{mol h}^{-1}$ ) according to Figure 2, we suggest that the formation of CO is most likely caused by decarbonylation of formaldehyde (eq 11).



Nakahara *et al.* reported that (eq 11) was based on the proton-transferred decarbonylation of formaldehyde, where one proton was intramolecularly transferred to the other proton attached to the same carbonyl group to form a hydrogen-hydrogen bond, followed by carbonyl group elimination through a breakage of two hydrogen-carbon bonds resulting in carbon monoxide and hydrogen.<sup>28</sup> It seems likely, however, that the photocatalytic oxidation of formaldehyde was the dominant pathway for hydrogen production.

## 5.6 CONCLUSIONS

The effect of  $\text{D}_2\text{O}$  on the photocatalytic  $\text{H}_2$  and  $\text{CO}_2$  evolution during the degradation of 20% formaldehyde has been extensively studied using different concentrations of  $\text{D}_2\text{O}$  (0-80%). The experimental results have shown clearly the role of the solvent in both hydrogen production and formaldehyde oxidation as an electron acceptor (protons) and electron donor respectively. The solvent isotopic effect indicated that the photocatalytic oxidation of formaldehyde was found to take place through  $\bullet\text{OH}$  radicals at the valence band, while the photocatalytic hydrogen production mainly occurred at the conduction band by the reduction of two protons originating from water and formaldehyde.

## 5.7 ACKNOWLEDGEMENTS

Belhadj H. gratefully acknowledges a scholarship from the Deutscher Akademischer Austauschdienst (DAAD) providing the financial support to perform his Ph.D. studies in Germany. The present study was performed within the Project “Establishment of the Laboratory ‘Photoactive Nanocomposite Materials’” No. 14.Z50.31.0016 supported by a Mega-grant of the Government of the Russian Federation.

**5.8 REFERENCES**

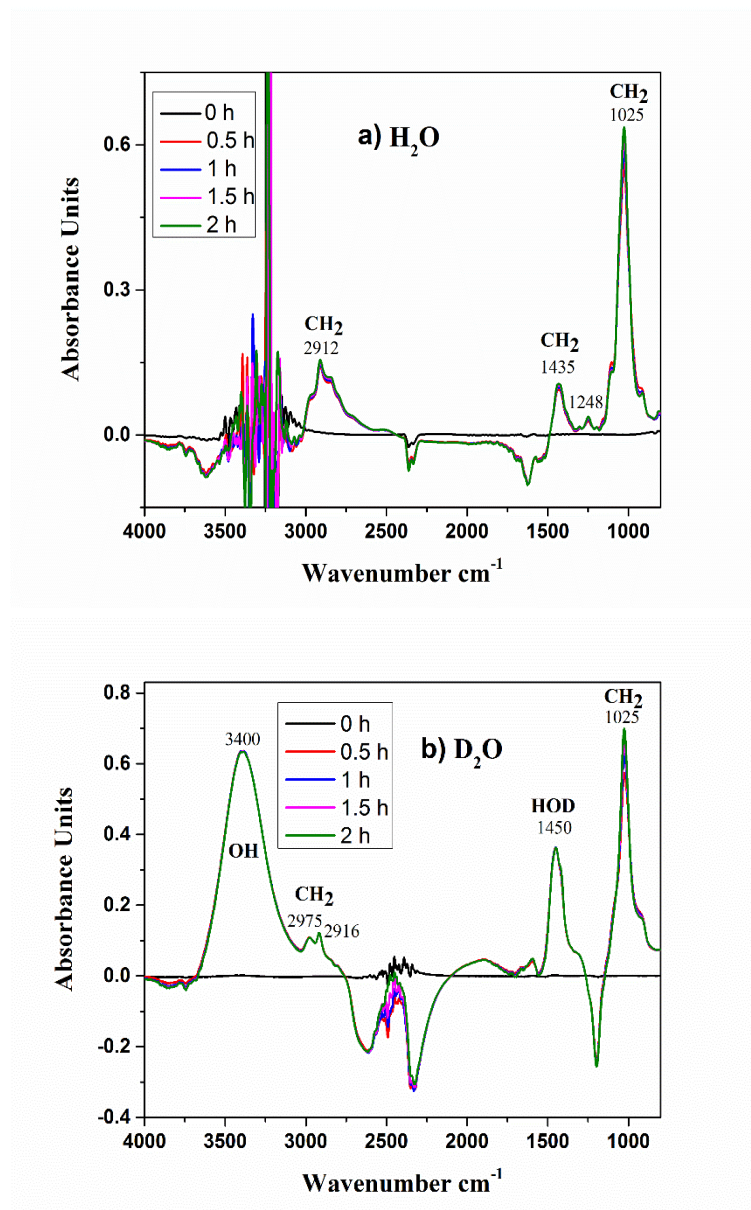
- (1) Chen, X.; Shen, S.; Guo, L.; Mao, S. S. *Chem. Rev.* **2010**, *110*, 6503–6570.
- (2) Kim, J.; Monllor-Satoca, D.; Choi, W. *Energy Environ. Sci.* **2012**, *5*, 7647.
- (3) Patsoura, A.; Kondarides, D. I.; Verykios, X. E. *Catal. Today* **2007**, *124*, 94–102.
- (4) Kandiel, T. a.; Dillert, R.; Robben, L.; Bahnemann, D. W. *Catal. Today* **2011**, *161*, 196–201.
- (5) Rossetti, I. *ISRN Chem. Eng.* **2012**, *2012*, 1–21.
- (6) Kandiel, T. a.; Ivanova, I.; Bahnemann, D. W. *Energy Environ. Sci.* **2014**, *7*, 1420.
- (7) Hug, S. J.; Sulzberger, B. *Langmuir* **1994**, *10*, 3587–3597.
- (8) Busca, G.; Lamotte, J.; Lavalley, J. C.; Lorenzelli, V. *J. Am. Chem. Soc.* **1987**, *109*, 5197–5202.
- (9) Atitar, M. F.; Belhadj, H.; Dillert, R.; Bahnem, D. W. In *Emerging Pollutants in the Environment - Current and Further Implications*; InTech, 2015.
- (10) Mudunkotuwa, I. a; Minshid, A. Al; Grassian, V. H. *Analyst* **2014**, *139*, 870–881.
- (11) Belhadj, H.; Hakki, A.; Robertson, P. K. J.; Bahnemann, D. W. *Phys. Chem. Chem. Phys.* **2015**, *17*, 22940–22946.
- (12) Szczepankiewicz, S. H.; Colussi, a J.; Hoffmann, M. R. *J. Phys. Chem. B* **2000**, *104*, 9842–9850.
- (13) Rotzinger, F. P.; Kesselman-Truttman, J. M.; Hug, S. J.; Shklover, V.; Grätzel, M. *J. Phys. Chem. B* **2004**, *108*, 5004–5017.
- (14) Gao, H.; Xu, W.; He, H.; Shi, X.; Zhang, X.; Tanaka, K. *Spectrochim. Acta Part A Mol. Biomol. Spectrosc.* **2008**, *71*, 1193–1198.
- (15) Gong, D.; Subramaniam, V. P.; Highfield, J. G.; Tang, Y.; Lai, Y.; Chen, Z. *ACS Catal.* **2011**, *1*, 864–871.
- (16) Mendive, C. B.; Bredow, T.; Blesa, M. a; Bahnemann, D. W. *Phys. Chem. Chem. Phys.* **2006**, *8*, 3232–3247.
- (17) Chowdhury, P.; Malekshoar, G.; Ray, M. B.; Zhu, J.; Ray, A. K. *Ind. Eng. Chem. Res.* **2013**, *52*, 5023–5029.
- (18) Cunningham, J.; Srijaranai, S. *J. Photochem. Photobiol. A Chem.* **1988**, *43*, 329–335.
- (19) Robertson, P. K. J.; Bahnemann, D. W.; Lawton, L. a.; Bellu, E. *Appl. Catal. B Environ.* **2011**, *108–109*, 1–5.
- (20) Lawton, L. A.; Robertson, P. K. J.; Cornish, B. J. P. A.; Marr, I. L.; Jaspars, M. *J. Catal.* **2003**, *213*, 109–113.
- (21) Sun, S.; Ding, J.; Bao, J.; Gao, C.; Qi, Z.; Li, C. *Catal. Letters* **2010**, *137*, 239–246.
- (22) Krężel, A.; Bal, W. *J. Inorg. Biochem.* **2004**, *98*, 161–166.

- (23) Miller, K. L.; Lee, C. W.; Falconer, J. L.; Medlin, J. W. *J. Catal.* **2010**, *275*, 294–299.
- (24) Belhadj, H.; Melchers, S.; Robertson, P. K. J.; Bahnemann, D. W. *J. Catal.* **2016**, *344*, 831–840.
- (25) Belhadj, H.; AlSalka, Y.; Robertson, P.; Bahnemann, D. W. *ECS Trans.* **2017**, *75*, 101–113.
- (26) Avdeev, V. I.; Parmon, V. N. *J. Phys. Chem. C* **2011**, *115*, 21755–21762.
- (27) Davis, J. L.; Barteau, M. A. *J. Am. Chem. Soc.* **1989**, *111*, 1782–1792.
- (28) Morooka, S.; Matubayasi, N.; Nakahara, M. *J. Phys. Chem. A* **2007**, *111*, 2697–2705.

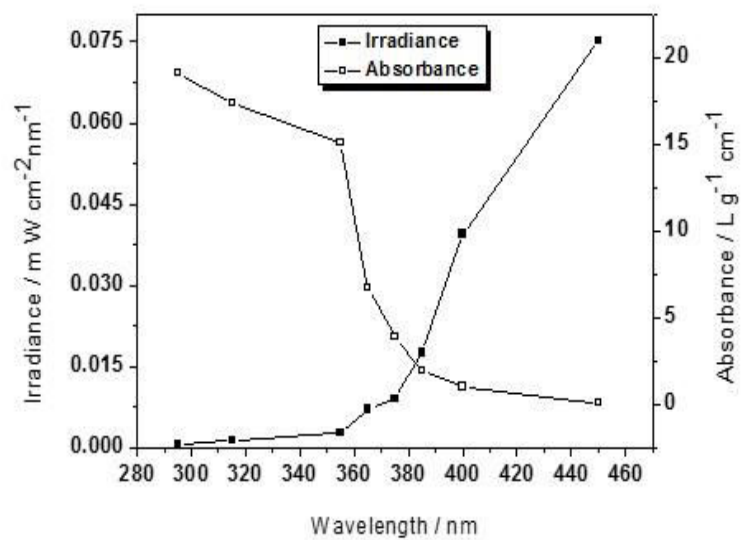
## 5.9 Supporting Information

Table S1. Evolution of traces of CO gas.

Experiments	0% D <sub>2</sub> O	20% D <sub>2</sub> O	40% D <sub>2</sub> O	60% D <sub>2</sub> O	80% D <sub>2</sub> O
CO (a.u.) × 10 <sup>-10</sup>	0.6	0.4	0.4	0.4	0.3



**Figure S1.** Time evolution of the ATR-FTIR spectra of adsorbed formaldehyde a) in pure water, b) in H<sub>2</sub>O-D<sub>2</sub>O mixture (20%/80%) on platinized TiO<sub>2</sub> in the dark for 2 h.



**Figure S2.** Absorption spectrum of suspended  $\text{TiO}_2$  particles in water and irradiance of  $30 \text{ mWcm}^{-2}$  Xenon lamp in the range of 295-450 nm.



# Chapter 6

## 6 Summary and Outlook

### 6.1 Summary and Conclusions

The surface chemistry of water interacting with  $\text{TiO}_2$  is crucial to many practical applications of photocatalysis, including photoinduced hydrophilicity, photocatalytic oxidation and hydrogen production.

This thesis presents spectroscopic and mechanistic studies of photocatalytic reactions employing  $\text{TiO}_2$  in aqueous solution. As an *in situ* technique, ATR-FTIR studies provide a better understanding of the mechanism of photocatalytic reactions at the  $\text{TiO}_2$ /water interface. This technique appears most efficient in characterizing surface hydroxyl groups, adsorbates and complexes or intermediates formed at the surface of  $\text{TiO}_2$  as shown below (Figure 6.1).

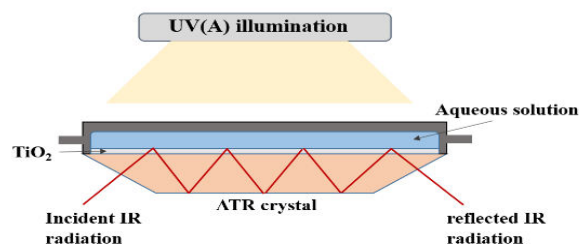


**Figure 6.1:** Scheme representing the ATR-FTIR principle.

A number of interesting and important conclusions emerge from the results of the isotopic studies of the  $\text{H}_2\text{O}/\text{D}_2\text{O}$  adsorption as a function of UV irradiation, and its impact on surface interactions and photocatalytic reaction behaviour for photoinduced hydrophilicity, photocatalytic degradation and hydrogen production. The results obtained are summarized below.

#### 6.1.1 Photoinduced Hydrophilicity of $\text{TiO}_2$

Since the photoinduced hydrophilicity was reported as a result of increasing the number of hydroxyl groups on the  $\text{TiO}_2$  surface upon UV irradiation, different models have been proposed to explain the mechanism leading to the hydrophilicity phenomenon

on the TiO<sub>2</sub> surface such as the generation of surface vacancies, the photo-induced reconstruction of Ti–OH bonds, and the photocatalytic decomposition of organic adsorbents. In an effort to determine the possible mechanism behind the formation of additional hydroxyl groups upon UV illumination, the interaction of adsorbates with TiO<sub>2</sub> surfaces has been investigated.

Here, the photoinduced hydrophilicity of the TiO<sub>2</sub> film was studied through *in situ* ATR-FTIR measurement of the OH/OD stretching bands during the adsorption of a H<sub>2</sub>O-D<sub>2</sub>O mixture on the TiO<sub>2</sub> surface. The results of this investigation showed that the deuteride ions exhibit stronger adsorption ability than hydroxyl ions resulting in an isotopic exchange reaction which takes place in the dark. The illumination of TiO<sub>2</sub> with UV light in the presence of O<sub>2</sub> leads to the formation of OH and OD groups, which in turn increase the hydrophilicity of the TiO<sub>2</sub> surface. Interestingly, when the system is subsequently stored again in the dark, no isotopic exchange is observed between hydroxyl groups and deuteride ions. These results suggest that the increase in the amount of OH and OD groups under UV irradiation is most likely caused by the photoadsorption of H<sub>2</sub>O and D<sub>2</sub>O rather than by the dissociative H<sub>2</sub>O and D<sub>2</sub>O adsorption at surficial oxygen vacancies.

For further understanding of the mechanistic details of the hydration of TiO<sub>2</sub> surfaces during UV illumination, information regarding the effect of electron acceptors and donors on the TiO<sub>2</sub> surface under illumination is required. Here, the influence of molecular oxygen (serving as an electron scavenger) and ethanol (serving as a hole scavenger) on the hydroxyl group and/or water hydration behaviour was examined. It was found that the adsorption of water and D<sub>2</sub>O are significantly increased in the presence of molecular oxygen. In contrast, when the solution was saturated with argon or nitrogen, no additional adsorption of water and D<sub>2</sub>O was detected and the hydrophilicity was strongly inhibited. These results clearly indicate that the presence of O<sub>2</sub> is necessary to enhance the photoadsorption of H<sub>2</sub>O and D<sub>2</sub>O on TiO<sub>2</sub> surfaces during UV(A) irradiation which is suggested to be caused by a photoinduced charge transfer process (Figure 6.2).



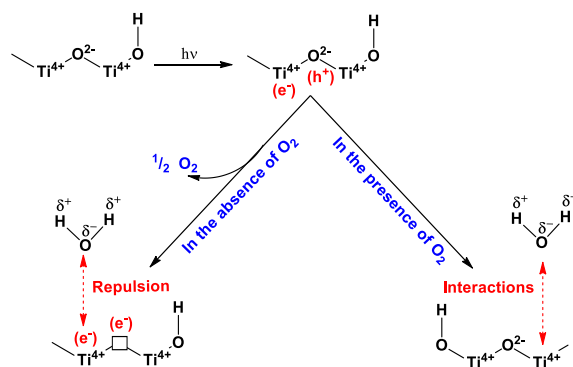
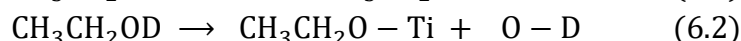
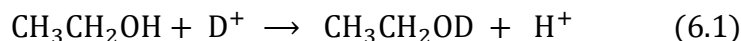


**Figure 6.2:** Interaction model of adsorbed water during UV(A) light irradiation in the absence and presence of oxygen molecules.

On the other hand, it was reported that the photogenerated holes play a crucial role in the photoinduced hydrophilicity. ATR-FTIR studies of the effect of adsorbed ethanol (hole scavenger) on water and deuterium oxide adsorption on the TiO<sub>2</sub> surface showed a stronger adsorption capacity for ethanol compared to both H<sub>2</sub>O and D<sub>2</sub>O. The adsorption of molecular ethanol on the TiO<sub>2</sub> surface in the presence of D<sub>2</sub>O revealed an isotopic exchange between ethanol and deuterium ions (D<sup>+</sup>) resulting in the formation of deuterated ethanol, Et(OD). It was also found that the dissociation of deuterated ethanol may occur on the TiO<sub>2</sub> surface in the dark resulting in the formation of ethoxide at Ti<sup>4+</sup> and D at neighboring basic surface sites. Eqs. (6.1)-(6.2).



When the system was subsequently illuminated with UV(A) light, the surface of TiO<sub>2</sub> becomes enriched with adsorbed H<sub>2</sub>O and D<sub>2</sub>O replacing photodesorbed ethanol molecules. Although the photocatalytic degradation of ethanol on the surface was taken into account, it seems that during UV light irradiation the particle network might be responsible for the enhancement of the water adsorption on a TiO<sub>2</sub> particle film due to a new distribution of the particle network by thermal processes. ATR-FTIR studies of the effect of O<sub>2</sub> revealed a similar behaviour of water and D<sub>2</sub>O adsorption even though these studies were performed in the absence of molecular oxygen. Several theories from the literature can explain this experimental observation, such as the replacement of surface impurities that are photocatalytically being destroyed, the exchange of adsorbed water

molecules by the thermal desorption of ethanol or the increase of hydroxylation by augmentation of surface area due to the deaggregation of the particle agglomerates.

On the basis of the results obtained here, it can be concluded that the photoinduced hydrophilic effect is achieved by an increase in the amount of adsorbed  $\text{H}_2\text{O}$  molecules and that this phenomenon occurs not only by a photoinduced charge transfer process (photoinduced adsorption/desorption and photocatalytic reaction) but also by a thermal process (thermal desorption of substrate and de-aggregation of particle) (Figure 6.3).

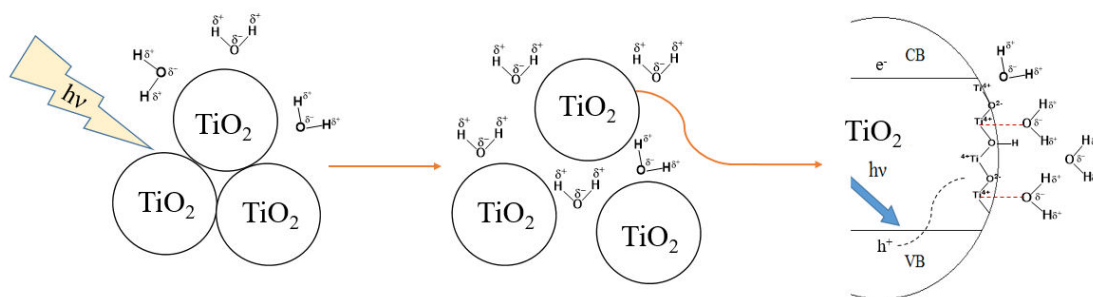


**Figure 6.3:** Proposed mechanism of photoinduced hydrophilicity on the  $\text{TiO}_2$  surface: thermal and photoinduced charge transfer processes.

### 6.1.2 Photocatalytic Degradation of Organic Compounds

For photocatalytic degradation systems, it is well known that the adsorption of molecular oxygen, water and organic compounds on the  $\text{TiO}_2$  surface play a significant role as electron donor/acceptors for photocatalytic degradation reactions. However, the competitive reactions between adsorbed species such as water and organic compound are expected to affect the photocatalytic reaction pathway. In the presence of  $\text{O}_2$ , it was found that the photocatalytic degradation of the organic compound (acetate) depends strongly on two factors, that is the adsorption behaviour of the substrate on the  $\text{TiO}_2$  surface and the effect of the reactive oxygen species formed. As expected, ATR-FTIR studies of the acetate adsorption in  $\text{D}_2\text{O}$  revealed a new constructive interaction between the acetate and the OD group at the  $\text{TiO}_2$ /liquid interface due to the isotopic exchange reaction which had a clear effect on the behaviour of adsorbed acetate. The isotopic study revealed that at pH values close to the  $\text{pH}_{\text{zpc}}$ , the acetate molecule preferentially adsorbs on the positively charged  $\text{TiO}_2$  surface in a monodentate structure as shown below (Figure 6.4).

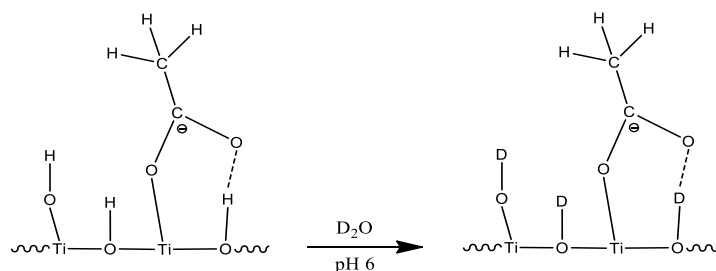


**Figure 6.4:** Schematic representation for the adsorption of acetate on anatase surface (UV100) in  $D_2O$  in the dark at pH 6.

Additionally, it was found that the adsorption behaviour and the photocatalytic activity for the decomposition of acetate both depend strongly on the pH of the suspension. ATR-FTIR studies on this pH effect clearly indicate that at low pH, the formation of a bidentate structure involving two distinct Ti atoms is favoured due to the interaction of  $TiO_2$  with acetate anions, while at high pH, the negatively charged surface repulses the negatively charged acetate anions resulting in weak bonds such as hydrogen bonds or dipole–dipole interactions (Figure 6.5).

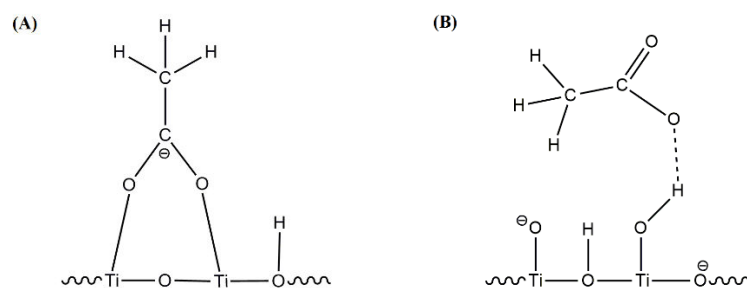


**Figure 6.5:** Schematic representation for the adsorption of acetate on anatase surface (UV100) in the dark at  $pH < pH_{zpc}$  (A) and  $pH > pH_{zpc}$  (B).

Furthermore, the effect of pH under UV irradiation, showed the formation of  $CO_2$  and  $H_2O_2$  at higher pH which can be considered as evidence for such adsorption intermediates being formed during the oxidation of acetate. In contrast, no formation of the product  $CO_2$  was observed at lower pH. These results suggest that the pathway for the degradation of acetate during UV irradiation is different and related to the pH of the solution.

Moreover, additional insight into the photocatalytic reaction pathways of acetate at different pH was obtained using EPR studies. The results of this investigation clearly showed the existence of different radical intermediates representing spin adducts of DMPO-OH at pH 9 and DMPO-OCH<sub>3</sub> at pH 3. This observation reveals that the oxidation

of acetate at low pH values occurs mainly through the direct oxidation by holes ( $h^+$ ) resulting in the well-known Kolbe decarboxylation with the formation of methyl radicals, while at high pH values the degradation of acetate mainly occurs by indirect oxidation via hydroxyl radical ( $\cdot OH$ ) attack (Figure 6.6).

Based on the conducted experiments it was suggested that the adsorption behaviour of acetate as well as the adsorption of water on the  $TiO_2$  surfaces play a vital role for the trapping of photogenerated charge carriers upon UV(A) irradiation, which is strongly dependent on the pH of the suspension.

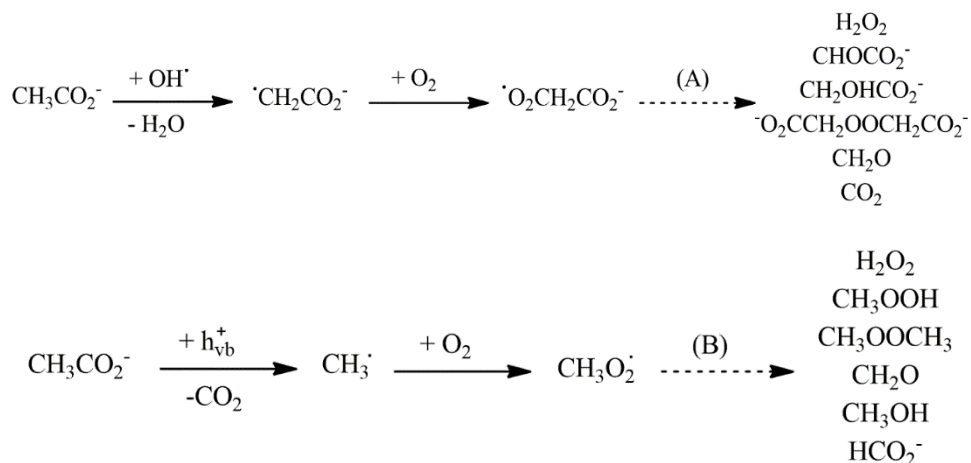


**Figure 6.6:** Proposed mechanism for the photocatalytic reaction of acetate at  $pH > pH_{zpc}$  (A) and at  $pH < pH_{zpc}$  (B).

### 6.1.3 Photocatalytic Hydrogen Production

For photocatalytic water splitting systems forming molecular hydrogen, water is expected to have an influence on the photocatalytic reaction in terms of the source of molecular hydrogen formed as well as for the oxidation of organic molecules. The experimental results show that the treatment of formaldehyde as organic compound in water with the use of Pt/ $TiO_2$  as the photocatalyst and UV radiation under oxygen free conditions results in the photocatalytic oxidation of formaldehyde with the simultaneous production of gas-phase hydrogen (Figure 6.7).

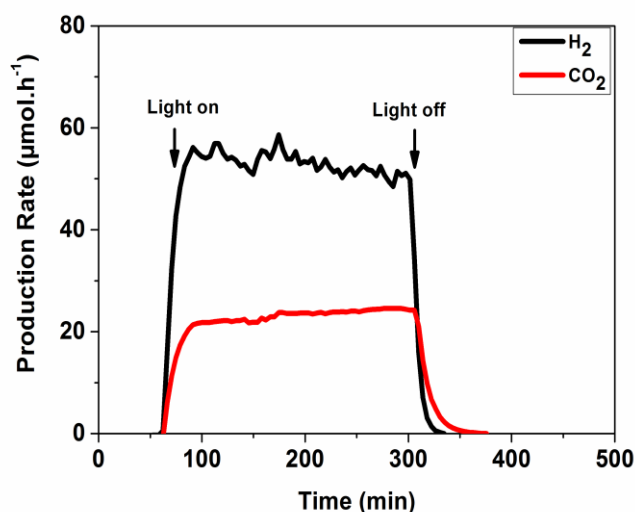
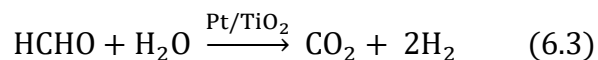


**Figure 6.7:** Photocatalytic H<sub>2</sub> and CO<sub>2</sub> evolution on platinized TiO<sub>2</sub> from formaldehyde solution.

It is well known that titanium dioxide is photocatalytically inactive for water splitting to produce molecular hydrogen, whereas the addition of formaldehyde as an electron donor can dramatically enhance its photocatalytic activity for hydrogen production. This effect has been attributed to the role of formaldehyde as a hole scavenger or hole trap allowing efficient separation of the electron-hole pair to help the separated electrons to catalyze the water splitting reaction.

The results of quadrupole mass spectrometry (QMS) investigations indicate that formaldehyde acts as a sacrificial reagent that is, as an electron donor and that the amount of evolved molecular hydrogen was found to be more than twice as high as the double of the quantity of CO<sub>2</sub> generated. However, it was assumed that the photocatalytic oxidation of formaldehyde occurred according to Eq. 6.3, where the ratio of evolved H<sub>2</sub> to CO<sub>2</sub> is 2/1.



Qualitative analysis of the isotopic studies showed the evolution of different isotopic hydrogen gases, namely H<sub>2</sub>, D<sub>2</sub>, and HD with different quantum yields for their evolution. These results indicate that during the photocatalytic oxidation of formaldehyde the protons from the water molecules were involved as electron acceptors to produce molecular hydrogen. Additionally, it was found that the evolution rate of CO<sub>2</sub> produced during UV

irradiation is the highest in pure water and then decreases with the addition of increasing concentration of D<sub>2</sub>O. This behaviour could be explained by the lower oxidation potential of <sup>•</sup>OD radicals in comparison to <sup>•</sup>OH radicals (2.8 (V/ENH)). This result again confirms the role of the solvent which as an electron donor is involved in the photocatalytic oxidation of formaldehyde. As expected, the isotopic exchange at the TiO<sub>2</sub>/D<sub>2</sub>O interface leads to a new constructive interaction between the adsorbate/intermediate and the OD group. Moreover, ATR-FTIR results of the solvent isotope effect on the degradation of formaldehyde revealed that during UV(A) irradiation, the formaldehyde in D<sub>2</sub>O is gradually converted to deuterated formic acid which is confirmed by different band shifting in FTIR spectra. The FTIR results also showed that water appeared to perturb the structure of adsorbed intermediates through the conversion of bidentate formate to monodentate formate as shown below (Figure 6.8).

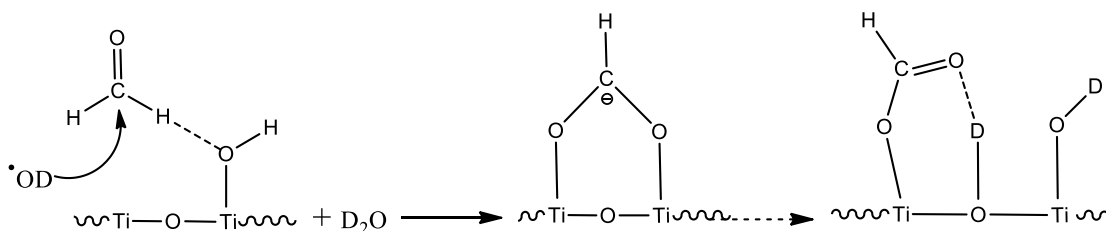


**Figure 6.8:** Effect of D<sub>2</sub>O on formaldehyde photocatalytic decomposition on Pt/TiO<sub>2</sub>.

The mechanistic investigations of the photocatalytic hydrogen production in the presence of D<sub>2</sub>O indicate that H<sub>2</sub> is mainly produced by the reduction of two protons originating from water and formaldehyde. Solvent isotopic effect studies demonstrate that the photocatalytic reaction pathways depend strongly on the water adsorption behaviour on the TiO<sub>2</sub> surface for the photocatalytic degradation and for the hydrogen production (Figure 6.9).

Finally, it is concluded that the interaction between H<sub>2</sub>O and titanium dioxide plays a central role in many photocatalytic reactions such photoinduced hydrophilicity, photodegradation of organic pollutants and photocatalytic hydrogen production.

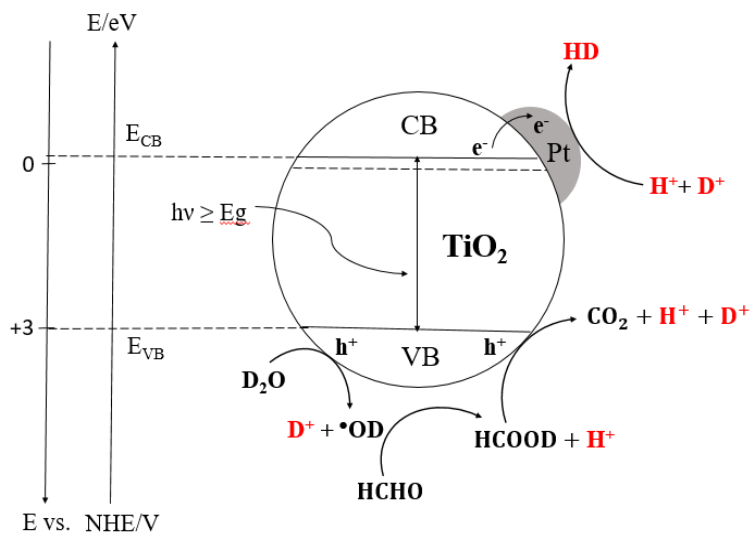


**Figure 6.9:** Proposed mechanism of the photocatalytic hydrogen formation from the oxidation of Formaldehyde in  $D_2O$ .

## 6.2 Outlook

The solid-liquid interface plays a fundamental role in many photocatalytic reactions. However, mechanistic studies of the processes occurring at solid/liquid interfaces still do not show a clear picture of these processes due to the complexity of the system. Investigations using isotopically labelled solvents present one of the most successful strategies to improve our understanding of the fundamental mechanism of TiO<sub>2</sub> photocatalysis.

The use of deuterium oxide (D<sub>2</sub>O) as solvent instead of water is advantageous because the catalytic properties of liquid/solid interface during the photocatalytic process may be drastically different thus allowing a good distinction between different reaction mechanisms.

*In situ* ATR-FTIR spectroscopy is one of the most promising spectroscopic methods applied in heterogeneous catalysis. It is a versatile technique that allows monitoring of the interaction between reacting molecules with the catalyst surface. Therefore, the combination of ATR-FTIR spectroscopy with solvent isotopic labeling (D<sub>2</sub>O) and molecular modeling appears to be very useful to assign specific vibrations of interacting species.

The results presented in this thesis shows the feasibility of the *in situ* ATR-FTIR spectroscopic method to investigate the behaviour of adsorbed species, intermediates and products at the catalyst surface, and also to study the reaction pathways and kinetics at the TiO<sub>2</sub>/water photocatalytic interface. The combination of ATR-FTIR studies with other spectroscopic methods such as QMS and EPR are important steps for further exploration. Another direction to expand the present studies at photocatalyst surfaces is to investigate the influence of UV(A) light on the behavior of different adsorbates on the TiO<sub>2</sub> particle network to elucidate not only the fundamental understanding of photoinduced charge transfer processes but also the thermal processes (thermal-desorption and deaggregation concept).

Further investigations are required using the combination of ATR-FTIR spectroscopy with pure isotope labeling (D<sub>2</sub>O<sup>18</sup>), kinetic modeling to provide a deeper understanding of the reactions taking place on the catalyst surface and also to reveal previously unknown mechanistic steps of TiO<sub>2</sub> photocatalysis.



## Publications

1. H. Belhadj, Saher Hamid, Peter K. J. Robertson and Detlef W. Bahnemann “Mechanistic Study of Molecular Hydrogen Formation from Photocatalysis of Formaldehyde in H<sub>2</sub>O and D<sub>2</sub>O” *ACS Catal.* 7 (2017) 4753–4758, doi: 10.1021/acscatal.7b01312
2. H. Belhadj, Y. AlSalka, P. Robertson, D.W. Bahnemann, In Situ ATR-FTIR Investigation of the Effects of H<sub>2</sub>O and D<sub>2</sub>O Adsorption on the TiO<sub>2</sub> Surface, *ECS Trans.* 75 (2017) 101–113. doi:10.1149/07550.0101ECST
3. H. Belhadj, S. Melchers, P.K.J. Robertson, D.W. Bahnemann, Pathways of the photocatalytic reaction of acetate in H<sub>2</sub>O and D<sub>2</sub>O: A combined EPR and ATR-FTIR study, *J. Catal.* 344 (2016) 831–840. doi:10.1016/j.jcat.2016.08.006
4. J. Modrejewski, J.-G. Walter, I. Kretschmer, E. Kemal, M. Green, H. Belhadj, C. Blume, T. Scheper, Aptamer-modified polymer nanoparticles for targeted drug delivery, *BioNanoMaterials.* 17 (2016) 43–51. doi:10.1515/bnm-2015-0027
5. H. Belhadj, A. Hakki, P.K.J. Robertson, D.W. Bahnemann, In situ ATR-FTIR study of H<sub>2</sub>O and D<sub>2</sub>O adsorption on TiO<sub>2</sub> under UV irradiation, *Phys. Chem. Chem. Phys.* 17 (2015) 22940–22946. doi:10.1039/C5CP03947A
6. M.F. Atitar, H. Belhadj, R. Dillert, D.W. Bahnemann, The Relevance of ATR-FTIR Spectroscopy in Semiconductor Photocatalysis, in: *Emerg. Pollut. Environ. - Curr. Furth. Implic., InTech*, (2015). doi:10.5772/60887

## Oral Presentation

1. Hamza Belhadj, Stephanie Melchers, Saher Hamid and Detlef W. Bahnemann “Mechanistic Study of Molecular Hydrogen Formation from photocatalysis of Formaldehyde in H<sub>2</sub>O and D<sub>2</sub>O” The 21<sup>st</sup> International Conference on Semiconductor Photocatalysis & Solar Energy Conversion (SPASEC-21), November 13-17, 2016, Holiday Inn Atlanta – Perimeter, Atlanta, Georgia, USA.
2. Hamza Belhadj, Peter K. J. Robertson and Detlef W. Bahnemann “Investigation on mechanism of photocatalytic degradation of acetate in H<sub>2</sub>O and D<sub>2</sub>O by ATR-FTIR and EPR spectroscopy” The First International Conference on New Photocatalytic Materials for Environment, Energy and Sustainability (NPM -1), June 7-10, 2016, Inter City Hotel, Göttingen, Germany.
3. Detlef W. Bahnemann, Hamza Belhadj, Peter K. J. Robertson “In Situ ATR-FTIR Investigation of the Effects of H<sub>2</sub>O and D<sub>2</sub>O Adsorption on the TiO<sub>2</sub> Surface” PRiME 2016/230<sup>th</sup> ECS Meeting (October 2-7, 2016) Hawai'i Convention Center. Hawaii.

4. Hamza Belhadj and Detlef W. Bahnemann "ATR-FTIR spectroscopic studies of the adsorption of water and deuterium oxide on TiO<sub>2</sub>" Russian-German-workshop 06-08 October 2014, Hanover. Germany.

### **Poster Presentation**

1. Hamza Belhadj and Detlef W. Bahnemann "New insights into the mechanism of photoinduced hydrophilicity on TiO<sub>2</sub> surface" 1<sup>st</sup> October 2015 – NanoDay, Hanover, Germany.
2. Hamza Belhadj, Amer Hakki, and Detlef W. Bahnemann " *In situ* ATR-FTIR study of surface hydroxyl groups on TiO<sub>2</sub> under UV irradiation" 1<sup>st</sup> Oct. 2014 – NanoDay, Hanover, Germany.
3. Hamza Belhadj, Faycal Atitar, Amer Hakki, and Detlef W. Bahnemann "ATR-FTIR Study of D<sub>2</sub>O Adsorption and Properties of Surface Hydroxyl Groups on TiO<sub>2</sub>" 20<sup>th</sup> International Conference on Conversion and Storage of Solar Energy (IPS-20), July 27-August, 2014, Berlin, Germany.

# Curriculum Vitae

## Personal Information

---

Surname, Name	Belhadj, Hamza
Nationality	Algerian
Date and Place of Birth	13/05/1984, Setif- Algeria
Marital Status	Married, one child

## Academic Education

---

<b>10/2013- 10/2017</b>	<b>PhD in Chemistry</b> Institute of Technical Chemistry, Leibniz University of Hanover, Germany <b>Thesis Title:</b> Solvent isotope effect (D <sub>2</sub> O) in photocatalytic systems
<b>11/2008–01/2011</b>	<b>Magister in Physical and Analytical Chemistry</b> Laboratory of Science and Environmental Technology, University of Constantine, Algeria <b>Thesis title:</b> “Photochemical degradation of rose bengal by different oxidation process into inorganic supports chromophore in aqueous solution”
<b>10/2003–07/2008</b>	<b>Diploma of Higher Education in Chemistry</b> Department of Chemistry, Faculty of science, University of Setif, Algeria

## Work experience

---

<b>04/2011–04/2013</b>	<b>Research Assistant</b> Laboratory of Science and Environmental Technology (LSTE), University of Constantine, Algeria
<b>10/2011–04/2013</b>	<b>Teaching Assistant (Physical and Analytical Chemistry)</b> Department of Chemistry, Faculty of science, University of Setif, Algeria